MERIDIAN INGINERESC

2
2013

ASOCIAȚIA INGINERILOR DIN MOLDOVA • UNIVERSITATEA TEHNICĂ A MOLDOVEI
MOLDAVIAN ENGINEERING ASSOCIATION • TECHNICAL UNIVERSITY OF MOLDOVA

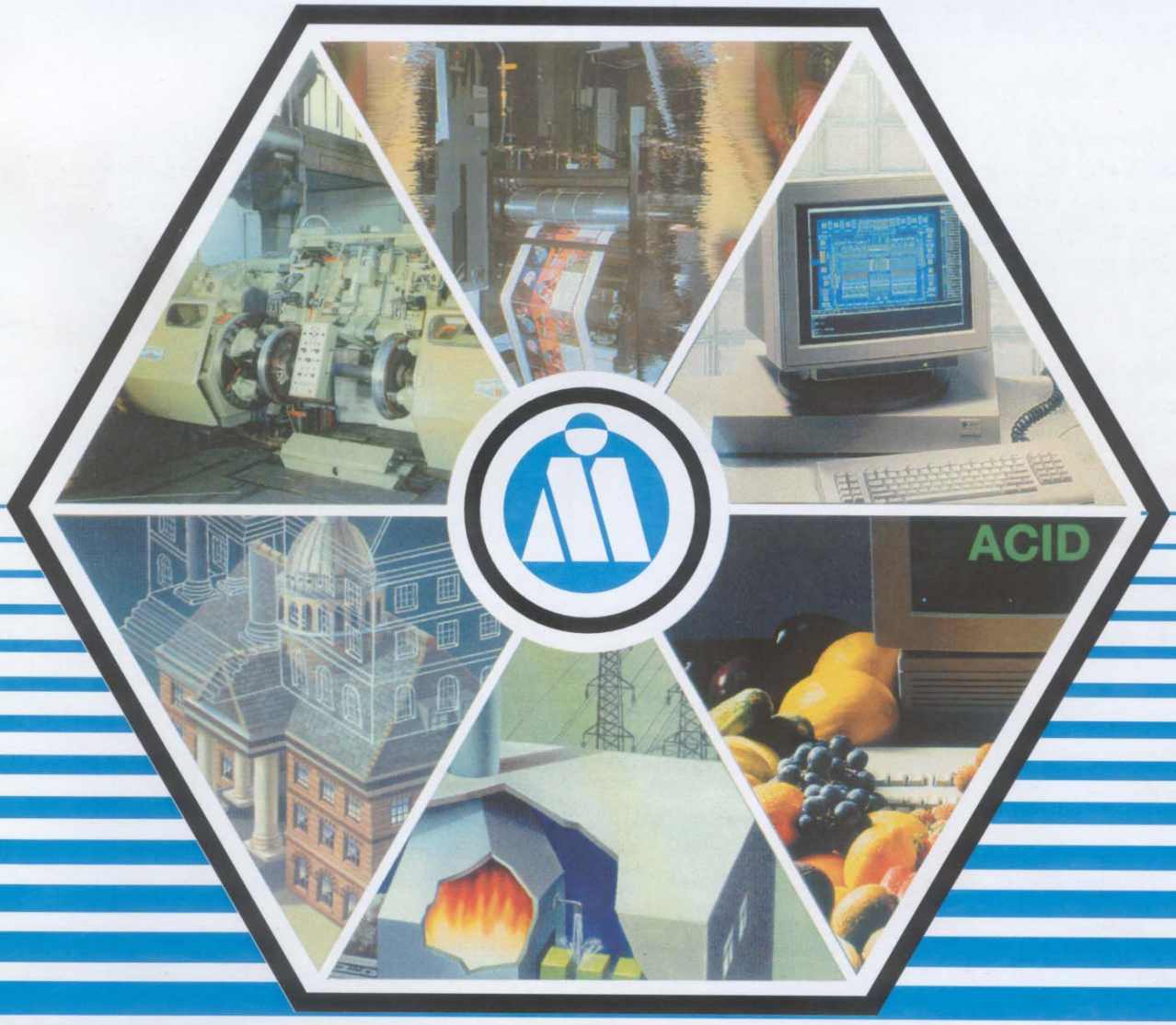

JOURNAL OF TECHNICAL UNIVERSITY OF MOLDOVA
AND MOLDAVIAN ENGINEERING ASSOCIATION

MERIDIAN INGINERESC

Technical and applied scientific publication founded in

9 February 1995

2

2013

ISSN 1683-853X
Published by Technical University of Moldova

C O N T E N T

REZUMATE

Bâzu M.I., Băjenescu T-M.I. **Încapsularea nanodispozitivelor şi fiabilitate.** Revoluţia ştiinţifică şi tehnică care a început se bazează pe capacitatea de a organiza şi manipula sistematic obiecte de dimensiuni nanometrice. Însă încapsularea dispozitivelor nano este o sursă importantă pentru analiza defectărilor. Nu dispunem de un prea mare număr de informaţii cu privire la durata de viaţă utilă a acestor produse sofisticate, cu toate cestea, ele au invadat piaţa. Teoriile convenţionale ale fiabilităţii trebuie restudiate pentru a putea fi folosite în ingineria nano. Folosirea cu încredere a acestor tehnologii depinde de capacitatea noastră de a înţelege mai bine mecanismele lor de defectare şi de a deduce respectivele modele de defectare.

Rusu M. **Metode de segmentare prin prăguire şi evaluarea cantitativă a rezultatelor.** Prezenta lucrare descrie principiu de bază a tehnicilor de prăguire a histogramei, menţionând câteva metode de referinţă. Este evaluată obiectiv metoda de segmentare propusă în lucrările anterioare şi comparată cu alte metode din literatură. Conform criteriilor de evaluare cantitativă a calităţii segmentării, metoda propusă este una eficientă şi dă rezultate satisfăcătoare.

Moraru V., Rusu M. ***Algoritm de separare liniară.*** Prezenta lucrare este consacrată problemei separării liniare a două mulţimi de date. Se prezintă o procedură efectivă de simplificare a rezolvării problemei cu sisteme de ecuaţii.

Mardar M.R. **Aplicarea metodei desfăşurării funcţiei de calitate în elaborarea unui nou produs extrudat.** În prezentul articol este cercetată aplicarea metodologiei de desfăşurare a funcţiei calităţii în elaborarea unui nou produs alimentar. Pe baza metodologiei QFD sunt specificate caracteristicile de calitate ale produsului extrudat elaborat, sunt identificate relaţia dintre priorităţile consumatorilor şi specificaţiile tehnice ale produsului. Rezultatele obţinute au permis identificarea direcţiei de dezvoltare a produsului elaborat în scopul de a asigura avantajele de piaţă ale produsului extrudat comparativ cu concurenţa.

Oprea D. **Vibraţiile turbo-generatorului la o centrala hidroelectrica.** Toate echipamentele rotative vibrează într-o oarecare măsură, dar la fel ca rulmenţii vechi şi componentele ajung la sfârşitul vieţii lor, după uzarea pe parcursul perioadei de funcţionare, ei încep să vibreze mai dramatic şi în moduri diferite. Monitorizarea permanentă a echipamentului permite aceste semne de uzură şi deteriorare să fie identificate cu mult înainte de deteriorarea, ce devine o problemă costisitoare. In acest articolul, ne propunem sa analizam importanta măsurării vibraţiilor la o instalaţie hidro-electrica.

Marusic G. **Studiu cu privire la modelarea numerică a calităţii apei în sistemele acvatice de tip "*râu*".** Lucrarea prezintă un studiu bibliografic cu privire la sistemele informaţionale folosite pentru determinarea calităţii apei în sistemele de tip "*râu*". Se discută tipurile de programe care pot fi utilizate în scopul dat. Se evidenţiază cel mai optim, SMS (Surface - Water Modeling System). Se prezintă diferite studii de caz de modelare numerică a evoluţiei spaţio-temporale a sistemelor de tip "*râu*" cu aplicarea SMS.

Malai L. **Sporirea durabilităţii lagărelor de alunecare renovate cu materiale compozite polimerice.** Prezenta lucrare este dedicată sporirii nivelului de fiabilitate a îmbinărilor de tip lagăr renovate cu materiale compozite polimerice cu matrice poliamidoepoxidică ranforsate intensiv cu microsfere din sticlă cave S-a demonstrat experimental că ranforsarea materialelor compozite examinate cu microsfere de sticlă cave, în proporţie de până la 30%, practic, nu influenţează aderenţa şi stabilitatea acesteia pe substraturi din oţel carbon concomitent contribuind la sporirea durităţii şi capacităţii de înmagazinare a lubrifianţilor în straturile superioare. Testele tribologice au arătat că microsferele de sticlă cave determină o frecare mai mică în zona de contact polimer-metal pentru toate condiţiile de lubrifiere graţie capacităţii de

înmagazinare şi menţinere o durată de timp mai lungă a unsorii în zona de contact.

Perebinos M., Andries I. **Sinteza optimă după geometria în tehnica de antenă.** Având în vedere în mod explicit relaţiile funcţionale electrodinamice dintre geometria antenei, funcţie de excitare, distribuţie şi actualul model de antenă, am derivat strict modelul problemei sintezei de configuraţii geometrice, care pot fi descrise în formă vector-parametrică (radiatoare fire subţiri, corpuri de revoluţie). Acest model este transformat apoi într-o problemă standard de control optimal, fiind soluţionate direct problema non-liniară de programare matematică în spaţiu funcţional. Unele probleme de sinteză concrete s-au declarat şi rezolvate numeric în conformitate cu dorinţele inginereşti: minimizarea zonei laterale şi zonei fasciculului principal prin restricţii geometrice arbitrare, maximizarea fascicolului de vârf prin orice restricţie pe model ş.a.m.d.

Popov V., Ursu S., Gherţa A. **Compoziţia structurală a vinurilor roşii determinată de culoarea buteliei.** În prezenta lucrare sunt expuse rezultatele obţinute experimental ce vizează evoluţia compoziţiei structurale a vinurilor roşii Merlot şi Rară Neagră păstrate în butelii de culoare albă transparentă şi verde.

Galbinean S. **Erori de calcul ale plăcilor prin metoda elementelor finite.** Prezenta lucrare se referă la erorile şi neajunsurile calculului plăcilor prin metoda elementelor finite. Ca model de cercetare s-a ales o placă dreptunghiulară cu diferite moduri de rezemare a laturilor, încărcată cu o sarcină uniform distribuită. Pentru modelul cercetat s-au calculat eforturile în apropierea punctele singulare prin metoda analitică (exactă) şi prin metoda elementelor finite (aproximativă) şi s-au estimat erorile apărute la modelarea plăcii cu elemente finite. Pentru rezolvarea problemei date s-au propus soluţii.

Malai L. **Alegerea şi optimizarea constituţiei materialelor compozite poliamidice folosite la renovarea îmbinărilor de tip lagăr.** În lucrare sunt prezentate unele consideraţii cu privire la alegerea şi optimizarea unui material compozit pentru renovarea îmbinărilor de tip lagăr. În calitate de matrice a fost folosită poliamida PA 12 care a fost ranforsată cu bisulfură de molibden, microsfere de sticlă şi microfibre de bazalt. A fost studiată aderenţa materialului compozit pe substraturi din oţel carbon de calitate obişnuită şi comparată cu aderenţa materialului de bază.

Bostan V. **Microhidrocentrală cu rotor hidrodinamic.** Sisteme de conversie a energiei cinetice a debitului de apă liberă în energie electrică sau mecanică folosesc turbine fără baraje, eliminându-se astfel efectele negative asupra mediului, cum ar fi poluarea fonică, sedimentare excesivă, înrăutăţirea calităţii apei, efectele negative asupra faunei acvatice. În prezentul articol se propune un concept constructiv a două turbine de flux cu 3 şi 5 pale cu profil hidrodinamic NACA. Testarea experimentală a micro hidrocentralei MHCF D4x1, 5E în condiţii de teren reale a confirmat că hidrocentrala cu rotor hidrodinamic cu 5 pale asigură conversia energiei la clemele generatorului cu randamentul de 77,5%.

Goldman A., Fishman G., Toporet V., Rashcovoi A. **Cercetarea macroporozităţilor şi fisurilor în betoanele uşoare constructive.** Betonul uşor cu proprietăţile de rezistenţă caracteristice betonului constructiv a fost obţinut în rezultatul colaborării cercetătorilor din Universitatea Tehnică a Moldovei şi Departamentul Construcţiilor Civile din or. Ariel, Israel. Betonul uşor, prin structura sa, reprezintă un material cu porozitate înaltă, format din agregate uşoare ce asigură reducerea densităţii şi majorarea rezistenţei termice a betonului. Obţinerea betonului uşor cu proprietăţi de rezistenţă înaltă este determinat de incluzionarea în matriţa materialului macroîmplutură polimerică. Densitatea unuia astfel de beton constituie 2000-1600 kg/m^3 şi rezistenţa la compresiune la vârsta de 28 zile – 60-30 MPa.

Zubrilina Ya., Lupaşcu T., Şamis E. **Tehnologii efective noi de producere a materialelor şi articolelor de construcţie.** Lucrarea include descrierea tehnologiilor noi a materialelor de construcţie în baza lianţilor minerali. Metodele au fost probate în producere pe gips şi lianţilor de gips-ciment.

ABSTRACT

Bâzu M.I., Băjenescu T-M.I. **Nanodevices Packaging and Reliability.** A scientific and technical revolution has begun that is based upon the ability to systematically organize and manipulate matter on the nanometer length scale, but the nanodevices packaging is an important source of failure risks. We do not have a great deal of information about the useful life of these sophisticated products even though they are flooding the market. Conventional reliability theories need to be restudied to be applied to nano-engineering. A confident use of these technologies relies on our capacity to better understand their fault mechanisms, and our ability to deduce related fault models.

Rusu M. **Thresholding methods and quantitative evaluation of results.** This paper describes the basic principle of thresholding techniques, mentioning some reference methods. The segmentation method proposed in previous works is evaluated objectively and compared with other methods from the literature. According to the quantitative evaluation criteria of the segmentation, the proposed method is efficient and gives satisfied results.

Moraru V., Rusu M. **Algorithm for linear pattern separation.** This paper is dedicated to the problem of linear separation of two data sets. We presented an effective procedure to simplify the way of solving a problem with system of equations.

Mardar M.R. **Application of the method of quality functional deployment when developing a new extruded product.** Application of the method of quality functional deployment, when developing a new extruded product, has been considered in the article. On the basis of the methodology of QFD, the quality characteristics of the developed extruded product have been determined, the relations between the priorities of the customers and technical characteristics of the product, have been revealed. The obtained results allowed to reveal the directions of the development of the worked - out production witch the purpose of providing of the market advantages of the extruded product in comparison with competitors.

Oprea D. **Vibration on the turbo-generator at the small power plant.** All rotating equipment vibrates to some degree, but as older bearings and components reach the end of their product life, they begin to vibrate more dramatically and in distinct ways. Ongoing monitoring of equipment allows these signs of wear and damage to be identified well before the damage becomes an expensive problem. In this article we intend to analyze the importance of vibration measurement at the hydro-electrical power plant.

Marusic G. **Study on numerical modelling of water quality in "*river-type*" systems.** This paper presents bibliographic research on information systems used to determine water quality in "*river-type*" systems. It discusses the types of programs that can be used in this way. It highlights the most optimal, SMS (Surface - Water Modelling System). It presents several case studies of numerical modelling of the spatio-temporal evolution for "*river-type*" systems, using SMS application.

Malai L. **The increasing sustainability theme of refurbished bearings with polymer composite materials.** This paper is dedicated to increasing the level of reliability of bearing type joints refurbished with polymer composite materials intensively reinforced with polyamidepoxide material with hallow glass microspheres. It has been shown experimentally that reinforce of examined composite materials with hallow glass microspheres, by up to 30% practically does not affect the adhesion and stability of carbon steel substrates while helping to increase hardness and lubricant storage capacity in the upper layers. Tribology tests showed that the hollow glass microspheres results in less friction in the polymer-metal contact under all conditions of lubrication due to storage capacity and maintains the grease a longer period of time in the contact zone.

Perebinos M., Andries I. **Optimal synthesis after geometry in antenna technique.** Considering explicitly the functional electrodynamic relations between antenna geometry, excitation function, current distribution and antenna pattern, we have derived the strict synthesis problem model for geometrical configurations, which can be described in vector-parametrical form (thin-ware radiators, bodies of revolution). This model is transformed then into a standard optimal control problem being solved as the straight non-linear problem of mathematical programming in functional space. Some concrete synthesis problems were stated and numerically resolved in straight accordance with engineering desires: minimizing sidelobes and main beam area by arbitrary geometrical restriction, beam-peak maximizing by any restriction on pattern and s.o.

Popov V., Ursu S., Gherța A. **Structural composition of red wines determined by the colour of bottle.** This paper describes the experimental results regarding the evolution of structural composition of Merlot and Rară Neagră (Rare Black) red wines stored in green transparent bottles.

Galbinean S. **Calculation errors of the plates using finite element method.** This paper refers to errors and gaps in calculation of plates using finite element method. For research, as a model was chosen a rectangular plate with different conditions on boundary, with a uniformly distributed load on it surface. For the researched model were calculated the efforts near singular points using analytical method (exact) and finite element method (approximative) and were estimated the errors from finite element model of the plate. To solve this problem there have been proposed solutions.

Malai L. **The choice and optimization of a composite material used to renovate the bearing-type joints.** The paper presents certain considerations regarding the choice and optimization of a composite material used to renovate the bearing-type joints. The polyamide PA 12 was used as matrix and was reinforced with molybdenum disulphide, glass microspheres and basalt microfibers. Also, there was studied the composite material adhesion on the carbon steel substrates of common quality and it was compared with the base materials adherence.

Bostan V. **Micro hydro power station with hydrodynamic rotor.** Systems for conversion of the kinetic energy of the free water flow into electric or mechanical energy are using turbines in the absence of dams, thus eliminating the negative environmental impacts such as noise pollution, excessive sedimentation, low water quality, effects on aquatic fauna. In the present article is proposed a constructive concept of two flow turbines with 3 and 5 blades with NACA hydrodynamic profile. Experimental testing of the micro hydropower station MHCF D4x1,5E in real field conditions confirmed that the hydropower station with hydrodynamic 5− blade rotor assures the conversion of the energy at the rotor shaft to the generator clams with efficiency of 77.5%.

Goldman A., Fishman G., Toporet V., **Rashcovoi A. Study of macropores and cracks in structural lightweight concrete.** Structural lightweight concrete named GFC (lightweight high strength concrete), has been developed as result of cooperation between the TUM and the Department of Civil Engineering in Ariel. Lightweight concrete usually incorporates conventional cementitious matrix and artificial lightweight aggregates, thus providing reduced bulk unit weight, sufficient strength and improved thermal resistance. The GFC represents another concept: it is made by incorporating lightweight polymer macrofiller into High Performance Concrete, which serves as the matrix. The bulk unit weight of the GFC, as it has been obtained by now, is 2000-1600 kg/m^3, while the 28 days compressive strength has been 60-30 MPa.

Zubrilina Ya., Lupashku T., Shamis E. **Effective technologies of production of building materials and articles.** The work includes the summary data of new technologies of building materials and articles on basis of mineral bindings. The methods are tested in manufacturing environments on gypsum and gypsum-port land cement-active mineral admixtures binder.

SOMMAIRE

Perebinos M., Andries I. **Synthèse optimale après la géométrie de la technique d'antenne.** Considérant explicitement les relations électrodynamiques fonctionnelles entre géométrie d'antenne, fonction d'excitation, la distribution et actuelle modèle de l'antenne, nous avons dérivé le modèle strict de synthèse de problème pour les configurations géométriques, ce qui peut être décrit sous forme vectorielle paramétrique (radiateurs fils minces, de révolution). Ce modèle se transforme alors en un problème standardise de contrôle optimal, étant résolu le problème non-linéaire de la programmation mathématique dans l'espace fonctionnel. Certains problèmes de synthèse concrètes ont été formulées et numériquement résolues conformément directement avec les désirs d'ingénierie: minimiser les lobes latéraux et la zone du faisceau principal par restriction géométrique arbitraire, faisceau pointe maximisant par toute restriction sur le modèle.

Popov V., Ursu S., Gherța A. **Composition structurale des vins rouges déterminé par la couleur de la bouteille.** Dans cet article, les résultats expérimentaux sont présentés pour but le développement de la composition structurelle des vins rouges Merlot et Rară Neagră conservés dans les transparent blanc et vert bouteilles.

Galbinean S. **Erreurs de calcul des plaques en utilisant la méthode des éléments finis.** Ce document se réfère à des erreurs et lacunes dans le calcul des plaques en utilisant la méthode des éléments finis. Pour la recherche, en tant que modèle a été choisi une plaque rectangulaire avec différentes conditions aux limites sur la frontière, avec une charge uniformément répartie sur sa surface. Pour le modèle documenté ont été calculés les efforts près de les points singulier en utilisant la méthode analytique (exacte) et la méthode des éléments finis (approximative) et ont été estimés les erreurs du modèle éléments finis de la plaque. Pour résoudre ce problème ont été proposées des solutions.

Malai L. **La sélection et l'optimisation de la composition des polyamides utilisés pour rénover les combinaisons du type palier** Dans l'ouvrage sont présentés certaines considérations consternant le choix et l'optimisation d'un matériel composé pour la rénovation des polyamides du type palier. En qualité de matrice a été utilisé le polyamide PA 12 qui a été renforcé avec le sulfure de molybdène, microbilles de verre et microfibres de basalte. On a étudié le pouvoir adhésif du matériel composé des substrats d'acier carbone de qualité ordinaire et comparé à l'adhérence du matériel de base.

Bostan V. **Station micro hydro électrique avec rotor hydrodynamique.** Les systèmes de conversion de l'énergie cinétique de l'écoulement libre de l'eau en énergie électrique ou mécanique utilisent des turbines en l'absence de barrages, éliminant ainsi les impacts négatifs sur l'environnement tels que la pollution sonore, la sédimentation excessive, la qualité des eaux faible, les effets négative sur la faune aquatique. Dans le présent article est proposé un concept constructif de deux turbines de flux avec 3 et 5 pales à profil hydrodynamique NACA. Expérimentation de la micro centrale hydroélectrique MHCF D4x1,5E en conditions réelles sur le terrain a confirmé que la station hydroélectrique avec 5 pales rotor hydrodynamique assure la conversion de l'énergie à l'arbre du rotor du générateur avec une efficacité de 77,5%.

Goldman A., Fishman G., Toporet V., Rashcovoi A. **Investigations des macroporos et fissures dans le béton de force léger.** Le béton léger structurel apple haut béton de force léger, a été développé comme le résultat de coopération entre TUM et le Département de l'Ingénierie Civile en Ariel. Le béton léger incorpore d'habitude des ensembles légers matriciels conventionnels de béton et artificiels, en fournissant ainsi le poids d'unité en gros réduit, la force suffisante et la résistance thermale améliorée. Le haut béton de force léger représente un autre concept, est fait en incorporant le macro entonnoir de polymère léger dans le Haut Béton de Performance, qui sert de la matrice. Le poids d'unité en gros de haut béton de force léger, comme il a été obtenu à ce moment-là, est 2000-1600 kg/m^3, pendant que les 28 jours la force de compresseur a été 60-30 MPa.

Zubrilina Ya., Lupascu T., Samis E. **Les nouvelles technologies des matériaux et de produits de construction.** Le travail inclut la description des nouvelles technologies des matériaux et des produits de construction. Les méthodes de production en gypse et gypse-ciment astringent pouzzolane.

РЕЗЮМЕ

Bazu M.И., Băjenescu T-M.I. **Упаковка наноустройств и надежность.** Научно-техническая революция, которая началась, основана на способности систематически организовать и управлять материей на нанометровом масштабе длины. Однако упаковка наноустройств является важным источником анализа отказов. У нас нет много информации относительно полезного срока службы этих сложных продуктов, однако они наводняют рынок. Обычные теории надежности должна быть заново изучены чтобы использовать их в нано-технике. Уверенное использование этих технологий зависит от наших способностей лучшего понимания механизмов их отказа и вывести соответствующие моделей отказа.

Rusu M. **Пороговые методы сегментации и количественное определение результатов.** Эта статья описывает основной принцип пороговых методов сегментации; упомянуты некоторые эталонные методы. Метод сегментации предложенный в предыдущие работы оценивается объективно и сравнивается с другими методами из литературы. Согласно количественными критериями оценки качества сегментации, предлагаемый метод является эффективным и дает удовлетворительные результаты.

Moraru V., Rusu M. **Алгоритм линейной разделимости.** Эта статья посвящена задаче линейного разделения двух групп данных. Рассмотренный метод представляет собой эффективную процедуру для упрощения решения системы уравнений.

Мардар М.Р. **Применение метода развертывания функции качества при разработке нового экструдированного продукта.** В статье рассмотрено применение методологии развертывания функции качества при разработке нового пищевого продукта. На основе методологии QFD определены характеристики качества разрабатываемого экструдируемого продукта, выявлены взаимосвязи между приоритетами потребителей и техническими характеристиками продукта. Полученные результаты позволили выявить направления развития разрабатываемой продукции с целью обеспечения рыночных преимуществ экструдированного продукта по сравнению с конкурентами.

Опря Д. **Вибрации turbo-генератора гидроагрегата.** Всё оборудование, которое вращается в определенной степени вибрирует из-за этого впоследствии износа в процессе эксплуатации старые детали и их компоненты приходят в негодное состояние, они начинают вибрировать более драматично и различными способами. Постоянный мониторинг оборудования позволяет определить эти признаки износа задолго до повреждения, что в последствии становится дорогостоящей проблемой. В этой статье мы предлагаем проанализировать важность измерения вибрации на гидроэлектростанции (ГЭС).

Марусик Г. **К вопросу о численном моделировании качества воды в речных системах.** Статья представляет исследование по вопросу информационных систем, которые используются для моделирования качества воды в речных системах. Обсуждаются типы программ, которые могут быть использованы в данных целях и выделяется самая оптимальная под названием SMS (Surface - Water Modeling System). Представлены различные случаи использования SMS в целях численного моделирования пространственно-временной эволюции речных систем.

Малай Л. **Повышение долговечности подшипников скольжения восстановленных полимерными композитными материалами.** Данная работа посвящена повышению уровня надёжности подшипниковых соединений, восстановленных полимерными композитными материалами, состоящими из полиамидно-эпоксидной матрицы, и интенсивно наполненной полыми стеклянными микросферами. Экспериментально было доказано, что наполнение исследуемых композитных материалов полыми стеклянными микросферами в объеме до 30%, практически не влияет на прочность сцепления с основным материалом из углеродистой стали, в тоже время существенно увеличивает твёрдость,

маслоемкость и водопоглощаемость в поверхностных слоях. Трибологические опыты показали, что полые стеклянные микросферы уменьшают коэффициент трения в зоне контакта полимер - металл для всех условий смазки, благодаря способности накопления и сохранения смазочного материала в зоне контакта на более длительное время.

Перебинос М., Андриеш И. **Оптимальный синтез по геометрии антенной техники.** Учитывая явно функциональные электродинамические связи между геометрии антенны, в зависимости от возбуждения, распределение тока и диаграммы направленности антенны, мы получили точную модель задачи синтеза для геометрических конфигураций, которые могут быть описаны в – параметрически векториальной форме (обеспечение тонких радиаторов, тел вращения). Эта модель затем преобразуется в стандартную задачу оптимального управления, решаемую как прямой нелинейной задачей математического программирования в функциональном пространстве. Некоторые конкретные проблемы синтеза были сформулированы и численно решены в прямом соответствии с инженерными желаниями: сведение к минимуму боковой зоны и главного пучка через произвольные геометрические ограничения, увеличение пикового луча любыми ограничениями на модель и т.д.

Попов В., Урсу В., Герца А. **Структурный состав красного вина определенным цветом бутылки.** В данной работе, экспериментальные результаты, направленные на развитие структурный состав красных вин Мерло и Рарэ Неагрэ, храненные в прозрачной белой и зеленой бутылках.

Малай Л. **Выбор и оптимизация состава полиамидных композиционных материалов используемых при восстановлении подшипниковых узлов.** В работе представлены отдельные соображения по поводу выбора и оптимизации композитного материала для восстановления подшипниковых узлов. В качестве матрицы был использован материал полиамид ПА 12, который был усилен дисульфидом молибдена, стеклянными микросферами и базальтовым волокном. Была изучена адгезия композиционного материала на подложках из углеродистой стали обычного качества и сравнена с адгезией основного материала.

Бостан В. **Микро ГЭС с гидродинамическим ротором.** Системы для преобразования кинетической энергии свободного потока воды в электрическую или механическую энергию используют турбины в отсутствие плотины, тем самым устраняя отрицательное воздействие на окружающую среду, такие как шумовое загрязнение, чрезмерное осаждение, ухудшение качества воды, воздействие на водную фауну. В настоящей статье предлагается конструктивная концепция двух поточных турбин с 3-мя и 5-ю лезвиями с гидродинамическим профилем NACA. Экспериментальные испытания микро гидроэлектростанции MHCF D4x1,5E в реальных условиях подтвердили, что гидроэлектростанции с гидродинамическим 5-лопастным ротором обеспечивает конверсию кинетической энергии воды к разъемам генератора с эффективностью 77,5%.

Гольдман А., Фишман Г., Топорец В., Рашковой А. **Исследование макропористости и трещин в легком конструктивном высокопрочном бетоне.** Легкий конструктивный высокопрочной бетон был получен в результате совместной работы исследователей Технического Университета Молдовы и Департамента Гражданского Строительства Ариэля, Израиль. Легкий бетон представляет собой, как правило, матричные агрегаты, формирующие тело бетона на основе легких заполнителей, что обеспечивает уменьшение объемного веса и увеличение теплоизоляционных характеристик бетона. Создание легкого высокопрочного конструкционного бетона основано на совершенно другом принципе, который заключается в том, что в матрицу бетона вводится полимерный макронаполнитель. Объемный вес такого бетона составляет 2000-1600 кг/м^3, при прочности на сжатие в возрасте 28 суток - 60-30 МПа.

Зубрилина Я., Лупашку Т., Шамис Е. **Эффективные технологии производства строительных материалов и изделий.** Работа включает описание новых технологий строительных материалов и изделий на основе минеральных вяжущих. Методы опробованы в производстве на гипсе и гипсоцементно-пуццолановых вяжущих.

PACKAGING OF NANODEVICES AND RELIABILITY

[1]M.I. Bâzu, prof. [2]Titu-Marius I. Băjenescu
[1]National Institute for Microtechnologies, IMT-Bucharest
[2]Company for Consulting, C. F. C., La Conversion, Switzerland

1. INTRODUCTION

Considered initially as an accessory, indented only to protect the die from the environment, the package has become more and more an essential part of the electronic component. First, because the increasing level of integration led to the more sophisticated packages, with multiple dies in the same package and using modern manufacturing materials. But also because for the newest type of device, the microsystem, the package has not only to protect the die from the environment, but also to ensure the interaction between the die (containing a sensor) and the environment. The package has an essential role in the operation of electronic components, based on three main functions: *(1)* To interface the die with the external circuit. *(2)* To remove the heat generated by device operation. *(3)* To protect the die from the external environment (mechanical integrity, protection from temperature, radiation, moisture, ions and so on, chemical isolation from harsh environment). The package must find the best compromise between electrical, thermal and mechanical performances and physical dimensions to meet product-specific applications, reliability and cost objectives.

The predictable future trends are towards nano-packaging for nanosystems. The first nano-packaging proposed as collaboration between Georgia Institute of Technology NUS and Institute of Microelectronics (IME) of Singapore promises to bring nano-interconnections at wafer level. A team of about 40 faculty, researchers and graduate students are exploring ways to develop nano-structured connections in the short term to 20 to 100 micrometer pitch and nano-grain or nano-fiber connections in the long-term to 1-micrometer pitch.

An ambitious research program of the Packaging Research Center of Georgia Institute of Technology has four main directions [1]: *(a)* Electrical design: design for wafer-level packaging, design of chip-to-package rigid/compliant lead transitions, power distribution with minimum noise and electro-migration, signal integrity; *(b)* Interconnects: lead-free solder, nano links, nano interconnections, micro-electromechanical systems (MEMS)-fabricated interconnects; *(c)* Test and burn-in: interposer with built-in test-support processor and large bandwidth capability, mixed signal test at ultra-high optical signal rate; *(d)* Reliability: micro scale and nano-scale material characterization, fatigue modeling and design for reliability (DfR).

When multiple dies are put in one package, this is called *system in package* (SiP). When multiple dies are combined on a small substrate, often ceramic, this is called *multichip module* (MCM) [2].

In recent years, a new category of packaging technology has begun to be used: *wafer-level package* (WLP). An example is *chip-scale package* (CSP), which entered the industry's lexicon in 1994 [3], and is defined as a package with a perimeter that is no more than 1.2 times the perimeter of the die it contains. Such packages combine the best features of bare die assembly and traditional semiconductor packaging, and reduce overall system size, something that is to be desired in portable electronic products. WLP is used for the technologies of packaging an IC at wafer level, instead of the traditional process of assembling the package of each individual unit after wafer.

2. NANOTECHNOLOGY AND SOME ASPECTS OF THE WLP RELIABILITY

Nanotechnology is the creation of functional materials, devices, and systems through control of matter on the nanometer (1 to 100 nm) length scale and the exploitation of novel properties and phenomena developed at that scale.

The semiconductor industry faces serious problems with power density, interconnect scaling, defects and variability, performance and density overkill, design complexity, and memory-bandwidth limitations. Instead of raw clock speed, parallelism must now fuel further performance improvements, while few persuasive parallel applications yet exist. A candidate to replace complementary CMOS, nanoelectronics could address some of these challenges, but it also introduces new problems (figure 1).

There are two major factors limiting the reliability of WLP, especially for die sizes larger than 5×5 mm: *(i)* interconnect fatigue due to stresses generated by the coefficient of thermal expansion (CTE) mismatch between the die and the PCB and *(ii)* packaging cost. For WLPs that require a redistribution layer (RDL) for I/O redistribution and a compliant layer for reliability, the electroplating process and the dielectric layer make up a large portion of the overall packaging cost. The costs of RDL for a WLP with two metal layers are even greater. Recently, *Tessera* has developed a new compliant WLP that dramatically lowers cost versus previous compliant WLPs [4]. The compliant layer is more cost-effective than spin-on polyimide, benzocyclobutene (BCB) - employed as a filling material for encapsulation - or silicone dielectrics, which are used in conventional WLPs. The copper conductor is etched (which is cheaper than electroplating) to form traces and protected with solder mask. Wirebonds are used to connect the individual die pads to the copper traces, and eventually encapsulation and solder ball attach complete the packaging process.

Under filling (UF) is used to solve reliability problems, because UF reduces the effect of CTE mismatch between the silicon chip and the substrate. Also, UF protects the chip against impurities and makes the structure mechanically stronger by minimising the stress levels or fatigue in the solder joints. However, the adhesion of the die side passivation (polyimide) to UF is critical to the reliability of flip chip (FC) assemblies [5]. Weak interfaces between the die polyimide layer and the UF resin can result in yield loss during thermal cycling or when exposed to a highly accelerated stress test environment of heat and humidity. UF materials absorb moisture, and accumulation of moisture at the interfaces can lead to: *(a)* Crack propagation caused by swelling stress. *(b)* Weakening mechanical support. *(c)* Die-level interconnect failures. *(d)* Corrosion due to ionic contaminants resulting in metal migration failures.

3. 3D PACKAGE

A 3D package contains two or more chips stacked vertically so that they occupy less space. The concept was developed for IC, but could be applied to other electronic components. The names used are system-in-package (SiP) or chip stack multi-chip module (MCM). The wiring of the stacked chips is done along their edges, increasing the length and width of the package and usually requiring a supplementary layer between the chips. The solution to avoiding such an increase of package dimensions is to use through-silicon vias (TSVs) to wire the chips. TSVs are vertical connections through the body of the chips. Consequently, a TSV 3D package (also called TSS – through-silicon stacking) can also be flatter than an edge-wired 3D package, but is smaller in length and width. TSV technology has a wide range of applications: cell phones, MP3 players, notebooks and digital still cameras. Being a new technology, the reliability issues of TSVs are not yet completely understood.

3D interconnects offer an attractive option to reduce the energy dissipation and propagation delay of long on-chip wires (51 and 54% reduction in latency and energy dissipation respectively at 45 nm node). Also, optical interconnects offer reduced latency compared to scaled Cu/low-k technologies, but do not offer significant improvement compared to other technologies like WLP interconnects. A good solution might be the carbon nanotube (CNT) interconnects, which are compared favourably with scaled Cu/low-κ interconnects in terms of latency, with a 42% reduction in delay [6].

Heat-transfer analysis and thermal management of nanodevices become more complex when packing different functional components into a tight space. The miniaturization also raises issues such as coupling between system configurations and the overall heat dissipation to the environment.

4. PROCESS ERRORS

The main possible process errors are: *(i)* Faults in the seal glass (cracks, voids or migration), leading to leakage – intermittent or open circuit – to be identified by stress tests (seal, electrical, high-temperature-storage, temperature cycling and high-voltage tests). *(ii)* Incomplete hermetic seal (for metallic or ceramic packages), producing characteristic degradation or short circuit due to chemical corrosion or humidity. A seal test is needed to identify the failure risks. *(iii)* Dielectric particles floating in the package that may produce intermittent or short circuit. The recommended stress sequence for eliminating these failures is: constant acceleration, vibration (monitored), radiography, and shock (monitored) test. *(iv)* Broken or bent external lead, which leads to open circuit and can be identified by visual inspection followed by lead-fatigue test.

5. PLASTIC PACKAGE

The material used for plastic encapsulation is thermo-reactive resin: a combination of phenol and epoxy resins or silicone resins. The moulding material contains a basic resin, a drying agent, a catalyst, an inert material, an agent for firing delay and a material facilitating the detachment of the package after the moulding operation. If chosen properly, the moulding material may diminish the action of various failure mechanisms produced at wafer level, such as intermetallic Au bond–Al pad interface, which may lead to corrosion and failure at operation above 180°C. It is necessary to choose the right moulding compound alternatives, such as environmentally friendly halogen-free compounds, to mitigate high temperature corrosion. A study focused on this subject offered a characterization of bromine-related wirebond weakening processes, establishing the high-temperature reliability of halogen-free moulding compounds [7].

An ideal moulding compound has: low permeability to moisture, high strength at elevated temperatures, a high glass transition temperature and excellent adhesion. Much research on moulding compounds has been directed towards reducing their moisture permeability and raising their temperature gradient, in order to increase their high temperature strength. Newer biphenyl resins have been developed with filler content approaching 90%, considerably reducing the moisture permeability of the moulding compound. Though the strength of the moulding compound also decreases, the compensation derived from the reduction of moisture absorption counterbalances this at reflow temperatures.

It is important to determine the appropriate size of the spherical silica filler particles included in the package body to ensure thermal cycling-related reliability in plastic-encapsulated packages [8]. This is because the thermal shrinkage of the plastic package body can cause serious damage to the active pattern of the device due to the compressive stress resulting from the fillers pinned by the lead frame. In particular, the model suggested in this work indicates that the combined action of a large filler and smaller fillers can become a failure-causing factor in the plastic package. Thus the adoption of an appropriate filler size in the plastic encapsulation might allow a greater reliability margin for the modification of the lead-on-chip package structure.

In a plastic-encapsulated leaded surface-mount package, the failure mechanism known as *creep corrosion* will only be a reliability concern if the corrosion product is electrically conductive and bridges across two electrical paths, such as leads. The failure mode is generally current leakage [9].

When plastic encapsulated microcircuits (PEMs) underwent a few hundred hours in a steam pressure pot (SPP) test, a harsh moist environment, high leakage currents were noticed. Two possible causes were identified: *(i)* mould compound and *(ii)* the polyimide tape used for co-planarity of lead-frame fingers [10]. It seems however that the leakage current is independent of the frame and is not caused by the mould compound, but rather by the ionic content and acrylic-based adhesive layer of the polyimide tape. Ionic leakage current may occur as a result of moisture penetrating the package and accumulating at the chip. Moisture can reach the chip via penetration along the plastic–lead frame interface, through pores and cracks, as well as via vapour diffusion through the electromagnetic compatibility (EMC). Polyimides, like epoxies, can absorb several weight per cent of moisture, affecting both their mechanical and their electrical properties. The solution proposed for eliminating the high leakage current is to use polyimide tape with low ionic content and non-acrylic-based adhesive.

Failures in plastic packages caused by thermo-mechanical stress may occur at die or plastic level. The lead frame can initiate failure in the die or plastic, leading to an increase in the thermal resistance of the package. Die-related failures include: metal shift, die cracking, electrical failure, filler particle point failure and passivation damage. Plastic-related failures are concerned with the formation of cracks in the body of the package. Plastic cracks are usually derived from the delamination of the plastic from the plastic–silicon interface or the plastic–die paddle interface, which can give rise to the popcorn cracking [10].

The combination of moisture absorbed in the plastic and thermal stresses caused by the different expansions of the metal lead frame and the plastic may produce cracks in larger plastic surface mounting packages, initiated by internal stresses during soldering. Some results show that a critical amount of moisture absorption may lead to cracking, which can be diminished by baking procedures [11].

The primary cause of corrosion, stiction or other failure mechanisms within hermetically sealed enclosures has historically been viewed as due to increases in internal moisture concentrations. It has historically been postulated that the primary source of moisture in these enclosures is the failure to achieve at seal, or the loss of hermeticity post-seal.

Empirical observation of many data sets over the past 20+ years shows that this postulation does not always hold up in practice. The purpose of the current work is to test this postulation through the analysis of archival microelectronic packages and data sets of various ages [18].

6. ASPECTS OF MEMS/NEMS PACKAGING

As nanotechnology and MEMS are enabling new discoveries in diverse fields of science and engineering [12], a collection of review papers have been seen recently that try to summarize the various impacts that nanotechnology is bringing. Focusing on different physical and statistical issues, these review papers have provided a general background of reliability research in nano-engineering.

Motivated by a recent prediction made by Semiconductor Industry Association (SIA) in the International Technology Roadmap for Semiconductors (ITRS) [13] that the silicon technology will continue its historical rate of advancement with the Moore's law for a least of couple of decades, the paper [14] indicates that the silicon gate oxide will be scaled down to its physical limit. An alternative way is to replace oxide with a physically thicker high-k material to help solve most of the problems. However, new problems concerning reliability and performance have to be addressed. The paper [15] reviewed the status of reliability studies of high-k gate dielectrics and illustrated some concepts with experimental results.

Packaging is one of the key issues to be addressed for the evaluation of the reliability of MEMS/NEMS (nano-electro-mechanical switches) products. Any defects created during the sealing of packaging process may cause immediate device failure or may degrade the device performance over time. Furthermore, thermal stress induced by CTE mismatch is one of the main factors that affect the packaging reliability. In fact, the formation of the stress can happen not only during packaging process but also during the operation of devices. Such temperature variations cause the expansion of packaging materials when they are constrained by the package assembly. As a result of this mismatch, significant stresses are induced in the package and may cause the device to fail.

In addition to thermal mismatch, corrosion, creep, fracture, fatigue crack initiation and propagation, and delamination of thin films are all possible factors that may cause the failure of packaged devices. These failure mechanisms could be present or deferred by using proper packaging designs.

The strain can be further reduced if excellent thermal paths are built around interconnects to alleviate thermal stress originating from the temperature gradient between the ambient and operation temperature. On the other hand, delamination phenomena occur in the interface of adjacent material layers such as components made of dissimilar materials that are subsequently bonded together. Delamination can result in electrical or mechanical failures of devices such as mechanically cracking through the electrical via wall to make an electrical open because of the propagation of the delamination of metal line from the dielectric layer or overheating of the die because of delamination of the underside of the die, causing openings in the heath dissipation path. That is why the development of the packaging designs to increase the reliability is very important and requires extensive investigations.

Reliability testing is required before a new device can be delivered to the market. The test results can provide information for the improvement of packaging design and fabrication. The analyse method is to use the mathematical tools of probability and statistical distribution to evaluate data to understand the patterns of failure and to identify the sources of failure [16].

7. CONCEPTS AND TERMINOLOGY

A clear understanding of several concepts and terminology related to reliability is needed to proceed with the understanding of the methodologies which are applied to guarantee optimal operability of VLSI and ULSI systems, fault tolerance, and circuit architectures implementing them. IEEE defines reliability of a system or component to perform its required functions under stated conditions and for a specified period of time. The process yield of a manufacturing process is defined as the fraction, or percentage, of acceptable parts among all parts that are fabricated. A system failure occurs or is present when the service provided by the system differs from the specified service or the service that should have been offered.

Nano-reliability measures the ability of a nano-scaled product to perform its intended functionality. At the nano-scale, the physical, chemical, and biological properties of materials differ in fundamental, valuable ways from the properties of

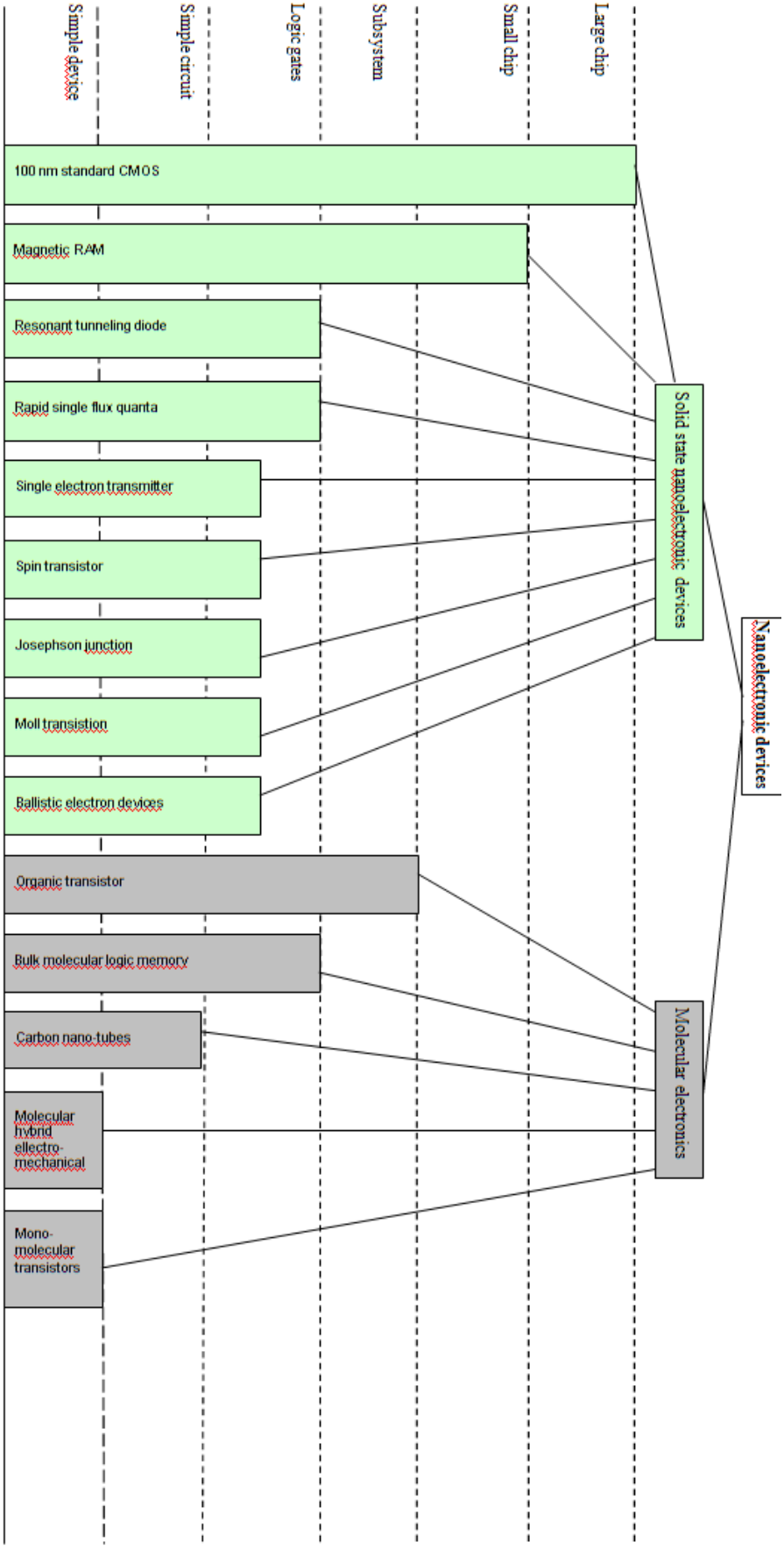

Figure 1. The roadmap for nanotechnology presents many nanodevices currently being investigated as an alternative to standard CMOS [13].

individual atoms, molecules, or bulk matter.

Conventional reliability theories need to be restudied to be applied to nano-engineering. Research on nano-reliability is extremely important due to the fact that nano-structure components account for a high proportion of costs, and serve critical roles in newly designed products.

The ability to measure, and manipulate matter at the atomic/molecular scale has led to the discovery of novel materials. A nanometre is 10^{-12} metre, a single human hair is about 8×10^5 nanometres wide.

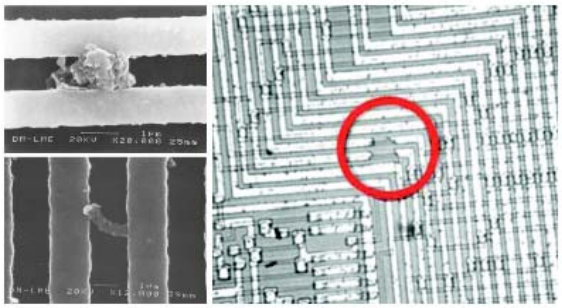

a. *b.*

Figure 2. Defect images: **(a)** Bridging defects with low-resistance electrical behaviour on the top and high-resistance electrical behaviour on the bottom microphotograph, and **(b)** Open defect inside the circle [17]

The upper layer of a fault model models various physical defects such as missing spot, unwanted spot, gate oxide short (GOS) with channel, floating gate coupled to a conductor, and bridging faults. Some of the physical defects are depicted in figure 2. The fault models have been developed from structural and lithography defects, and each defect model is described in terms of electrical parameters of its components. Thus, for simulation purposes, physical defects are translated into equivalent electrical linear devices such as resistors, capacitors and nonlinear devices such as diodes and scaled transistors [17].

CMOS technology on silicon is the dominating technology for microelectronic systems. Figure 3 shows a technology landscape until the year 2015 to give an overview about the whole area of potential technologies for information processing. Apart from solid-state nanoelectronics other technologies such as opto-electronics, super-conductive and molecular electronics are depicted.

A wrong output signal produced by a defective system is called an error. An error is an effect whose cause is some defect. Errors can be

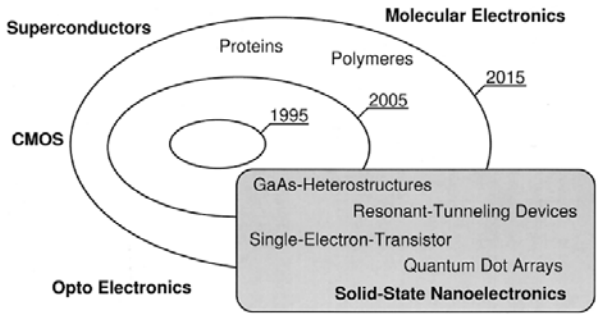

Figure 3. Landscape of different technologies for future information processing [19].

classified into three main groups: permanent, intermittent, and transient errors (the last ones are temporal single malfunctions caused by some temporary environmental conditions which can be an external phenomenon such as radiation or noise originating from other parts of the chip) [20].

8. CONCLUSIONS

The correct solution for modeling MEMS devices is to use physical models: full-finite element simulations of the naked die or packaged device. This is a time-consuming task, so the companies are reluctant in using such approach. Very often, independent research groups are involved in such activities. An example is the research group from the Polytechnic University of Milan led by Prof. Alberto Corigliano, which has developed a useful model for the effect of various mechanical and environmental factors on MEMS reliability [21, 22].

References

1. *Packaging Research Center, Georgia Institute of Technology, http:///www.nsf.gov/pubs/2000/nsf00137q.html*

2. Bâzu, M., Băjenescu T. *Failure Analysis. A Practical Guide for Manufacturers of Electronic Components and Systems, Wiley, Chichester and New York, 2011.*

3. Thomson P. *Chip Scale Packaging, IEEE Spectrum,* Vol. 36, pp. 36-43.

4. Gao G. et al. *Low-cost Compliant Waferlevel Packaging Technology. Tessera Internal Report,* 2008, http://www.tessera.com/ technologies

5. Pathangey B. et al. *Application of TOFSIMS for Contamination Issues in the Assembly World. IEEE Trans. Device Mater. Reliability, Vol. 7, No. 1, pp. 11-18.*

6. Bamal L. et al. *Performance Comparison of Interconnect Technology and Architecture Options for Deep Submicron Technology Nodes. Proc. of Internat. Interconnect Technology Conf., 2006, pp. 202-204.*

7. Chandrasekaran A. *Effect of Encapsulant on High-temperature of the Gold Wirebond-Aluminum Bondpad Interface, Master of Science Thesis, University of Maryland, 2003.*

8. Lee S. M. *Filler-induced Failure Mechanism in Plastic Encapsulated Microelectronic Package. Metals Mater. Int., Vol. 12, No. 6, pp.513-516.*

9. Xie J., Pecht M. *Palladium-plated Packages; Creep Corrosion and its Impact on Reliability," Advanced Packaging, February 2001.*

10. Kelly G. *The Simulation of Thermomechanically Induced Stress in Plastic Encapsulated IC Packages, Kluwer, Dordrecht, 1999.*

11. Lea C., Tilbrook D. *Moisture Induced Failure in Plastic Surface Mount Packages," Soldering Surf. Mount Technol., Vol. 1, No. 3, pp. 30-34.*

12. Huff M. *About MEMS and Nano-technology. http://www.memsnet.org/mems/*

13. *ITRS, "International Technology Roadmap for Semiconductors," http://www.itrs.net/reports.html*

14. Wong H., Iwai H. *On the Scaling Issues and High-Kappa Replacement of Ultra-Thin Gate Dielectrics for Nanoscale MOS Transistors. Microelectronic Engineering, Vol. 83, pp. 1867-1904.*

15. Ribes, G. et al. *Review of High-k Dielectrics Reliability Issues. IEEE Trans. Devices and Materials Reliab., Vol. 5, pp. 5-19.*

16. Bhushan, B. *Nanotechnology, 2nd edition, Springer, Berlin and New York, 2007.*

17. Stanislavjević M. et al. *Reliability of Nanoscale Circuits and Systems. Methodologies and Circuits Architecture, Springer, Berlin and New York, 2011.*

18. Lowry R. K., Kullberg R. C. *Examining internal gas compositions of a variety of microcircuit package types and ages with a focus on sources of internal moisture. Paper # 7206-1 presented during MF102 7206 Reliability, Packaging, Testing, and Characterization of MEMS/MOEMS and Nanodevices VIII, 28 Jan 2009 to 29 Jan 2009.*

19. Goser F. K. et al. *Aspects of Systems and Circuits for Nanoelectronics. Proc. of the IEEE, Vol.85, No. 4, pp. 558-573.*

20. Jeng Sh.-L. et al. *A review of Reliability Research on Nanotechnology. IEEE Trans. on Reliability, Vol. 56 (2007), No. 3, pp. 401-410.*

21. Mariani S., Ghisi A., Corigliano A., Zerbini S. *Multi-Scale Analysis of MEMS Sensors Subject to Drop Impacts. Sensors, Vol. 7, 2007, pp. 1817-1833.*

22. Mariani S., Ghisi A., Corigliano A., Zerbini S. *Modeling Impact-Induced Failure of Polysilicon MEMS, a Multi-Scale Approach. Sensors, Vol. 9, 2009, pp. 556-567.*

Recommended for publication:16.04.2013.

THRESHOLDING METHODS AND QUANTITATIVE EVALUATION OF RESULTS

M. Rusu
Technical University of Moldova

INTRODUCTION

Segmentation represents division of the image into uniform regions according to certain criterion. This step is important in image processing and usually monitors extraction, detection or recognition of objects. Formed image regions are called segments and they represent separate objects from the background.

The performance of segmentation is influenced by quality of the image and of the scene complexity. A good segmentation occurs when objects in the image have well defined contours and do not present shadows or reflections of light. These effects lead to bad results in image segmentation, especially those represented in gray levels. The color images have advantage to include as segmentation criterion the factor of color.

1. USUAL METHODS OF IMAGE SEGMENTATION

Depends on image quality and their complexity we choose a specific segmentation algorithm. In some cases, before segmentation algorithm is applied, an improvement of quality may required (achieve higher contrast and better enhancement of contours).

In the specialized literature we can find many kinds of color (or grayscale) image segmentation techniques, which can be grouped into four main categories:

1. ***Pixel based segmentation*** – a region is defined as a set of pixels that have similar intensity / color.
   - *histogram based techniques* [1-3];
   - *clustering techniques* [4];
   - *Fuzzy clustering techniques* [5-7].
2. ***Region based segmentation.*** The methods for detection of regions are based on similarity and spatial proximity between pixels. We know:
   - *the region growing techniques* – choose a pixel position and looking in the 8 directions if neighboring pixels corresponding to a criterion of similarity, forming homogeneous regions [8-9];
   - *the splitting and merging algorithms* [10] – the purpose is to divide the image in regions. Each region, according to a certain sense is homoge-neous, but the concatenation of two adjacent regions is not homogeneous with the same sense.
3. ***Edge based segmentation*** [11, 12] – when a region is defined as a set of pixels defined by a color contour. For contour determination is important the change rate of gray levels (or color values of pixel).
4. ***Hybrid segmentation techniques*** [13-15] – improve the results of the segmentation by addition and / or combination of the above methods.

In the literature we found other techniques, such as those based on graphs [16]; special algorithms have been adapted to segmentation techniques using neural networks [17], Markov models, algorithms based on texture, color and other.

To apply a method or another depends on:

– the nature of image: capture mode, resolution, lighting, noise level

– the type of useful information (textures, text & etc..)

– the purpose of segmentation: location object recognition forms, interpretation, quality control, diagnostics & etc..

– the characteristics that must be extracted also influence the choice of segmentation methods: contours, regions, shape and texture.

An irregular lighting negatively affects the segmentation results, especially in methods based on the histogram. Also the presence of *salt and pepper* noise negatively affects the segmentation results and requires some preprocessing before applying segmentation methods.

For the gray images is indicated to use the histogram based segmentation, for the color images – the regions based segmentation. The method for edges detection can be implemented for both type of image: in grayscale and color.

2. SEGMENTATION METHODS BASED ON HISTOGRAM

The method described in previous works [18-19] is part of the segmentation methods based on

pixel classification depending on their intensity.

The segmentation techniques based on histogram calculates the pixel values frequency. These techniques are based on thresholding of histograms and are effective when there is a relatively clear separation of pixel values between analyzed objects. In this case the given range of color represents a single class of objects.

Thresholding method consists in choosing an N number of thresholds: $Th_1, Th_2, \ldots Th_N$ and create an labeled image, based on the original image, as follows:

if g(i,j)<=Th_1
then g(i,j)∈ $segment_1$
if g(i,j)>Th_1 && g(i,j)<=Th_2
then g(i,j)∈ $segment_2$
…
if g(i,j)>Th_{N-1} && g(i,j)<=Th_N
then g(i,j)∈ $segment_{N-1}$
if g(i,j)>Th_N
then g(i,j)∈ $segment_N$

where *g(i,j)* – the value of pixel, $segment_1$ - $segment_{N-1}$ – the objects in the image.

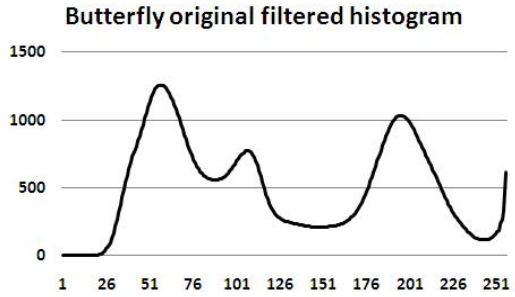

Figure 1. Example of the filtered histogram (image *butterfly* [20]).

On this histogram mentioned three well-defined peaks, therefore have two thresholds. Applying the Otsu method described below we achieved Th1=69 and Th2=141.

Figure 2. Original image *butterfly* [20] and segmented image (3 segments).

One of the reference segmentation methods on the histogram is Otsu's method. This method aims minimizing the intra-class variance. By default, the method is designed for image binarization, so obtaining of two classes (object and background), but the method can be adapted to obtain several classes.

Regions with a high homogeneity have low variance. For each threshold T (from 1 to 255) is calculated:

$$\sigma_W^2(t) = q_1(t)\sigma_1^2(t) + q_2(t)\sigma_2^2(t),$$

where t – the determined threshold, σ_i^2 – the variance of respective classes, $\sigma_W^2(t)$ – the weighted sum of variances of the two classes;
$q_1(t)$ and $q_2(t)$ are the probabilities of the two separate classes by the threshold t and are determined as the sum of the probability that the pixels of a class are a certain intensity (gray level) on the specified interval (from 1 to t for the first class and from t to the highest intensity – for the second):

$$q_1(t) = \sum_{i=1}^{t} P(i) \text{ and } q_2(t) = \sum_{i=t+1}^{I} P(i), \quad (1)$$

An implementation of Otsu's method can be found at http://www.mathworks.com/matlabcentral/fileexchange/26532-image-segmentation-using-otsu-thresholding/content/otsu.m.

t=85 t1=71, t2=136

a. b. c.

Figure 3. a) Test image *blood cells* [21]; b) binarized image (segmented with one threshold); c) segmented image with two thresholds (three segments).

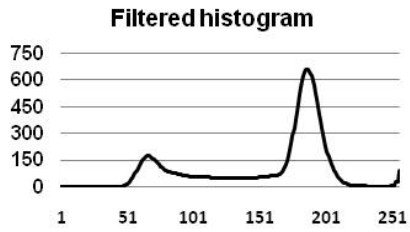

Figure 4. Filtered histogram of *blood cells* [21].

Many of the methods based on histogram, mentioned in the literature, refer to the binarization of the image that means determine a single threshold. Obviously for images containing multiple objects such methods are not effective, it is necessary to separate the image into as many

segments as many objects are in the picture, so *n* thresholds. Papamarkos N. and Gatos B. in "*A new approach for multithreshold selection*" (1994) are proposed a program that performs segmentation with multiple thresholds. Their method determines the histogram peaks (the maximum values), and finds the minimum between two maximums.

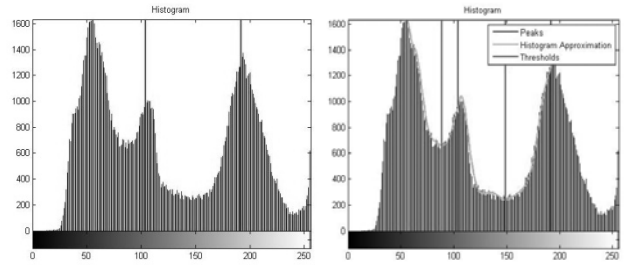

Figure 5. a) Maximums determination of the histogram (of image *butterfly* [20]); b) thresholds determination;

The irregular lighting influences the histogram: the peaks are not sharp and could not be separated by "valleys" they may look like in the figure below.

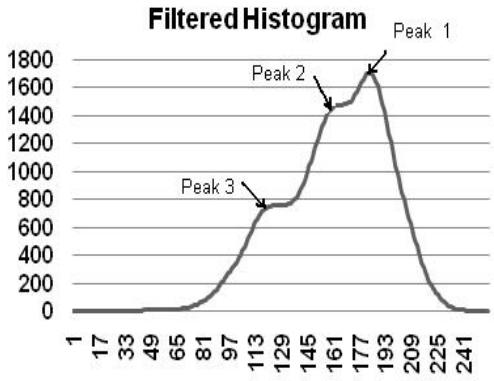

Figure 6. The test image #260058 [20] and the corresponding filtered histogram.

Notice in Figure 6 that histogram contains 3 Gaussians and the segmentation based on thresholds algorithm could detect only one (there peaks are not sharp and there are no "valleys"). In these cases it is recommended a Gaussian Mixture Model (GMM). This model is described in detail by Reynolds and Rose D.C. in "Robust Text-Independent Speaker Identification Using Gaussian Mixture Speaker Models". In the present work the authors refer to the model for acoustic signals. The model was taken over and implemented to the image segmentation, for example [22-23].

A Gaussian mixture model is a probability density function represented as a weighted sum of

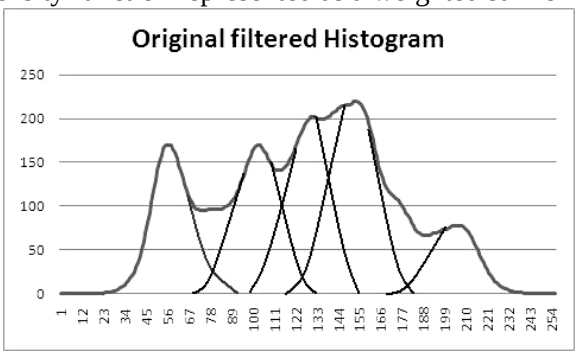

Figure 7. Gaussian Mixture Model (5 Gaussians)

$\boldsymbol{M}$ components with the Gaussian densities and can be written:

$$\boldsymbol{p}(\boldsymbol{x}\,|\,\lambda) = \sum_{\boldsymbol{i}=1}^{\boldsymbol{M}} \boldsymbol{w}_{\boldsymbol{i}}\, \boldsymbol{g}\left(\boldsymbol{x}\,|\,\boldsymbol{\mu}_{\boldsymbol{i}}, \sum_{\boldsymbol{i}},\right)$$

where $\boldsymbol{x}$ – represents a random vector with D dimension, $\boldsymbol{w}_{\boldsymbol{i}}$ where i=1,...M – the mixture weights and $\boldsymbol{g}\left(\boldsymbol{x}\,|\,\boldsymbol{\mu}_{\boldsymbol{i}}, \sum_{\boldsymbol{i}}.\right)$ – the components densities.

The components densities are the D- varied functions and can be expressed as:

$$\boldsymbol{g}\left(\boldsymbol{x}\,|\,\boldsymbol{\mu}_{\boldsymbol{i}}, \sum_{\boldsymbol{i}}.\right) = \frac{1}{(2\pi)^{\boldsymbol{D}/2}\,|\sum_{\boldsymbol{i}}|^{1/2}} \times$$

$$\times \exp\left\{-\frac{1}{2}(\boldsymbol{x}-\boldsymbol{\mu}_{\boldsymbol{i}})' \sum_{\boldsymbol{i}}^{-1} (\boldsymbol{x}-\boldsymbol{\mu}_{\boldsymbol{i}})\right\} \qquad (2)$$

with the average of distribution $\boldsymbol{\mu}_{\boldsymbol{i}}$ and covariance matrix $\sum_{\boldsymbol{i}}$. Mixtures weights must satisfy the condition $\sum_{\boldsymbol{i}=1}^{\boldsymbol{M}} \boldsymbol{w}_{\boldsymbol{i}} = 1$.

A Gaussian mixture model is considered complete if it is characterized by the average distributions, covariance matrix and the weights of all components. This model can be expressed as a function of the parameters listed above:

$$\lambda = \{\boldsymbol{w}_{\boldsymbol{i}}, \boldsymbol{\mu}_{\boldsymbol{i}}, \sum_{\boldsymbol{i}}\}, \qquad (3)$$

where $\boldsymbol{i} = 1,..., \boldsymbol{M}$.

GMM is poorly implemented in the image segmentation. Huang Z.K. and Chau K.W. [22] have developed an algorithm that can be applied only for bimodal histograms. Tang H. et al. [23]

believe that Gaussian mixture model based only on the distributions of intensity, is insufficient if the image is affected by noise. To solve this problem they propose a model that includes weight neighborhood (neighborhood weighted Gaussian mixture model). Experiments performed by the authors showed that their proposed method gets a better result in classification and is less affected by noise.

Completing the classical (basic) algorithms leads to better results.

A G-U-MM implementation is described in the article "Improved heterogeneous Gaussian and Uniform Mixed Models (G-U-MM) and Their use in Image Segmentation", authors Teodorescu H.N., Rusu M. sent to ROMJIST in May 2013. The flowchart of the developed algorithm is given below:

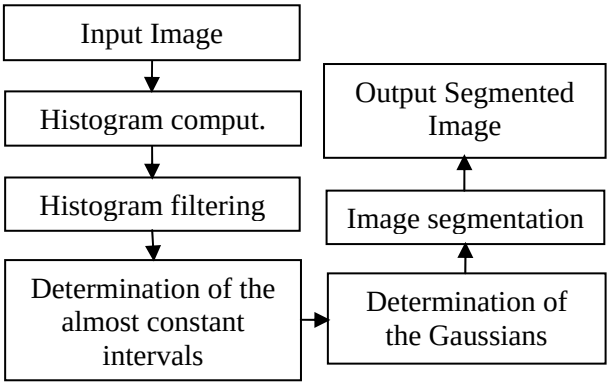

Figure 8. Flowchart of the proposed method used for image segmentation

The source code developed in C++ can be found at the address http://francophonie.utm.md/rusu_mariana/.

3. QUANTITATIVE QUALITY ASSESSMENT OF SEGMENTATION

Evaluation of segmentation is done either manually by experts, or by using machine account. Supervised evaluation (involving human factor) is the delineation of regions by experts and comparing the results with obtained results and after algorithms implementation.

http://www.eecs.berkeley.edu/Research/Projects/CS/vision/bsds/ site contains manually segmented images that can be used to assess the quality of segmentation.

This method is tedious and time consuming, so it tends to use quality assessment indices that would allow a non-supervised evaluation (without the involvement of experts).

In case of unsupervised evaluation is suggested more assessment metrics that would determine: the homogeneity of regions, the difference of averages between regions, the contrast between object and background, if too many or too few segments are obtained and others [24-26]. An important factor in quality assessing of segmentation is the evaluation of texture. Test images for this work do not contain textures, but the texture based segmentation is widely used in literature [27-28]. Sharma M., Markou M. and Singh S. analyse textural characteristics for precise regions determination [28]. An evaluation of the preliminary obtained results is described in the work "Quality Analysis of Image Segmentation based on G-UN-MMs", the authors Rusu M., Teodorescu H.N., presented at 2nd International Conference on Nanotechnologies and Biomedical Engineering, Chisinau, Republic of Moldova, April 2013.

A good segmentation evaluation method must be independent of the contents and types of image. It is necessary to determine most accurately the segmentation performance with minimal human involvement.

In order to make a comparison of the results using the proposed method with other methods from the literature, we primarily take into account the number of obtained segments. For each method the number of obtained segments should be the same for an objectively comparison.

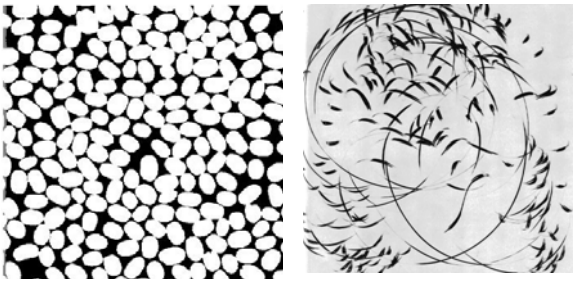

a. b.

Figure 9. Original synthetic images *D75* (a) and *D45* (b) [20].

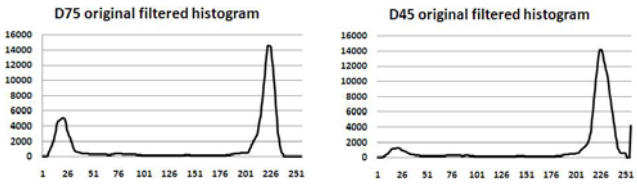

Figure 10. Original filtered histograms of synthetic images *D75* and *D45* [20].

We can observe that the histogram is composed of two Gaussians separated by one uniform distribution (3 segments). We need two thresholds.

The Multithresh (Papamarkos method) recommends other number of thresholds and we cannot make an objectively comparison between our (or Otsu) and this method because the number of obtained segments are different.

Table 1. Thresholds of synthetic images *D75*.jpg and *D45*.jpg

	*Thresholds of D75.jpg**
Multithresh	*0, 17, 73, 113, 153, 231, 255*
Otsu's method	*0, 25, 70, 255*
our method	*0, 54, 185, 255*
	*Thresholds of D45.jpg***
Multithresh	*0, 68, 81, 113, 152, 255*
Otsu's method	*0, 32, 76, 255*
our method	*0, 36, 185, 255*

* The recommended number of Thresholds is 6
** The recommended number of Thresholds is 5

In the literature are many quantitative objective evaluation methods [24-26], including:

- F, proposed by Liu and Yang;
- F′ and Q, proposed by Borsotti, Campadelli and Schettini;
- Intra-region uniformity criterion of Levine and Nazif;
- E – based on empirical analysis, proposed by Zhang et al.

The criteria we use are briefly presented below, paraphrasing the literature [24-26].

1) ***Liu and Yang's evaluation function***:

$$F = \sqrt{N}\sum_{j=1}^{N}\frac{e_j^2}{\sqrt{S_j}} \tag{4}$$

where N is number of obtained regions after segmentation, S_j – area of region j and e_j^2 – squared color error (or the gray level) that is calculated as

$$e_j^2 = \sum_{k\in S_j}(x_k - \bar{x})^2 \tag{5}$$

where x_k is the gray level of the pixel, and the $\bar{x}$ means gray level of the region.

We can observe that F is biased towards small numbers of segments or large numbers of small segments. F tends to zero when is over segmentation (F is 0 when the color error is zero for all segments, it is only when each pixel form its own region).

2) ***Borsotti, Campadelli and Schettini function*** **F′** to improve upon Liu and Yang's method:

$$F' = \frac{1}{1000\cdot S_I}\sqrt{\sum_{a=1}^{MaxArea}[N(a)]^{1+1/a}}\sum_{j=1}^{N}\frac{e_j^2}{\sqrt{S_j}}$$

were S_I – image surface;
$N(a)$ – denote the number of regions in the segmented image having an area exactly the size *a;*
MaxArea – the area of the largest region in segmented image.

F' is better than F when the segmentation has lots of regions consisting of small number of pixels.

3) ***Borsotti criterion***

$$Q = \frac{1}{10000\cdot S_I}\sqrt{N}\sum_{j=1}^{N}\left(\frac{e_j^2}{1+\log S_j}+\left(\frac{N(S_j)}{S_j}\right)^2\right) \tag{6}$$

were $N(S_j)$ – denote the number of regions in the segmented image having an area exactly S_j.

The segmentation with large numbers of regions is not penalized as heavily.

4) ***Intra-region uniformity criterion of Levine and Nazif*** [25]:

$$Lev = \sum_j\sum_{x\in R_j}\left(f(x)-\frac{1}{S_j}\sum_{x\in R_j}f(s)\right)^2 = \sum_j\frac{\sigma_j^2}{C} \tag{7}$$

$f(x)$ – the intensity of pixel x
C – normalized coefficient, equal to the maximum possible variance

$$C = \frac{(f_{\max}-f_{\min})^2}{2} \tag{8}$$

This criterion computes the sum of rapports between the normalized standard deviation of each region and the contrast of that region.

5) ***Entropy-based evaluation method*** [24]

As the authors say the entropy is a measure of the disorder within a region and is a natural characteristic to incorporate into a segmentation evaluation method.

The entropy for region *j* is defined as:

$$H_v(R_j) = -\frac{L_j(m)}{S_j}\log\frac{L_j(m)}{S_j} \tag{9}$$

where $L_j(m)/S_j$ represents the probability that a pixel in region R_j has a luminance value of m.

The notation $H_v(R_j)$ was simplified to

$H(R_j)$ with the default feature v being luminance. Zhang H. et al. define the expected region entropy of image I:

$$H_r(I) = \sum_{j=1}^{N} \left(\frac{S_j}{S_I} \right) H(R_j), \tag{10}$$

and the layout entropy:

$$H_l(I) = -\sum_{j=1}^{N} \left(\frac{S_j}{S_I} \right) \log \frac{S_j}{S_I}. \tag{11}$$

They propose to combine the both the layout entropy and the expected entropy measuring the effectiveness of a segmentation method:

$$E = H_l(I) + H_r(I). \tag{12}$$

For the natural images (standard test images), we determine the thresholds [see 29], that represent the limits of the Gaussian and uniform intervals, but we not obtained such good results as for synthetic images.

Table 2. Quantitative evaluation of the segmented image *butterfly* [20] using different methods.

The metrics	*Multithresh method*	*Otsu's method*	*Proposed method*
F	*333665*	*189539*	*278709*
F′	*0.0026*	*0.0015*	*0.0021*
Q	*0.0109*	*0.0040*	*0.0080*
Lev	*1.37*	*1.23*	*1.21*
E	*7.5*	*6.96*	*7.24*

For more details see [29]. Visually is difficult to assess which result of segmentation method is better, but the quantitative parameters show a difference.

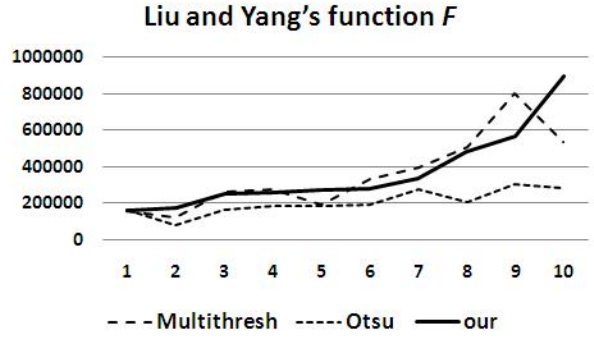

Figure 11. Representation of results using Liu and Yang's evaluation function.

According to the criterion of efficiency, the proposed method is a simple one, having a minimal resource consumption and fast computation. The results achieved are numerically close to those obtained with other more complex methods.

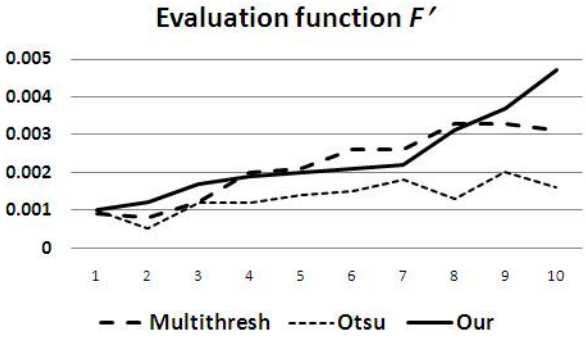

Figure 12. Representation of results using evaluation function F'.

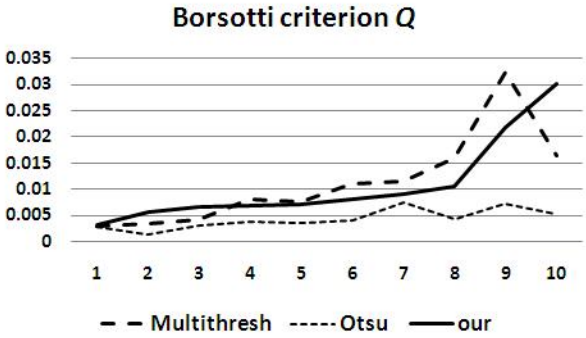

Figure 13. Representation of results using Borsotti criterion.

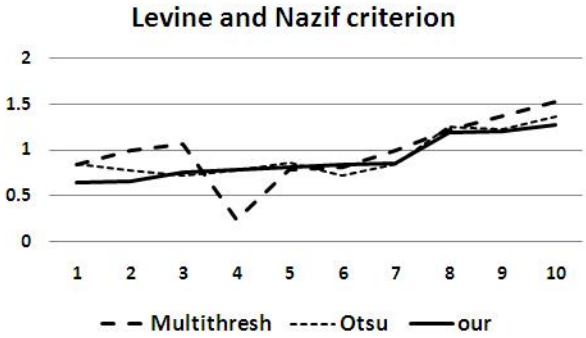

Figure 14. Representation of results using Levine and Nazif criterion.

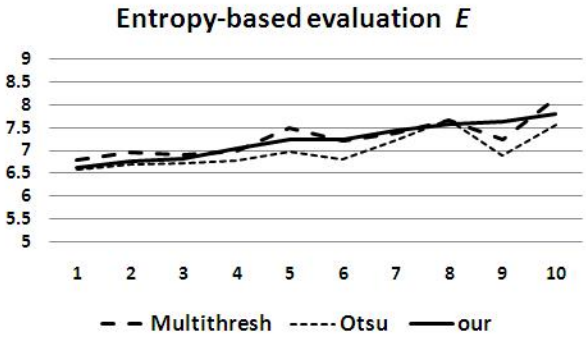

Figure 15. Representation of results using entropy-based evaluation method.

Therefore, we conclude that the method is effective and satisfactory.

The quality of the results indirectly validates the use of the Model of Mixtures of Gauss and Uniform Noises (G-UN-MM) proposed in our previous papers [18-19].

CONCLUSIONS

Segmentation is an essential step in image processing, of obtained results in this stage depends on interpretation quality of the scene by the computer (unsupervised method). Due to the many types of images (natural, SAR, medical) and the factors (irregular lighting, noise) that can influence the representation of objects in the scene was not yet developed an unique segmentation method that will produce satisfactory results for any type of image.

After preprocessing (filtering) we choose the segmentation method: pixel-based classification, edge based or regions based depending on the features required to extract: shapes, contours, regions, textures, text, etc. When choosing we consider the image type and the color spectrum. For example, the ultrasonic images are processed more complex methods using the wavelet. For the gray test images most effective (low complexity and fast computational) methods are based on pixel classification – thresholding and clustering; for the color images – regions based methods. Edge based methods are also widely used, because they are based on the determination of the color transition of values, which are effective for both cases.

Impulse noise (salt and pepper) influences greater the histogram based methods. All pixels with value 0 (black) are assigned of an area, and the pixels with the highest value (255 - white) on other areas. Another disadvantage of the histogram based methods is that the obtained segments are not adjacent homogeneous regions.

The edge based methods often get multiple or false contours. Because of irregular illumination (shadows, light spots) the edges of objects in the scene can be represented with dashed lines leading to erroneous interpretation of the scene.

Region-oriented segmentation methods are time consuming (each pixel in the image is compared to a randomly chosen pixel (germ) and check similarity to form homogeneous areas). It is more effective for color images.

The complexity of segmentation algorithm represents a compromise between the time spent on implementation and required accuracy of the results.

Bibliography

1. ***Souza, F., Valle, E., Chávez, G., Aráujo, A.,*** *Hue histograms to spatiotemporal local features for action recognition, Computer Vision and Pattern Recognition, Vol. 1, 4 pag., 2011*
2. ***Navon, E., Miller, O., Averbuch, A.,*** *Color image segmentation based on adaptive local thresholds, Image and Vision Computing, Vol. 23, pag. 69-85, 2005*
3. ***Suryanto, Kim, D.H., Kim, H.K., Ko, S.J.,*** *Spatial color histogram based center voting method for subsequent object tracking and segmentation, Image and Vision Computing, Vol. 29, pag. 850-860, 2011*
4. ***Bong, C.W., Rajeswari, M.,*** *Multi-objective nature-inspired clustering and classification techniques for image segmentation, Applied Soft Computing, Vol.11, pag. 3271-3282, 2011*
5. ***Chien, B.C., Cheng, M.C.,*** *A color image segmentation approach based on fuzzy similarity measure, IEEE, International Conference on Fuzzy Systems,* ***Vol.*** *1, pag. 449-454, 2002*
6. ***Sowmya, B., Rani, B.S.,*** *Colour image segmentation using fuzzy clustering techniques and competitive neural network, Applied Soft Computing, Vol. 11, pag. 3170-3178, 2011*
7. ***Murugesan, K. M., Palaniswami, S.,*** *Efficient colour image segmentation using multi-elitist-exponential particle swarm optimization, J. of Theoretical and Applied Information Technology, Vol. 18, No. 1, 2010, pp. 35-41*
8. ***Deng, Y., Manjunath, B. S., Shin, H.,*** *Color image segmentation, IEEE Computer Society Conference on Computer Vision and Pattern Recognition, Vol. 2, pag. 446-451, 1999*
9. ***Shih, F.Y., Cheng, S.,*** *Automatic seeded region growing for color image segmentation, Image and Vision Computing, Vol. 23, pag. 877-886, 2005*
10. ***Liu, L., Sclaroff, S.,*** *Region segmentation via deformable model-guided split and merge, Proc. Eighth IEEE International Conference on Computer Vision, Vol.1, pag. 98-104, 2001*
11. ***Ma, W.Y., Manjunath, B.S.,*** *EdgeFlow: A technique for boundary detection and image segmentation, IEEE Transactions on Image Processing, Vol. 9, No. 8, pag. 1375-1388, 2000*
12. ***Rao, S.R. and al.,*** *Natural image segmentation with adaptive texture and boundary encoding, Proceedings of the 9th Asian conference on Computer Vision, Vol. 1, pag. 135-146, 2009*
13. ***Angulo, J., Serra, J.,*** *Modelling and segmentation of colour images in polar representations, Image and Vision Computing, Vol. 25, pag. 475-495, 2007*

14. ***Nikolaev, D. P., Nikolayev, P.P.,*** *Linear color segmentation and its implementation, Computer Vision and Image Understanding, Vol. 94, pag. 115-139, 2004*

15. ***Haris, K. et al.,*** *Hybrid image segmentation using watersheds and fast region merging, IEEE Transactions on Image Processing, Vol. 7, No. 12, pag.1684 – 1699, 1998*

16. ***Kim, J.S., Hong, K.S.,*** *Color–texture segmentation using unsupervised graph cuts, Pattern Recognition, Vol. 42, pag. 735-750, 2009*

17. ***Verikas, A., Malmqvist, K., Bergman, L.,*** *Colour image segmentation by modular neural network, Pattern Recognition Letters, Vol. 18, No. 2, pag. 173-185, 1997*

18. ***Teodorescu, H.N., Rusu, M.,*** *Yet Another Method for Image Segmentation based on Histograms and Heuristics, Computer Science Journal of Moldova, Vol. 20, No. 2 (59), pag. 163-177, 2012*

19. ***Teodorescu, H.N., Rusu, M.,*** *Image Segmentation Based on G-UN-MMs and Heuristics - Theoretical Background and Results –" Proceedings of the Romanian Academy, Series A, Vol. 14, No. 1, pag. 78-85, 2013*

20. Berkeley Segmentation Dataset: Images, Available: http://www.eecs.berkeley.edu/Research/Projects/CS/vision/bsds/BSDS300/html/dataset/images.html

21. Test Image blood cells. Available: http://www.pudn.com/downloads58/sourcecode/math/detail206012.html

22. ***Huang, Z.K., Chau K.W.,*** *A new image thresholding method based on Gaussian mixture model, Applied Mathematics and Computation, Vol. 205, pag. 899–907, 2008*

23. ***Tang, H. et al.,*** *A vectorial image soft segmentation method based on neighborhood weighted Gaussian mixture model, computerized Medical Imaging and Graphics, Vol. 33, pp. 644–650, 2009*

24. ***Zhang H. et al.,*** *Image segmentation evaluation: A survey of unsupervised methods, Computer Vision and Image Understanding, Vol. 110, No.2, pag. 260–280, 2008*

25. ***Udupa K., et al.,*** *A framework for evaluating image segmentation algorithms, Computerized Medical Imaging and Graphics, Vol. 30, pag. 75–87, 2006*

26. ***Sezgin, M., Sankur, B.,*** *Survey over image thresholding techniques and quantitative performance evaluation, Journal of Electronic Imaging, Vol. 13, No. 1, pag. 146–165, 2004*

27. ***Ilea, D.E., Whelan P.F.,*** *Image segmentation based on the integration of colour – texture descriptors – A review, Pattern Recognition, Vol. 44, pag. 2479–2501, 2011*

28. ***Sharma, M., Singh, S.,*** *Evaluation of Texture Methods for Image Analysis, The Seventh Australian and New Zealand Intelligent Information Systems Conference, pp. 117-121, 2001*

29. ***Rusu, M., Teodorescu, H.N.,*** *Improved Heterogeneous Gaussian and Uniform Mixed Models (G-U-MM) and their use in Image Segmentation, Available: http://francophonie.utm.md/rusu_mariana/*

Recommended for publication: 12.02.2013.

ALGORITHM FOR LINEAR PATTERN SEPARATION

Dr.prof. V. Moraru, M. Rusu,
Technical University of Moldova

INTRODUCTION

The linear separation problem of data sets is an important concept in the data analysis. This theory is widely used and applied in many fields such as pattern recognition [1], decision making [2], disease diagnosis [3], biometrics [4], automatic document processing [5] and others.

For example, there are two sets of objects (attributes)

$$A = \{a^1, a^2, ..., a^m\}$$

$$B = \{b^1, b^2, ..., b^k\}$$

where a^i and $b^i \in R^n$ for $\forall i = 1, 2, ..., m$, $\forall j = 1, 2, ..., k$ and $A \cap B = \varnothing$.

The aim of the linear separation is to build a decision function of the form:

$$f(x) = w^T x - w_0$$

which divides the space into two subsets such

$$f(a^i) < 0 \text{ şi } f(b^i) > 0$$

where $\forall i \in A$ and $\forall j \in B$.

Here w is a column vector of R^n, and w_0 is a scalar: $w_0 \in R$. The symbol „T" means transposition operation, in this case all vectors are column vectors.

Separation (classification) can be formulated as a quadratic programming problem. In this paper we will discuss three models of linear separation. For one of these models we will introduce an effective procedure for numerically solving.

1. THE MODEL OF MAXIMUM SEPARATION [6]

We choose a hyperplane

$$w^T x - w_0 = 0 \qquad (1)$$

which maximizes the minimum distance from any point of the sets A and B. The distance from the point $z \in R^n$ to the hyperplane (1) is equal to

$$d(z) = \frac{f(z)}{\| w \|} = \frac{w^T z - w_0}{\| w \|}.$$

Here and below $\| . \|$ is the Euclidean norm. So

$$d(a^i) = \frac{w_0 - w^T a^i}{\| w \|},$$

$$d(b^i) = \frac{w^T b^i - w_0}{\| w \|},$$

$$d_{\min} = \min\{d(a^1), d(a^2), ..., d(a^m), d(b^1), ..., d(b^k)\}.$$

The problem consists in maximizing the size $d_{\min}$ which is equivalent to the following problem:

$$\left.\begin{array}{l} \delta \to \min \\ \text{subject to} \\ w_0 - w^T a^i \ge \delta \| w \|, i = 1,2,...,m \\ w^T b^i - w_0 \ge \delta \| w \|, i = 1,2,...,k. \end{array}\right\} \qquad (2)$$

The problem (2) is a nonlinear problem (non-convex) towards the unknowns

$$\delta \in R, \; w_0 \in R, \; w \in R^n.$$

We impose the following restriction: $\| w \| = 1$. Then, introduce the variables

$$u = \frac{w}{\delta} \in R^n \text{ and } v = \frac{w_0}{\delta} \in R,$$

problem (2) is equivalent to the following problem:

$$\left.\begin{array}{l} \frac{1}{2} u^T u \to \min \\ \text{subject to} \\ [b^i]^T u - v \ge 1, i = 1,2,...,k, \\ -[a^i]^T u + \delta \ge 1, i = 1,2,...,m, \\ u \in R^n, v \in R. \end{array}\right\} \qquad (3)$$

The problem (3) is a convex quadratic programming problem with $(n+1)$ variables and $(m+k)$ linear constraints. If $u^* \in R^n$ and $v^* \in R$ is an optimal solution of problem (3), then the solution of (2) is:

$$w^* = \frac{u^*}{\| u^* \|}, w_0^* = \frac{v^*}{\| u^* \|}, \delta^* = \frac{1}{\| u^* \|}.$$

The vector w^* is perpendicular to the considered hyperplane and has a length equal to 1,

and the size w_0^* is shortest distance between the hyperplane and origin of the coordinate system.

2. SUPPORT VECTOR MACHINES (SVM) [7]

In this method the elements of set A are labeled with $t=-1$, and the elements of set B with $t=1$. In other words,

$$t(x)=\begin{cases}-1, \text{if } f(x)<0,\\ +1, \text{if } f(x)>0,\end{cases}$$

i.e.

$$\left.\begin{aligned} w^T x - w_0 < 0, \text{if } t(x)=-1,\\ w^T x - w_0 > 0, \text{if } t(x)=+1\end{aligned}\right\} \quad (4)$$

We note that the hyperplane (1) does not change if w and w_0 are multiplied by the same positive constant. It is convenient to choose this constant such bellow

$$\left.\begin{aligned} w^T a^i - w_0 = -1, i=1,2,...,m,\\ w^T b^i - w_0 = +1, i=1,2,...,k.\end{aligned}\right\}$$

Thus, taking into consideration the (4) we can write

$$t(x^i)(w^T x^i - w_0) \geq 1, \forall x^i \in A \cup B.$$

Determination of the optimal separating hyperplane is reduced to solving the problem:

$$\left.\begin{aligned} &\frac{1}{2} w^T w \to \min\\ &\text{subject to}\\ &t(x^i)(w^T x^i - w_0) \geq 1, \forall x^i \in A \cup B.\end{aligned}\right\} \quad (5)$$

The problem (5) is similar to the problem (3). The constraints of (5) ensure that in the optimal solution w^*, w_0^* we have:

$$f(x^i)=\begin{cases}+1, \text{for } t(x^i)=1,\\ -1, \text{for } t(x^i)=-1.\end{cases}$$

3. REFORMULATING THE PROBLEM IN THE TERMS OF THE CONVEX QUADRATIC PROGRAMMING

Let the convex hulls of the sets A and B:

$$conv(A)=\left\{x : x=\sum_{i=1}^{m}\alpha_i a^i, \sum_{i=1}^{m}\alpha_i = 1, \alpha_i \geq 0, i=1,2,...,m\right\}$$

$$conv(B)=\left\{y : y=\sum_{i=1}^{k}\beta_i b^i, \sum_{i=1}^{k}\beta_i = 1, \beta_i \geq 0, i=1,2,...,k\right\}$$

Then the problem of optimal separation of the sets A and B can be formulated as:

$$\left.\begin{aligned} &\frac{1}{2}\| x-y \|^2 = \frac{1}{2}(x-y)^T(x-y) \to \min\\ &\text{subject to}\\ &\sum_{i=1}^{m}\alpha_i = 1, \alpha_i \geq 0, i=1,2,...,m,\\ &\sum_{i=1}^{k}\beta_i = 1, \beta_i \geq 0, i=1,2,...,k.\end{aligned}\right\} \quad (6)$$

Let the matrices $U_{m\times m}, V_{k\times k}$ and $Z_{m\times k}$ defined in the following way:

$$U_{m\times m}=\begin{pmatrix} (a^1,a^1) & (a^1,a^2) & ... & (a^1,a^m)\\ (a^2,a^1) & (a^2,a^2) & ... & (a^2,a^m)\\ ... & ... & ... & ...\\ (a^m,a^1) & (a^m,a^2) & ... & (a^m,a^m)\end{pmatrix}$$

$$V_{k\times k}=\begin{pmatrix} (b^1,b^1) & (b^1,b^2) & ... & (b^1,b^k)\\ (b^2,b^1) & (b^2,b^2) & ... & (b^2,b^k)\\ ... & ... & ... & ...\\ (b^k,b^1) & (b^k,b^2) & ... & (b^k,b^k)\end{pmatrix}$$

$$Z_{m\times k}=\begin{pmatrix} (a^1,b^1) & (a^1,b^2) & ... & (a^1,b^k)\\ (a^2,b^1) & (a^2,b^2) & ... & (a^2,b^k)\\ ... & ... & ... & ...\\ (a^m,b^1) & (a^m,b^2) & ... & (a^m,b^k)\end{pmatrix}$$

Also note

$$\gamma=(\alpha_1,\alpha_2,...,\alpha_m,\beta_1,\beta_2,...,\beta_k)^T \in R^{m+k},$$

$$Q=\begin{pmatrix} U_{m\times m} & -Z_{m\times k}\\ -Z^T_{k\times m} & V_{k\times k}\end{pmatrix},$$

$$B=\begin{pmatrix} \underbrace{1\ 1\ ...\ 1}_{m\ ori} & \underbrace{0\ 0\ ...\ 0}_{m\ ori}\\ \underbrace{0\ 0\ ...\ 0}_{k\ ori} & \underbrace{1\ 1\ ...\ 1}_{k\ ori}\end{pmatrix},$$

$$e=\begin{pmatrix}1 & 1^T\end{pmatrix}.$$

The matrices $U_{m\times m}$, $V_{k\times k}$ and Q are positive semidefined.

With these notations the problem (6) becomes:

$$\left.\begin{array}{l} \dfrac{1}{2}\gamma^T Q\gamma \to \min \\ \text{subject to} \\ B\gamma = e, \\ \gamma \geq 0. \end{array}\right\} \quad (7)$$

Note that the objective function depends only on the scalar product of the vectors a^i and b^j. The problem (7) is a convex programming problem and therefore it has a global optimal solution.

4. SVM AS A PROBLEM TO SOLVE A SYSTEM OF EQUATIONS

Using Kuhn-Tucker theorem, it demonstrates that the dual problem (5) is:

$$\left.\begin{array}{l} \dfrac{1}{2}\gamma^T Q\gamma - \sum\limits_{i=1}^{m+k}\gamma_i \to \min \\ \text{subject to} \\ \sum\limits_{i=1}^{m+k} t(x_i)\gamma_i = 0, \\ \gamma_i \geq 0, \forall i = 1,2,\ldots,m+k. \end{array}\right\} \quad (8)$$

The vectors a^i, b^i *which* $\gamma_i > 0$ are called support vectors.

It is noted that the problems (7) and (8) give one and the same results. In the following we will show how the problem (7), which is equivalent to the problem (8) can be reduced to solving a quadratic equation system.

If $\gamma^* \in R^{m+k}$ is an optimal solution of the problem (7) then there is $\lambda^* \in R^2$ such that [8]:

$$\left.\begin{array}{l} B\gamma^* = e, \\ \Gamma^*\left(Q\gamma^* + B^T\lambda^*\right) = 0, \\ \gamma_i^* = 0 \Rightarrow \left[Q\gamma^* + B^T\lambda^*\right]_i \geq 0, \forall i. \end{array}\right\}$$

where $\Gamma = Diag(\gamma)$ is a diagonal matrix:

$$\Gamma = \begin{pmatrix} \gamma_1 & \cdots & 0 \\ \vdots & \ddots & \vdots \\ 0 & \cdots & \gamma_{m+k} \end{pmatrix},$$

and the notation $[c]_i$ here and further mean the component i of the vector c.

Note the $G = Diag\left(Q\gamma + B^T\lambda\right)$ and

$$F(\gamma,\lambda) = \begin{pmatrix} \Gamma\left(Q\gamma + B^T\lambda\right) \\ B\gamma - e \end{pmatrix}.$$

Such the problem (7) is reduced to solve the system of equations and inequalities:

$$\left.\begin{array}{l} F(\gamma,\lambda) = 0, \\ \gamma \geq 0, G \geq 0. \end{array}\right\}$$

Theorem. *For* $\forall\gamma \in D = \{\gamma : B\gamma = e, \gamma \geq 0\}$ *the Jacobian matrix*

$$\nabla F = \begin{pmatrix} G + \Gamma Q & \Gamma B^T \\ B & 0 \end{pmatrix}$$

is non-singular.

Demonstration of this theorem is analogous of proof the **Theorem 1** from [9].

We define now the functions $p, q : R \to R_+$:

$$p(x) = x^2 \max(0,x) = \frac{1}{2}\left(x^3 + |x|x^2\right),$$

$$q(x) = -x^2 \min(0,x) = -\frac{1}{2}\left(x^3 - |x|x^2\right).$$

The functions $p(x)$ and $q(x) = p(-x)$ are twice continuously differentiable:

$$p'(x) = \frac{3}{2}\left(x^2 + |x|x\right), p''(x) = 3\left(x + |x|\right),$$

$$q'(x) = \frac{3}{2}\left(-x^2 + |x|x\right), q''(x) = 3\left(-x + |x|\right).$$

It is easily established that:

1. $\left\{\begin{array}{l} p(x)q(x) = 0, p'(x)q'(x) = 0, \\ p''(x)q''(x) = 0, \forall x \in R. \end{array}\right.$

2. $\left\{\begin{array}{l} p(x) + q(x) > 0, p'(x) + q'(x) \neq 0, \\ p''(x) + q''(x) > 0, \forall x \neq 0. \end{array}\right.$

3. $\left\{\begin{array}{l} p(x) = 0 \text{ if and only if } p'(x) = 0, \\ q(x) = 0 \text{ if and only if } q'(x) = 0. \end{array}\right.$

Considering this and introducing auxiliary variables $\eta_1, \eta_2, \ldots, \eta_m$, $\mu_1, \mu_2, \ldots, \mu_k$, λ_1 and λ_2 the problem (7) can be reduced to solve a system of $2(m+k+1)$ equations with same number of unknowns [9]:

$$\left.\begin{array}{l} p(\eta_i)=\alpha_i . i=1,2,\ldots,m, \\ q(\eta_i)=\left[U_{m\times m}\alpha - Z_{m\times k}\beta+\lambda^1\right]_i, \\ i=1,2,\ldots,m, \\ p(\mu_i)=\beta_i, i=1,2,\ldots,k, \\ q(\mu_i)=\left[-Z_{m\times k}\alpha + V_{k\times k}\beta+\lambda^2\right]_i, \\ i=1,2,\ldots,k, \\ B\gamma=e. \end{array}\right\} \quad (9)$$

This was noted as follow:

$$\lambda^1=(\lambda_1,\lambda_1,\ldots,\lambda_1)^T\in R^m,$$
$$\lambda^2=(\lambda_2,\lambda_2,\ldots,\lambda_2)^T\in R^k.$$

The system (9) may be reduced to the $(m+n+2)$ equations with the $(m+n+2)$ unknowns, replacing the vectors α and β using functions p and q:

$$\alpha=(p(\eta_1),p(\eta_2),\ldots,p(\eta_m))^T,$$
$$\beta=(p(\mu_1),p(\mu_2),\ldots,p(\mu_k))^T.$$

The best-known method for solving nonlinear systems of equations (9) is the Newton method [10]. Newton's method has very attractive theoretical and practical properties, because of its fast convergence: under the nonsingularity of the Jacobian matrix it will converge locally superlinearly.

Let be

$$\alpha^*=(\alpha_1^*,\alpha_2^*,\ldots,\alpha_m^*)^T$$

and

$$\beta^*=(\beta_1^*,\beta_2^*,\ldots,\beta_k^*)^T$$

the optimal solution of problem (8). When the decision function is given by:

$$f(x)=\frac{2}{\left\|x^*-y^*\right\|^2}\left[(x^*-y^*)x-\left\|x^*\right\|^2+\left\|y^*\right\|^2\right],$$

where

$$x^*=\sum_{i=1}^{m}\alpha_i^* a^i,\ y^*=\sum_{i=1}^{k}\beta_i^* b^i.$$

5. CONCLUSIONS

In this paper we presented an overview of mathematical problem separating two data sets. The classification methods are based on search for an optimal hyperplane which separates the considered data. A special place is occupied by SVM introduced in 1995 by Vladimir Vapnik and discussed in the literature by many researchers [11].

Here was introduced reformulation of Kuhn-Tucker optimality conditions in an equivalent system of smooth linear equations (cubic). The system of equations can be solved efficiently using Newton method. In the neighborhood of the optimal solution γ^* the rate of convergence of Newton's sequence is superlinear. The numerical examples clearly show that the proposed method is promising.

Bibliography

1. ***Mangasarian, O. L.*** *Linear and nonlinear separation of patterns by linear programming. Operations Research, Vol. 13, Nr. 3, pag. 434-452, 1965.*

2. ***Viveros, M. S., Nearhos, J. P.,*** *and* ***Rothman, M. J.****, Applying Data Mining Techniques to a Health Insurance Information System. Proc. of the 22th International Conference on Very Large Data Bases (VLDB '96), pag. 286-294, 1996.*

3. ***Mangasarian, O. L., Street, W. N.*** *and* ***Wolberg, W. H.*** *Breast Cancer Diagnosis and Prognosis via Linear Programming, Operations Research, Vol. 43, No. 4, pag. 570-577, 1995.*

4. ***Ferreira, C.*** *Gene Expression Programming: Mathematical Modeling by an Artificial Intelligence. Springer Verlag, 478 pag., 2006.*

5. ***Merrikh-Bayat, F., Babaie-Zadeh, M.,*** *and* ***Jutten, C.*** *Linear-quadratic blind source separating structure for removing show-through in scanned documents, International Journal on Document Analysis and Recognition (IJDAR), Vol. 14, No.4, pag. 319-333, 2011.*

6. ***Freund, R. M.*** *Pattern Classification, and Quadratic Problems, Massachusetts Institute of Technology, 2004.*

7. ***Vapnik, V.*** *The nature of statistical learning theory, Springer-Verlag, New York, 1995.*

8. ***Gill, P. E., Murray, W.,Wright, M. H****. Practical Optimization, Academic Press, London,1981.*

9. ***Moraru, V.,*** *A Smooth Newton Method for Nonlinear Programming Problems with Inequality Constraint, Computer Science Journal of Moldova, Vol. 19, Nr. 3 (57), pag. 333-353, 2011.*

10. ***Ypma, T. J.*** *Historical development of the Newton-Raphson method, SIAM Review, Vol. 37, No. 4, pag. 531-551, 1995.*

11. ***Byun, H., Lee, S. W.,*** *Applications of Support Vector Machines for Pattern Recognition: A Survey, Pattern Recognition with Support Vector Machines, Vol. 2388, pag. 213-236, 2002.*

Recommended for publication: 11.03.2013.

APPLICATION OF THE METHOD OF QUALITY FUNCTIONAL DEPLOYMENT WHEN DEVELOPING A NEW EXTRUDED PRODUCT

PhD assistant professor M.R. Mardar
Odessa National Academy of Foods Technologies

During the new product creation the researcher quite often bases on the subjective judgment and it sometimes leads to appearance of the product on the market which doesn't meet the requirements of the customers. One of the perspective directions in the field of creation of a new food product is application and adaptation of the modern instruments and methods of quality management, such as methodology of QFD (Quality Function Deployment) [1, 2]. The above - mentioned method was developed at the end of 1960-s in Japan. Its aim is to provide customers′ demands when planning and designing the products and when designing the technology of making and producing of the production as well. The first ideas, stated concerning the questions of quality, connecting the parameters of a product quality and the process of its creating with the customers expectations, were practically realized in Bridge stone Tire and Matsushita Electric at the end of 1966 and got the name "*Quality Assurance Plan*". The first table of quality in the form of a matrix diagram was developed in 1972 in Mitsubishi Heavy Industries. We should take into account that the greatest contribution into the new methodology development was made by Iy. Akao, S. Mizuno who published the book with the title "*Quality Function Deployment: the approach to the General quality control*" [3, 4]. Since this moment the development of QFD methodology development according to distribution of the general Quality management, has begun.

Application of QFD method for constructing the new food product is based on receiving the consumers' demands for the new product, revealing the most important and perspective from them and transferring of the given demands into the quantitative technical characteristics of the product. The peculiarity and advantage of this method application is contained in getting not only stated during the public- opinion poll demands for the product but also unacknowledged demands, fulfillment of which will allow the enterprise to offer the customer the goods with the unique characteristic and to win the struggle witch competitors [5].

The main instrument, when using the given method, is building of a correlation matrix, with the help of which the QFD team, consisting of the specialists of different profiles, makes estimations at different stages of the research. All the results of the similar estimations can be brought together into one and the same table. The visual proof of the method made it popular under the title "*Quality House*", in which every element of the "*House*" represents the results of one of the conducted stages of the new product development [1, 2]. The given method includes application of a number of other quality instruments, such as an affinity diagram, a tree - like diagram, benchmarking methods and others. The customers demands for the product quality are developed by stages, beginning witch determining of the product necessity on the market and ending with the ways of quality control. The final estimation of the project concerning the product development belongs to the customer, that's why it′s particularly important that during all the work at the project the consumers should directly or indirectly take part in the work.

Application of the structuring method of Quality function at all the stages of production creating allows to realize such most important principles of quality management, as catering for the consumer and making decisions, based on the facts obtained. Structuring of Quality function also provides realization of quality conception, which proclaims Total Quality Management (TQM) - one should not correct a drawback (a fault) but prevent it.

The new product development when using QFD method includes the following stages[1]:

- ✓ collecting of the information:
- ✓ the information processing:
- ✓ generalization and structuring of the consumers' demands
- ✓ prioritization of the customers' demands
- ✓ building of "Quality house"
- ✓ development of the new product conception
- ✓ development of the technical task for the product.

Application of the given method for creating the new food product, and particularly in our case,

the extruded product, should end in development of the technical task and approval of the recipes. At the first stage of QFD – the analysis during selective investigation, "*the consumers' voice*" was determined. The consumers' estimation is a necessary stage of the new product development. It allows to reveal the most preferable sample and to determine if it corresponds to the conception and if it needs some changes [1, 2]. For collecting the information, the written questionnaires of the respondents were used. The answers to the open question "*Please, make up a list of your wishes concerning the extruded product quality*", allowed to determine the list of the consumers' demands for the expected production. At this stage of the information processing the methods of composing "*The consumers' voice*" table, were used. In this table the consumers' demands were specified, simplified and concretized. Generalization and structuring of the consumers' demands were carried out with the help of two quality instruments: an affinity diagram and a tree - like diagram. When using the affinity diagram the demands were distributed by relative groups and then were generalized. As a result of carrying out of this procedure the amount of demands essentially decreased, because the identical demands were deleted and the similar ones were generalized. The given demands then were divided with the help of the tree-like diagram into the implied stated and unrealized demands. Application of the tree-like diagram gives an opportunity to reveal the secret, unrealized consumer′s wishes. Fulfillment of such demands helps the researcher to leave the competitors behind and to increase the audience having a special purpose. The demands for safety and normative documents for the product, which must be followed by all means, should be concerned to the implied demands for the food product. Eventually the consumer's′ demands for the extruded product have been determined: a pleasant taste, crunching structure, high nutritional value, being natural, presence of the biologically active substances (BAS), a low calorie content, being healthy, a reasonable price.

At the stage of prioritization of the consumers' demands, the repeated address to the consumers′ demands are always contradictory and it′s impossible to create the production, which would meet all the consumers' demands. As a result it is necessary to have a clear idea about the demands which must be satisfied by all means and the demands which can be neglected to a certain degree. To answer these questions it′s necessary to regulate the list of the consumers′ demands by the degree of importance. So further questioning was directed to determination of the importance factors of consumers′ preferences indices by a five-mark scale, namely: 5 - very valuable, 4 - valuable, 3- less valuable but it would be nice to have it, 2 - not very valuable, 1 - isn′t valuable. By the consumers' demands rating it has been stated that the most important things for the consumers' of the extruded product are its pleasant taste and crunching structure, being healthy, being natural, high nutritional value, presence of BAS and, of course, reasonable price. The results of the consumers' demands, their priorities are included in the special columns of "*Quality House*" (fig. 1).

After finishing of the stage, connected with visualization and estimation of importance of the consumers' expectations, it was necessary to solve guaranteeing of the given expectations fulfillment in practice. With this purpose, on the basis of studying of the normative and technical documents, we have determined the technical characteristics of the extruded product, which are connected with wishes and expectations of the consumers' and are included into the "top" of Quality house, namely: mass protein portion, mass starch portion, mass cellulose portion, BAS content, applying additives, energy value, mass moisture portion, coefficient of outburst, mass by volume, the expiration date, safety indices, preventive properties, price.

In the central "*room*" of Quality House, the conventional signs of the quantities of the correlation coefficient between the consumers' demands and technical characteristics of the product are included. For every characteristic the criterion, taking into account meanings of the correlation coefficients of the particular characteristic and the demands priority, put forward by the consumers', was calculated. As it turned out, transformation of the consumers' demands into the technical characteristics has shown, that formation of gustatory characteristics of the product depends on the chemical composition of the extruded product, namely on BAS content (in this case on presence of aroma forming compounds), on the amount of the additives introduced, the product′s being healthy depends, first, on the chemical composition of the product, on the amount of the included additives and presence of the preventive properties of the finished product. Also the expiration date, energy value of the finished products directly influences the products being healthy.

During the correlation matrix building, so called "*the roof of the house*", the relations of quantitatively measured quality indices between one another, have been filled in; and the directions of

their change for providing the necessary meanings of the consumers′ demands, have been determined.

The results of the benchmarking have been put down into the "*veranda*" of Quality House. The purpose of conducting of the benchmarking is determining of the degree of the competitors′ demands, revealing of strong and weak points of the competitive organizations and discovery of the real possibilities for "*break - through*" improvement of the own product [5].

As a result the understanding has been achieved concerning the fact: to what degree the product, developed by us, is perfect in comparison to the best analogues of the competitive companies.

In this case the expert method has also been used and a five - mark scale from "*a bed mark*" to "*an excellent mark*", has also been used, namely 5 - excellent; 4 - good; 3 satisfactory (mainly corresponds); 2 - barely satisfactory (corresponds partly); 1 - badly (doesn't correspond to expectations). The results of such comparison are presented in the "*veranda*" of Quality House. The extruded product of the famous trade company "*Corn figured items with bacon taste*", has been chosen as a competitive product.

When filling the "*basement*" of Quality House the priority of the developed product was calculated (estimated). Generalizing the data concerning strength of the connection between the technical characteristics of grain bread and the consumers′ demands, taking into the account the importance of the latter ones, the priority of optimization of the recipe composition of the extruded product, has been determined. As it has been shown, it′s first necessary to provide the preventive direction of the new developed product at the expense of introduction of the natural additives into its composition as well as to provide the increased BAS content and it′s necessary to pay special attention to the product safety indices.

So, application of the methods of quality function deployment allowed to reveal the most important characteristics of the extruded product for the consumer, to determine the correlation between the priorities of the consumers and the technical characteristics of the product, and further on it will be taken into account when developing the technical task and recipe composition of the new product with the aim of providing its competitive advantages.

Bibliography

1. Ponomaryov S.V. *Upravlenie kachestvom produkczii. Instrumenty I metody menedzhmenta kachestva/S.V. Ponomaryov, S.V. Mishhenko, B.Ya.Belobragin, V.A. Samorodov I dr. M.:RIA "Standarty I kachestvo". 2005. 248 s.*

2. Suvorova L.A. *Primenenie metodologii QFD I statisticheskih metodov d upravlenii kachestvom produkczii na promyshlennom predpriyatii/ L.A. Suvorova, R.P. Czvirov //Kachestvo, innovaczii, obrazovanie. 2005. №2. S.72-78.*

3. Akao Y. *Quality Function Deployment (QFD). Integrating customer requirements into product design. – Portland, OR: Productivity Press, 1990. – 369 p.*

4. Misuno, S. *QFD. The customer-driven approach to quality planning and deployment/S. Misuno, Y. Akao.- Tokyo, Japan: Asian Productivity Organization, 1994. – 365p.*

5. Matison V.A. *Primenenie metoda razvyortyvaniya funczii kachestva dlea konstruirovaniya produlta v pishhevoj promyshlennosti //V.A. Matison, N.A. Demidova. //Pishhevaya promyshlennost'. 2012. №4. S.44–45.*

Recommended for publication: 22.03.2013.

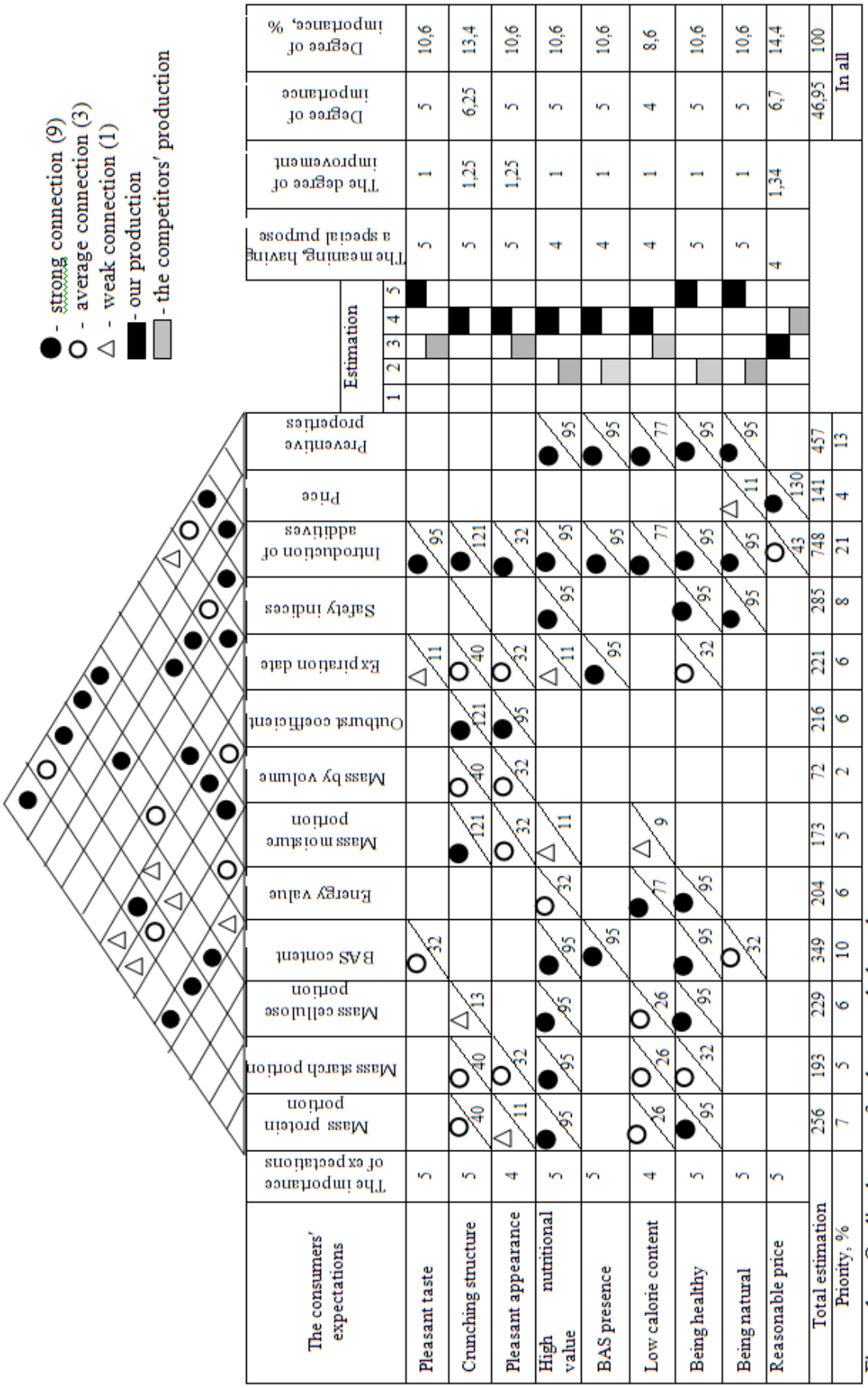

The consumers' expectations	The importance of expectations	Mass protein portion	Mass starch portion	Mass cellulose portion	BAS content	Energy value	Mass moisture portion	Mass by volume	Outburst coefficient	Expiration date	Safety indices	Introduction of additives	Price	Preventive properties	Estimation 1	2	3	4	5	The meaning, having a special purpose	The degree of improvement	Degree of importance	Degree of importance, %
Pleasant taste	5				○ 32					△ 11		● 95								5	1	5	10,6
Crunching structure	5	○ 40	○ 40	△ 13			● 121	○ 40	● 121	○ 40		● 121						■		5	1,25	6,25	13,4
Pleasant appearance	4	△ 11	○ 32				○ 32	○ 32	● 95	○ 32		● 32						■		5	1,25	5	10,6
High nutritional value	5	● 95	● 95	● 95	● 95	○ 32	△ 11			△ 11	● 95	● 95		● 95				■		4	1	5	10,6
BAS presence	5				● 95					● 95		● 95		● 95				■		4	1	5	10,6
Low calorie content	4	○ 26	○ 26	○ 26		● 77	△ 9					● 77		● 77				■		4	1	4	8,6
Being healthy	5	● 95	○ 32	● 95	● 95	● 95				○ 32	● 95	● 95		● 95					■	5	1	5	10,6
Being natural	5				○ 32						● 95	● 95	△ 11	● 95					■	5	1	5	10,6
Reasonable price	5											○ 43	● 130						■	4	1,34	6,7	14,4
Total estimation		256	193	229	349	204	173	72	216	221	285	748	141	457								46,95	100
Priority, %		7	5	6	10	6	5	2	6	6	8	21	4	13								In all	

Figure 1 - «Quality house» for the extruded product

Figure 1. «*Quality house*» for the extruded product.

VIBRATION ON THE TURBO-GENERATOR AT THE SMALL POWER PLANT

D. Oprea, PhD student
Czech Technical University

INTRODUCTION

All rotating equipment vibrates to some degree, but as older bearings and components reach the end of their product life, they begin to vibrate more dramatically and in distinct ways. Ongoing monitoring of equipment allows these signs of wear and damage to be identified well before the damage becomes an expensive problem. In this article we intend to analyze the importance of vibration measurement at the hydro-electrical power plant.

1. VIBRATION FOR TURBINE GENERATOR SHAFT

Vibration of turbine-generator shaft occurs due to the disturbance of electric power system. The coupling interaction between disturbance of electric power system and vibration of shafts makes turbine-generator oscillate. Alternating stress due to large vibration decreases the life of shafts, even results in shaft broken. It is very important in time to do the measurement and analyzes of the system condition [2].

Power plant turbo-generator sets should run around the clock – not only to keep power flowing but also to improve the machinery´s life expectancy, which is shortened every time machines are started up and shut down. While it is unfortunate when a turbo-generator set needs to be shut down for diagnosis or due to excessive vibration, it is entirely futile if no faults are subsequently found.

In the fig. 1 is illustrate the cross-section view of a generating unit.

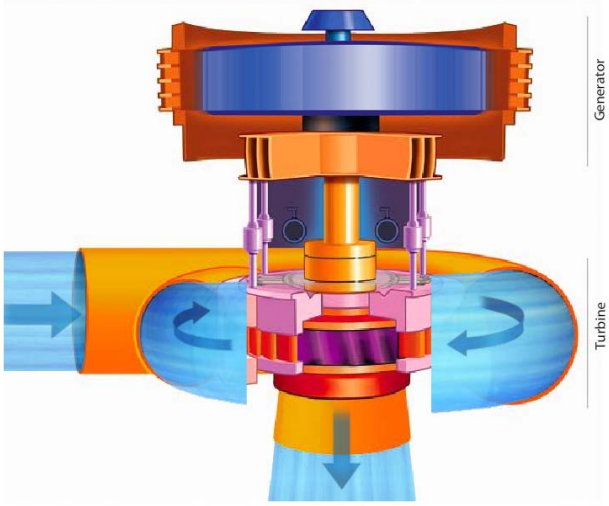

Figure 1. Cross-section view of a generating unit, update 10.04.13[1].

2. EXAMPLE

Decrease downtime and increase savings, is generically known as condition monitoring. When used correctly, it can result in huge cost savings compared to traditional maintenance methods.

Traditional maintenance methods are preventive - Components are replaced according to a fixed schedule whether worn or not. Traditional

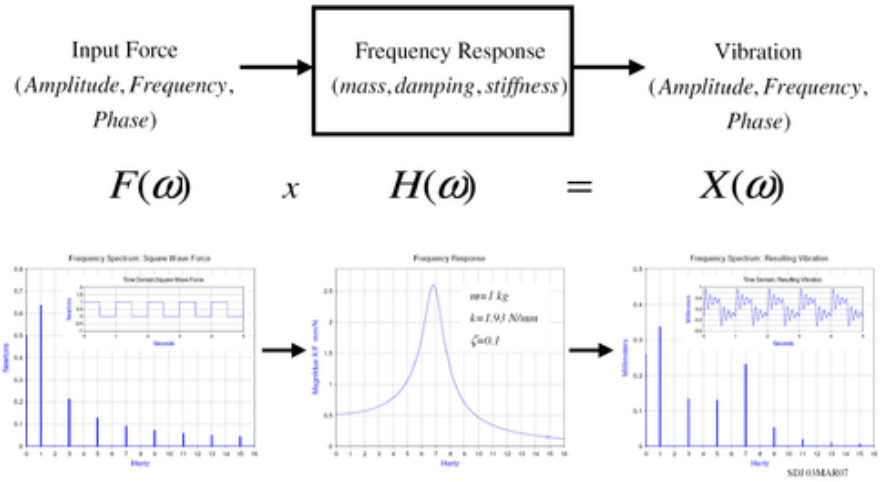

Figure 2. Frequency response model, update 10.03.13.

maintenance methods are also reactive, repairing components only after they have broken down.

Neither of these methods is ideal, although both are very common throughout the heavy industry sector, and both tend to incur much higher costs than methods that use vibration analysis.

3. USED STANDARDS

For evaluate the results at the Hydro electrical Power Plant from Czech Republic, the real data was according to the standard ČSN ISO 10816 – 3, for the power equipment from 300 kW to 50 MW:

Table 1. Standard ČSN ISO 10816 – 3.

Categories	V_{ef} (mm/s)
A/B	2,3
B/C	4,5
C/D	7,1

Categories:

A – this class is characteristic for a new installations.

B – installations, whose vibrations are placed in these limits are characteristic by a long time of function.

C – installations, whose vibrations are placed in these limits are considered dangerous in function/running for a long time.

D – installations, whose vibrations are placed in these limits are considered dangerous in function/running.

As an example of importance to control in time the vibrations, we are going to illustrate the real values for the Small Power Plant from Czech Republic.

The devices used was: VIBROTEST – 60, VIBROPORT – 41, acceleration sensor AS – 060 (Schenck Vibro).

Turbine characteristics: Kaplan, 110 rotation/min.

Generator characteristics: Synchronous, P_{max}=525 kW, 600 rotations/min.

Next we are going to illustrate the vibrations for the generator, bridge (on which is placed the generator) and the turbine- shaft vibrations in different time of measuring.

4. MEASUREMENT RESULTS

Measuring at the 16.02.10

Vibration measurement locations are shown in fig. 3. For clarity, all spectra are displayed with uniform amplitude scale 1.5 mm/s, for each set separately as spectrum overlay, first measuring point for generators and then measuring point for turbine - shafts.

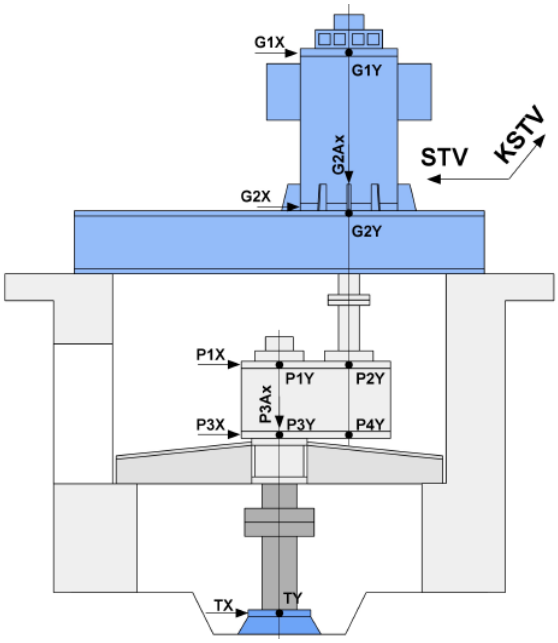

Figure 3. Frequency response model, update 16.02.10.

Figure 4. Frequency response model, update 16.02.10.

Figure 5. Frequency response model, update 16.02.10

Table 2. The average value of vibration at the various levels.

Part of system	Vef [mm/s]		
	Measuring Place	P=290 kW	Pmax=370 kW
Generator	G1X	1,58	1,51
	G1Y	1,54	1,50
	G2X	0,32	0,43
	G2Y	1,38	1,44
	G2Ax	1,00	0,84
Ax	P1X	0,50	-
	P1Y	0,52	-
	P2Y	0,40	-
	P3X	0,40	-
	P3Y	0,39	-
	P3Ax	0,37	-
	P4Y	0,31	-
Turbine	TX	0,12	-
	TY	0,15	-

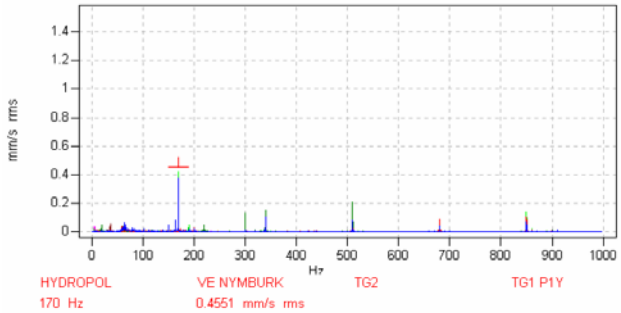

Figure 6. Vibrations of the shaft, update 16.02.10.

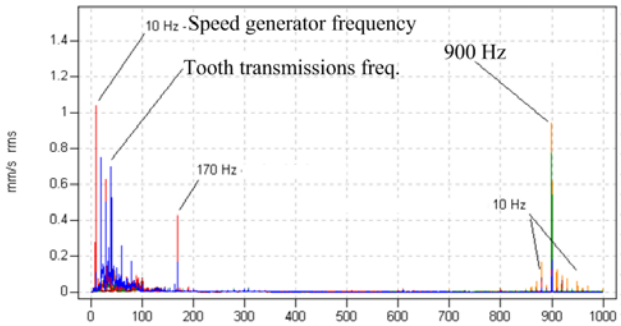

Figure 7. Vibrations of the generator, update 16.02.10.

All spectra contain the following basic components, see fig. 7:

- Speed generator frequency 10 Hz and his harmonics (20 Hz, 30 Hz, … etc).
- Tooth transmissions frequency 170 Hz and his harmonics (340 Hz …).
- Splined generator frequency 900 Hz lateral modulation band with a distance of 10 Hz.

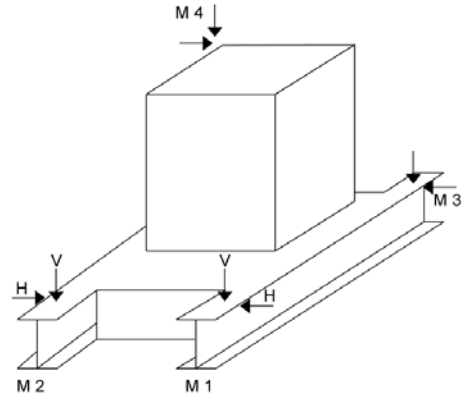

Figure 8. Scheme of the generator and bridge placement.

The measurements, witch was effectuated on the bridge are illustrated in fig. 8.

Measuring 21.03.13

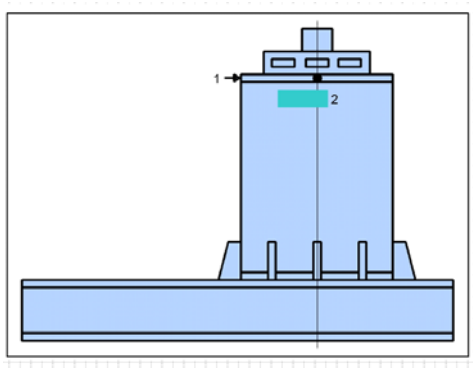

Figure 9. The scheme of the measuring places.

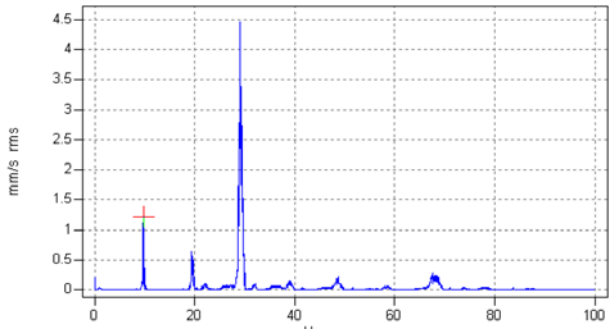

Figure 10. Vibrations of the generator, direction 2, update 21.03.13.

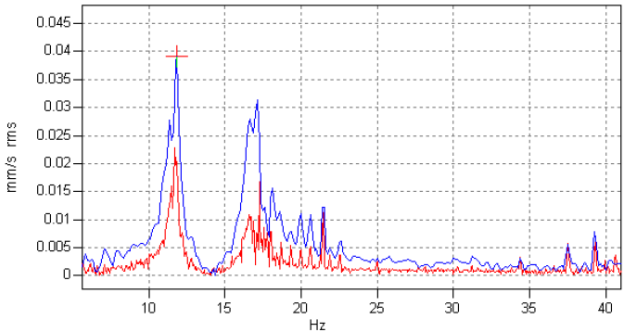

Figure 11. Vibrations of the bridge, update 21.03.13.

Analyzing the results of measurement the engineers detect the big values of the generator vibration.

Following detailed analysis of the measured values the engineers concluded that the problem is somewhere in the section bridge - generator.

To detect cause of the excessive vibration were performed several additional steps. First of all were taken out the cover anti-noise from the generator and performed new measurement.

Were detected thought of vibration the damage side – namely the instability in the location of shaft between generator and the bridge on witch generator is placed.

CONCLUSION

Analyzing the vibration levels it can be recommended to avoid operation at partial load, close to minimum values, but not over maximum, in order to keep relatively low levels of vibrations.

The hydro units don´t have problems in normal operation, in the vibration signals frequency spectra being observed remarkable amplitudes at frequencies identified as runner fundamental frequency and network frequency. Otherwise the signals are relatively clean.

From the example shown in the article is well seen the importance of performing regular measurements and their correct analysis.

Bibliography

1. *Hydro Quebec http://www.hydroquebec.com/ learning/hydroelectricite/turbine-lternateur.html, update 10.04.2013.*

2. Qing, He, Dongmei, Du. *Modeling and Calculation Analysis if Torsional Vibration for Turbine Generator Shaft. Journal of Information and Computer Science 7: 10(2010) 2174-2182. Hydropower and Hydroelectricity http://environment.about.com/library/weekly/blrenew6.htm, update 8.11.2012.*

3. *"Energy" Facts about hydropower http://wvic.com?hydro-facts.htm. www.arpmnv6.ro/fondul_de_mediu.htm.*

4. *"The future of hydropower" "Advantages of hydropower" "Hydropower's effects on the environment "http://library.thinkquest.org/17531/hydro.html#future*

5. Chemisinec I., Marvan M., Necesan, J., Sykora T., Tuma J. *Obchod s elektrinou. Praha 2010, CONTE spol s.r.o., ISBN 978-80-254-6695-7*

6. *Historical Timeline "Hydropower and Hydroelectricity", update 8.11.2012. http://environment.about.com/library/weekly/blrenew6.htm*

7. Krejcar R. *Rozvoj energetických systém, přednášky rok 2011.*

8. *Energetický Regulační Úřad. www.eru.cz [cit. 20.11.2012]*

9. *OTE. www.ote-cr.cz [cit. 05.11.2012]*

10. *Ministerstvo Průmyslu a Obchodováni (MPO): http://www.mpo.cz/ [cit. 20.11.2012]*

Recommended for publication: 29.03.2013.

STUDY ON NUMERICAL MODELING OF WATER QUALITY IN „RIVER-TYPE" SYSTEMS

G. Marusic, PhDc
Technical University of Moldova

INTRODUCTION

Water from rivers is used in most fields of human activities, so water quality maintenance is a global problem. It is monitored by the Water Framework Directive 2000/60/EC (Amended by Directive 2008/32/EC), approved by the European Commission, stating that by 2015 it is necessary to provide the state "*very good*" for all Water Bodies [1].

Lately, information systems have been widely used for assessing processes that occur in "*river-type*" systems and determining water quality. These systems consist of two main components: mathematical models and software packages [2].

A study on mathematical modelling of water quality in aquatic systems of "*river-type*" is presented in [3].

There is now a wide range of software packages used to model the environment, which can be classified into 3 types: based on spreadsheets, based on solving equations and based on dynamic simulation [4].

The purpose of this paper is the analysis of software packages and the study on numerical simulation of water quality in "*river-type*" systems.

1. SOFTWARE FOR NUMERICAL MODELING

Some packages based on spreadsheets include: Excel®, Quattro® Pro[7] and Lotus®[8]. They have incorporated a wide range of mathematical, statistical and logical functions. Also, they contain a lot of options for storing, keeping and sorting data, plotting, analyzing and exporting data. However, the above packages do not contain advanced mathematical functions and numerical procedures and are not able to perform the operations of differentiation and integration [4].

For environmental modelling, mathematical packages are used, such as Mathcad®, Mathematica®, MATLAB®, and TK Solver. These arrays have incorporated operating functions, complex numbers, animation, interpolation and numerical procedures. Not all listed packages have drawing tools, but they have the ability to import graphical format from other applications [4, 5, 6].

Lately, for modelling environmental systems, dynamic simulation packages have been used, such as Extend™[9], ithink®[10], Simulink®[11], ANSYS CFX, WASP (Water Analysis Simulation Program), CE-QUAL-W2, WMS (Watershed Modelling System), AGNPS (Agricultural Non-Point Source Pollution), GWLF (Generalised Watershed Loading Function), MONERIS (Modelling Nutrient Emissions in River Systems), QUAL2E, WQRRS (Water Quality for River Reservoir Systems), SMS (Surface - Water Modelling System), etc.

Extend™[9], ithink®[10], and Simulink®[11] have a flow GUI and support modelling linear and nonlinear systems in continuous or discrete time. The main features of these packages are animation, customizable GUI, sensitivity analysis and optimization. The downside is that they do not automatically maintain dimensional consistency [7].

ANSYS CFX is a program of finite element analysis. It is used for simulation in engineering, such as fluid flow calculation, electronic and electromagnetic optimization. It was used for numerical simulation of pollutant dispersion in rivers Argeş and Dâmboviţa in Romania. The pollutants dispersion discharged from the two points on the surface was simulated. The obtained numerical models allow tracking pollutants concentration in time and space and distance estimation of the polluted river [8].

A water quality model was developed for water basin "*Argazi - Miass - Shershni*" in Russia. WASP6 dynamic simulation program was used, developed by the Environmental Protection Agency of USA. It is designed for the analysis and prediction of water quality in various sources of surface water supply. This program incorporates two special submodules: TOXI, for modelling, taking into consideration toxic substances and EUTRO, for modelling water quality by standard indicators. Mathematical apparatus of WASP6 contains 171 equations. The program allows choosing equations used for modelling, depending on model objects, input data available and established boundary conditions. The obtained

model allows analyzing the actual situation, predicting changes and taking decisions for an appropriate management [9].

The results of hydrodynamics and water quality modelling for river Severnaia Sosiva from Russia is presented in [10]. It was developed a modelling system, the nucleus of which is the numerical simulation program of water quality, CE-QUAL-W2. This program was developed by the U.S. Army Corp of Engineers. A 3-D model of the studied sector was made by means of ArcGIS program. Based on data from hydrological stations Sosiva and Sartini, a database was developed with the following modules: Meteorology, Hydrology and Hydrochemistry. The obtained model calculates water quality parameters [10].

A water quality monitoring system was developed for the river Neva in Russia. The main components of the system are: the mapping of the river studied sector, "*Neva*" database, simulation model of the pollutants dispersion. The mapping was developed with ArcInfo version 9.1 program, which has been connected to "Neva" database. The numerical simulation model was developed based on the "*Ghidroecoprognoz*" version 2.97.001. The obtained results allowed state estimation of the water system in real-time, with the condition of changing various modelling parameters [11].

An information system was developed for Teleczkoe water basin and the estuary sector of the river Chiulyshman from Russia. The hydrodynamic and water quality model was developed. The developed system contains three modules: WMS basin modelling system, 3.5 version of the model CE-QUAL-W2, the database. The database is composed of lake bathymetry, the relief of the shore, meteorology, hydrology, water quality parameters [12].

The AGNPS program is very useful for forecasting loading basins with nutrients from agricultural sources and forecasting water quality. It was developed by the Research Center for Agriculture and Natural Resources Center USA [13, 14].

The evaluation of nitrogen and phosphorus emissions in surface waters is done using GWLF program. It was applied to the Cannonsville watershed in the USA. The model provides reasonable estimations of monthly flow and nutrient and sediment loading. This program was successfully applied for modelling nutrient export in Choptank River Basin on the coastal plain of the Chesapeakedrainage [15, 16].

MONERIS program is widely used for assessing watershed loading with nitrogen and phosphorus from point and diffuse sources. For example, it was used to assess nutrient and pollutant loading for the German part of the Elbe River basin [17] and for nutrient emissions modelling in "*river-type*" systems [18].

In the United States, QUAL2E water quality model is widely used, which was developed by the United States Environmental Protection Agency (EPA) in 1998. QUAL2E simulates temperature, DO, BOD, chlorophyll, nitrogen (organic nitrogen, ammonia NH_3, and NO_3^- nitrate), organic and inorganic phosphorus and coliform bacteria [19].

Another model, WQRRS, developed by the United States Army Corps of Engineers, simulate DO, total dissolved solids, P, NH_3, NO_2^-, NO_3^-, alkalinity, total carbon, organic constituents, and a number of aquatic biota, including plankton, algae, coliform bacteria, and several species of fish. It models hydrodynamic shape, determines depths and speeds [19].

The disadvantage of the listed programs is that they do not fully support the modelling process, but depend on other programs and systems, including those related to topography and databases.

The most useful software package for modelling water quality in "*river-type*" systems is the SMS system, which is a software package for modelling surface waters. It was developed by the USA experts from Aquaveo Company. It can solve dynamic and static problems. It is widely used in simulating processes in "*river –type*" water systems, as it manages the entire modelling process: from importing topographic and hydrodynamic data up to visualizing and analyzing solutions. The modelling process includes river hydrodynamics, floods in rural and urban area, waves modelling, following the dynamics and physical properties of water particles, the determination and analysis of pollutant dispersion.

SMS program is often used to determine the concentration of pollutants field. This process is done in two steps: first, it is determined the hydrodynamics of the studied sector using the SMS module named RMA2, then the results are used as input data for the module RMA4, in order to determine the pollutant dispersion. The base module of RMA2is the system of Navier-Stokes equations in the form of Reynolds by Cartesian coordinates x and y (1), (2), together with the continuity equation (3) for incompressible fluid in turbulent motion of the free surface:

$$h\frac{\partial u}{\partial t}+hu\frac{\partial u}{\partial x}+hv\frac{\partial u}{\partial y}-\frac{h}{\rho}\left(E_{xx}\frac{\partial^2 u}{\partial x^2}+E_{xy}\frac{\partial^2 u}{\partial y^2}\right)+gh\left(\frac{\partial H}{\partial x}+\frac{\partial h}{\partial x}\right)+$$
$$+\frac{gun^2}{\left(h^{1/6}\right)^2}\times\left(u^2+v^2\right)^{1/2}-\varsigma V_a^2\sin\psi+2h\omega v\sin\varphi=0 \quad (1)$$

$$h\frac{\partial v}{\partial t}+hu\frac{\partial v}{\partial x}+hv\frac{\partial v}{\partial y}-\frac{h}{\rho}\left(E_{yx}\frac{\partial^2 v}{\partial x^2}+E_{yy}\frac{\partial^2 v}{\partial y^2}\right)+gh\left(\frac{\partial H}{\partial y}+\frac{\partial h}{\partial y}\right)+$$
$$+\frac{gvn^2}{\left(h^{1/6}\right)^2}\times\left(u^2+v^2\right)^{1/2}-\varsigma V_a^2\sin\omega+2h\omega v\sin\phi=0 \quad (2)$$

$$\frac{\partial h}{\partial t}+h\left(\frac{\partial u}{\partial x}+\frac{\partial v}{\partial y}\right)+u\frac{\partial h}{\partial x}+v\frac{\partial h}{\partial y}=0 \quad (3)$$

Where h is the water depth (m), u - local velocity in the x direction (m/s), v - the local velocity in the y direction (m/s), t - time (s), ρ - density of water (kg/m^3), g - gravity acceleration (m/s^2), E - coefficients of turbulent viscosity (Pa.s or kg / m / s), H - geodetic elevation of the riverbed (m), n - Manning's roughness coefficient, ζ - empirical coefficient on air friction, V_a - wind speed (m/s), ψ - wind direction (degrees counterclockwise from the positive x-axis), ω - angular velocity of rotation of the Earth (rad/s), φ - place latitude.

The base module of RMA4 is the two-dimensional form of the advection-dispersion equation ADE applied to the turbulent flow regime:

$$h\left(\frac{\partial c}{\partial t}+u\frac{\partial c}{\partial x}+v\frac{\partial c}{\partial y}-\frac{\partial}{\partial x}D_x\frac{\partial c}{\partial x}-\frac{\partial}{\partial y}D_y\frac{\partial c}{\partial y}-\sigma+kc+\frac{R(c)}{h}\right)=0 \quad (4)$$

Where c is the concentration of pollutant (mg/L), D_x and D_y - turbulent diffusion coefficients in the x and y, k - decay constant (s^{-1}), σ - the local term source of pollutant (unit measure of concentration/s), $R(c)$ - precipitation/evaporation (concentration unit x m/s) [20].

2. NUMERICAL SIMULATION USING SURFACE-WATER MODELING SYSTEM (SMS)

Case studies using SMS program are presented in [21, 22, 23, 24, 25].

An industrial water pollution coming from the textile factory was found for a sector of the river Olt, city of St. George, Romania. The problem of determining the spatio-temporal dispersion of pollutants for the mentioned sector was developed, which was solved using SMS program. Two chemical indicators were analyzed: BOD_5 and COD - Mn. Data were obtained on the lateral and longitudinal dispersion of pollutants coming from the treatment plant. It was found that the SMS package can be applied to a project aimed at wastewater treatment using fitotehnologia [21].

The SMS program was used to determine the spatio-temporal evolution of petroleum products for a sector of the Prut River, Costesti, Moldova. Simulations were performed on a real river section with a length of 2.4 km and 1.2 km wide. It was determined the hydrodynamics and the field evolution of pollutant concentrations in all the finite elements of the studied domain [22].

The dispersion of oil products depending on the time is shown in Fig. 1:

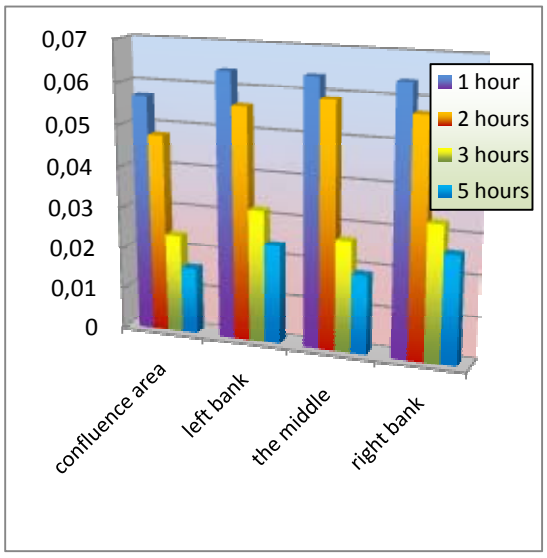

Figure 1. Temporal evolution of the concentration field of petroleum products.

The problem of dispersion modelling of chemical pollutants on a sector of the Prut River in the town Ungheni was made in August 2011, when the mentioned sector was polluted with copper compounds. To solve the problem, we used the SMS program. The simulation was carried out in dynamic way [23]. The dispersion of copper compounds was determined in all finite elements of the studied sector (Fig. 2).

The problem of mathematical modelling and numerical simulation of the process of fluoride dispersion in "*river-type*" systems is developed in [24]. The fluoride influence on the human body is being discussed. The problem was solved by using the SMS program. It was determined the fluoride dispersion for a sector of the Prut River [24]. Fig. 3 shows the temporal evolution of fluoride concentrations field.

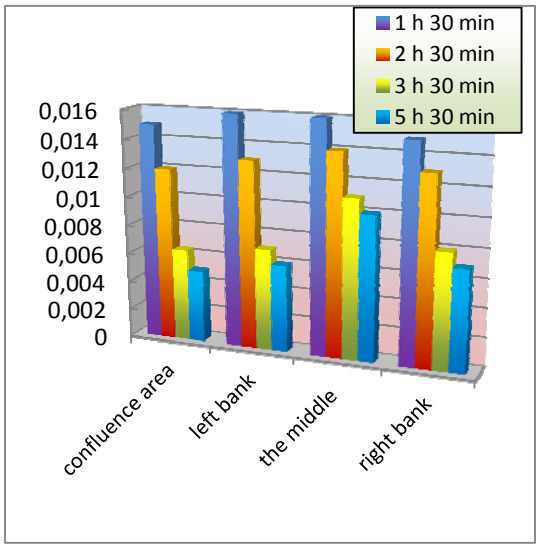

Figure 2. Temporal evolution of the concentration field of copper compounds.

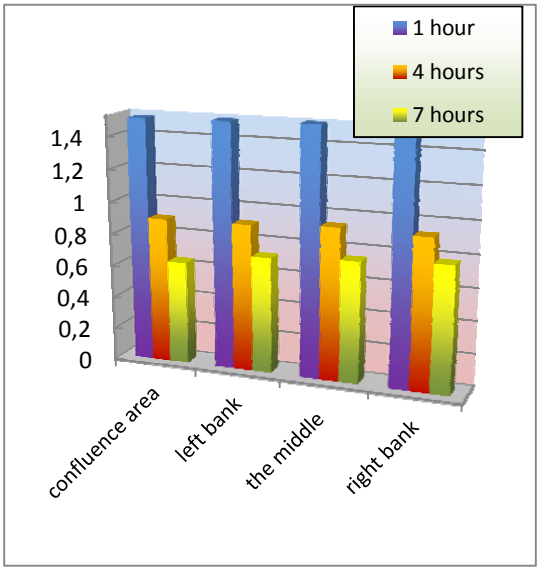

Figure 3. The temporal evolution of fluoride concentrations field.

The negative consequences of iron water pollution are discussed in [25]. The SMS software is used to determine the hydrodynamics and pollutant dispersion for a sector of the Prut River in the town Ungheni, Moldova. The iron dispersion at different time intervals from the moment with water confluence is shown in Fig. 4.

The obtained numerical model allows the determination of iron concentration field evolution in space and time throughout the studied sector.

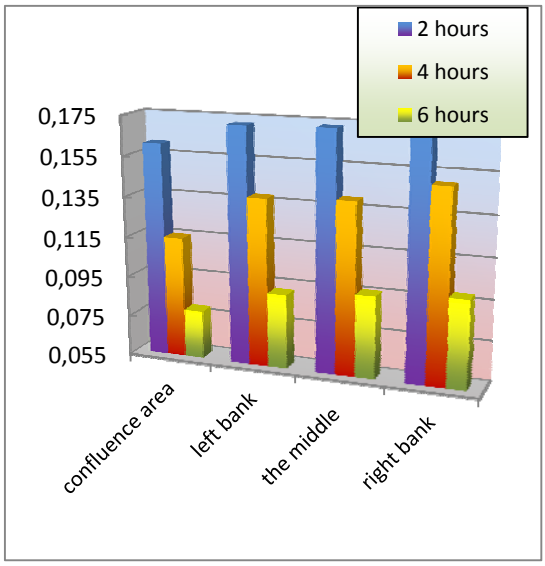

Figure 4. Temporal evolution of the iron concentrations field.

CONCLUSIONS

A review was conducted concerning the software packages used to assess water quality in "*river-type*" systems. It was found that the most optimal software is SMS (Surface-water Modelling System). This observation is argued by the fact that the mentioned system manages the entire modelling process and can be applied in dynamic or static regime.

Taking into consideration the case studies presented in other papers, it can be assumed that applying the mentioned package makes possible to track the spatio-temporal evolution of the pollutant dispersion in all the finite elements of studied sector. This will allow us to determine and forecast the correct water quality and predict pollution exceptional phenomena.

References

1. **** European Parliament and Council Directive EU 2000/60/EC establishing a framework for Community action in the field of water, 2000.*

2. Găgescu, R., Tertişco, M., Junie, P., Eremia, C. *Ensuring sustainable use of water on Earth by computerized environmental monitoring. Romanian Journal of Information and Automation, vol. 21, No. 3, pag. 5-12, 2011.*

3. Marusic, G. *A study on the mathematical modeling of water quality in "river-type" aquatic systems. Journal WSEAS Transactions on Systems, E-ISSN: 2224-2678, under review.*

4. Nirmala Khandan, N. et all. *Modeling Tools for Environmental Engineers and Scientists*, *CRC Press, 2001.*

5. Pritchard, P. J. *Mathcad — A Tool for Engineering Problem Solving, McGraw-Hill, New York, 1999.*

6. Palm III, W. J. *Introduction to Matlab 6 for Engineers, McGraw-Hill, New York, 2001.*

7. Marusic, G., Sandu, I., Moraru, V., Vasilache, V., Crețu, A., Filote, C., Ciufudean, C. *Software for modeling spatial and temporal evolution of river-type systems// Proceedings of the 11th International Conference on DEVELOPMENT AND APPLICATION SYSTEMS, Suceava, Romania, May 17-19, pag. 162-165, 2012.*

8. Mocanu, C., Fodor, D. *Numerical simulation of pollutant dispersion in natural courses*. *Ecoterra, No. 28, pag. 119-125, 2011.*

9. Iulaeva, E. O., Raznopolov, K. O., Suharev, Iu. I. *Overview of WASP6 program applied to the problem of the aquatic ecosystem research "Argazi - Miass - Shershni"// Proceedings of the Chelyabinsk Scientific Center, No. 28, pag. 89 – 94, 2005.*

10. Puşistov, P. Iu., Alsînbaiev, K. S. et all. *Numerical modeling of spatial and temporal structure of hydrodynamics and water quality characteristics of the river Severnaia Sosiva. Journal Atmospheric and Oceanic Optics, No. 11, pag. 956 – 960, 2006.*

11. Shishkin, A. I., Epifanov, A. V. *The system of monitoring water quality in the basin of the river Neva on the basis of GIS technology// Proceedings of the Southern Federal University, No. 12, pag. 113 – 118, 2006.*

12. Danchev, V. N., Pushistov, P. Yu. *Experience and results of the development of information and computational complex for simulation of hydrodynamics and water quality of rivers and lakes OB basin. Part 2 – Lake Teletskoye and section of the river Chulyshman. Bulletin of the Buryat State University. No. 9, pag. 154 – 161, 2012.*

13. Serban S. A., *Surface water quality in the lower basin of the river Jiu. // Thesis, Bucharest, 2012.*

14. Koelliker, J.K., Humbert, C. E., Joseph Mich, St. *Applicability of AGNPS model for water quality planning, Paper No. 89-2042, Am. Soc. of Agric. Engrs., pag. 13, 1989.*

15. Schneiderman, Elliot M., Pierson, Donald C. et all. *Modeling the hydrochemistry of the Cannonsville watershed with GENERALIZED WATERSHED LOADING FUNCTIONS (GWLF). Paper No. 01032 of the Journal of the American Water Resources Association. Vol. 38, No. 5, pag. 1323–1347, 2002.*

16. Lee K. Y., Thomas R. Fisher, T. R. et all. *Modeling the hydrochemistry of the Choptank River Basin using GWLF and Arc/Info: 1. Model calibration and validation. Journal Biogeochemistry, Vol. 49, No.2, pag. 143-173, 2000.*

17. Berlekampa, J., Lautenbachb, S. et all. *Integration of MONERIS and GREAT-ER in the decision support system for the German Elbe river basin. Journal Environmental Modelling & Software, Vol. 22, Issue 2, pag. 239–247, 2007.*

18. Venohr, M., Hirt, U. et all. *Modelling of Nutrient Emissions in River Systems – MONERIS – Methods and Background. International Review of Hydrobiology, Vol. 96, Issue 5, pag. 435–83, 2011.*

19. McKinney Daene C. et all. *Modeling Water Resources Management at the Basin Level: Review and Future Directions. SWIM Paper 6. International Water Management Institute, Colombo, Sri Lanka, 1999.*

20. ** *„SMS Tutorials", SMS v.10.1.11, AquaVeo, 2011.*

21. Sumbasacu G. O. *Methods and means of monitoring and preventing rivers pollution // Thesis, Bucharest, 2009.*

22. Besliu, V., Cufudean, C. Filote, C., Marusic, G., Moraru, V., Ştefănescu, B. *Mathematical modeling of hydrodynamics and chemical pollutant dispersion in rivers// Proceedings of the 7th International Conference on Microelectronics and Computer Science ICMCS – 2011, Technical University of Moldova, Chişinău, vol. 1, pag. 160 - 165, 2011.*

23. Marusic, G., Moraru, V. *Mathematical modeling of pollutant transport for a sector of the Prut River// Proceedings of the 3th International Conference "Mathematical modelling, optimization and information technology", Academy of Transport, Information and Communications of Moldova, Chişinău, pag. 86 - 98, 2012.*

24. Marusic, G., Sandu, I., Moraru, V., Filote, C. Ciufudean, C., Beşliu, V., Vasilache, V., Ştefănescu, B., Şevcenco, N. *Fluoride Dispersion Modeling for "River-Type" Systems. Meridian Ingineresc No. 4, pag. 28 – 32, 2012.*

25. Marusic, G., Filote, C., Ciufudean, C. *The Spatial - Temporal Evolution of Iron Dispersion in "River-type" System// Proceedings of the 17th WSEAS International Conference on APPLIED MATHEMATICS (AMATH '12), Montreux, Switzerland, pag. 95 – 98, 2012.*

Recommended for publication: 19.02.2013.

INCREASING THE SUSTAINABILITY OF BEARINGS RENOVATED WITH POLYMER COMPOSITE MATERIALS

L. Malai
State Agrarian University of Moldova.

INTRODUCTION

Estimates made by many home and abroad scholars show that one of the major causes influencing on the cost of the agricultural machinery repair is bearing wear, especially those in the housing, and of bearings parts. The reason for seeking of some effective ways to increase the sustainability of mounting locations of bearings as well as of contact surfaces of bearings was and is always a current concern of scientists and of agricultural equipment manufacturers.

The overall goal of this study is to increase the joints sustainability of bearing type refurbished with polymer composite materials (PCM). As the research object served the joints of bearing type components of agricultural equipment and of related branches refurbished with PCM. The study of the research subject, in terms of reliability and especially of durability and maintainability in particular, presents the topic of discussion and great interest for specialists concerned with the operation and maintenance of agricultural equipment and related industries.

The paper presents the results of testing a polyamidepoxy material intensively reinforced with hollow glass microspheres proposed to renovate worn bearings surfaces and places of bearings.

1. MATERIAL AND METHODS

Experiments were conducted to study two groups of PCM the constitution of which was established based on the analysis of data from the literature and as the result of some preventive experiments [1-3].

In the first group of PCM, as a matrix was used polyamide ПА12 (ОСТ 6-05-425), which is an assortment of polyamide with improved resistance to UV radiation and weather and has an increased resistance to wear and shocks showing physics-mechanical properties in a wide temperature range, with the lowest density of all known polyamides today. It is also resistant to most chemicals, the fats, oils, fuels, hydraulic fluids, various organic solvents (aliphatic and aromatic hydrocarbons, ketones, esters, ethers, oils, etc.). For comparison, the grip of the composite material was confronted with that of the base material.

In the second group of PCM, as a matrix was used the hybrid material on the basis of a mixture of the epoxy oligomer of the type П-ЭП354 and polyamide ПА12, 30% volume proportion of the epoxy oligomer the remaining part polyamide.

CM reinforcement was performed with the following agents: molybdenum disulphide MD-1 (ТУ 48-19-133-90), used to improve the behavior of CM load and wear without affecting shock and fatigue resistance, hollow glass microspheres (glass microballoons) СМ-ВП gr.5 with the following chemical composition: SiO_2: 76-78%; Na_2O; 10-12%; CaO: 6%; ZnO: 1-1,5%; B_2O_3; 4%, properties: 0,37 to 0,42 g/cm^3 density, compression strength 150 kg/cm^2 (attrition 10%) moisture, not more than 0,3% basalt microfibers (ТУ У В.2.7-26.8-32673353-001/2007), used to increase tensile strength, stiffness, shrinkage during training, improving lubrication.

Composite was obtained by mixing the components in the ball mill ZE-101 for 30 min. the speed of drum 80…120m^{-1}.Crushing of the basalt microfibers and their sorting was done in the shredding device Ц-10 with subsequent sorting through oscillating sieves. The coatings were applied by hot pressing of carbon steel substrates of usual quality in delivery state by hydraulic press DV 2428. The dimensions and shape of the samples were determined according to the investigated properties. Processing parameters were maintained under semi-automatic system.

The research was carried out in four distinct phases according to the matrix - 3 Factors Box program - Benkin presented in table 1 [1, p.51], and the data were processed by applying the following schedule STATGRAPHICS: Special ► Experimental design ► Create design► Response surface.

Physics-mechanical properties were determined by standard methods or approved in respective areas. Thus, adhesion was estimated by the method of pins, hardness SHORE method, SR ISO868-95 scale D, the degree of hydrophilicity / hydrophobicity of the studied CM was estimated according to ISO (ASTM D570).

2. EXPERIMENTAL RESULTS AND DISCUSSION

2.1. Ensuring reliability level by choosing and optimizing the material constitution of wear compensator layer

Experiments made in order to optimize the PCM by studying the adhesion of filler material on steel substrates have shown different behavior of the materials of the reinforcement of the relative adhesion of PCM on carbon steel substrates Rz80 roughness μm. This behavior is observed both in family PCM polyamide matrix and the matrix of polyamidepoxy and is described by regression equations which in the coded coordinates have the following form:

$$A_r = 0,91 - 0,002x_1 - 0,07x_2 - 0,04x_3 + 0,008x_1^2 + \\ +0,01x_1x_2 - 0,008x_2^2 - 0,03x_2x_3 - 0,008x_3^2, \quad (1)$$

$$A_{r\text{-PPECM1}} = 1,6 - 0,02x_1 - 0,025x_2 - 0,035x_3 + 0,005x_1^2 - \\ -0,035x_2^2 - 0,03x_2x_3 - 0,055x_3^2, \quad (2)$$

$$A_{r\text{-PPECM2}} = 1 - 0,012x_1 - 0,016x_2 - 0,022x_3 + \\ +0,003x_1^2 - 0,022x_2^2 - 0,019x_2x_3 - 0,034x_3^2, \quad (3)$$

where A_r is the relative adhesion of PCM family of polyamide matrix determined by reference to polyamide adhesion; $Ar._{PPECM1}$ - relative adhesion of PCM family of polyamidepoxy matrix determined by reference to polyamide adhesion; $Ar._{PPECM2}$ - relative adhesiveness of PCM family of polyamidepoxy matrix determined by reference to matrix adhesion (mixture of hybrid polyamidepoxy) x_1, x_2 and x_3 represents the percentage of components of coded coordinates, respectively MoS_2, and hollow glass microspheres and basalt microfibers.

Based on the analysis equations 1-3 show that, for both groups of composite materials, all reinforcing agents adversely affect adhesion of PCM on carbon steel substrates (b_1, b_2 and b_3 in all regression equations differs from 0 with negative values). Relative adhesion of PCM of polyamide matrix is most significantly influenced by the hollow glass microspheres, followed by basalt microfibers ($|b_2|>|b_3|>|b_1|$).

In the PCM family of polyamidepoxy matrix the relative adhesion is most influenced by basalt microfibers, followed by hollow glass microspheres ($|b_3|>|b_2|>|b_1|$).

With regard to the percentage of the basalt microfibers much lower than that of the glass microspheres and molybdenum disulfide can be concluded more significant negative influence of these reinforces on the adherence in relation to the hollow glass microspheres.

At the same time it is found that the influence of the content of MoS_2 on adhesion to both sets of experiments, it is insignificant ($b_1<0$). Moreover, the PCM family of polyamide matrix, under certain conditions, disulfide Mo has a beneficial effect that is increasing along with the increasing of the glass microspheres *($b_{11}>0$ and $b_{12}>0$)*, this influence being diminished for polyamidepoxy PCM family *($b_{12} = 0$ in equations 2 and 3)*.

As a result of optimization of relationships 1-3 in order to maximize and minimize the relative adhesion were obtained the results shown in table 1. The data presented clearly demonstrate the possibility of increasing adhesion by changing the PCM matrix by mixing the addition of epoxy oligomer. As a result of this change an increase of relative adhesion of 1,63 times was obtained.

Evolution of relative adherence of PCM families for optimal concentration can be seen in figures 1 and 2. From these figures it appears that for the PCM family of polyamide matrix, in the case of CM reinforcement with an insignificant quantity of molybdenum disulfide (1%) microspheres of glass and basalt microfibers decrease the relative adhesion to a relatively small range (from 0,98 to 0,8), and for the PCM family of polyamidepoxy matrix this range is extremely small (1,6 -1,5). These findings are sufficient to conclude that PCM of polyamidepoxy matrix the glass microspheres practically do not affect the adhesion of these materials on steel substrates.

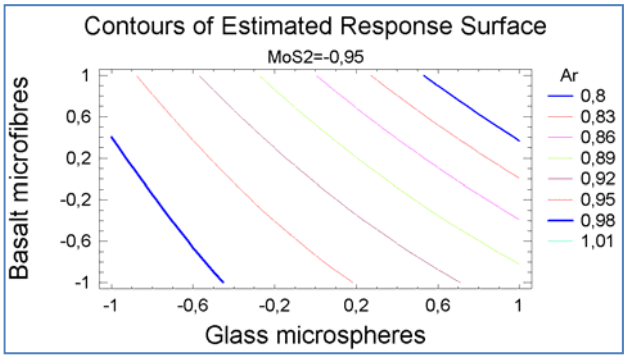

Figure 1. Estimating the PCM relative adherence of poliamide matrix to the concentration of polyamide matrix constituents (for the case of disulphide Mo concentration -0,95 (code) 1,1% (real).

The results of the foregoing experiment on adherence PCM polyamide demonstrated that the addition of epoxy oligomer has lead to obtain such

Table 1. Optimum values on the relative adhesion strength according to constitution for PCM polyamide matrix and polyamidepoxy matrix.

Factor	Optimum values											
	Minimize						Maximize					
	PPCM		PPECM1		PPECM2		PPCM		PPECM1		PPECM2	
	code	real	code	real,	code	real	code	real	code	real	code	real
MoS_2	1	5	1	5	1	5	-1	1	-1	1	-1	1
Glass microspheres	1	30	-0,99	10,1	-0,99	10,1	-0,97	10,3	-0,56	14,3	-0,56	14,3
Basalt microfibres	1	6	1	6	1	6	-1	2	-0,47	3,06	-0,47	3,06
A_r	**0,742**		**1,446**		**0,903**		**1**		**1,63**		**1,01**	

Legend: PPECM1 - relative adhesion of PCM family of polyamidepoxy matrix determined by reference to polyamide adhesion; PPECM2 - relative adhesion of PCM family of polyamidepoxy matrix determined by reference of polyamidepoxy matrix adhesion.

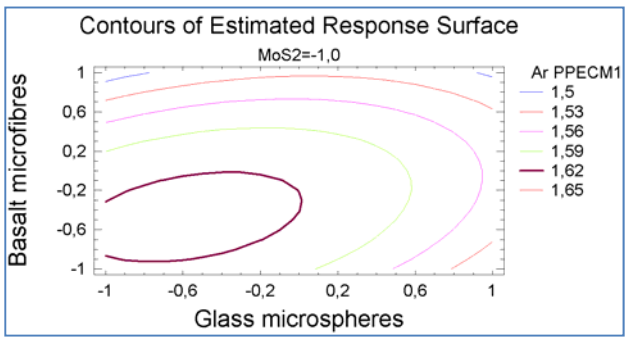

Figure 2. Estimating the relative adhesion of the PCM of polyamidepoxy matrix by reference of the concentration of the constituents (for the case of Mo concentration of disulfide 1 (code) 1% (real).

an adhesion of applied material to the carbon steel substrate which equals, virtually the tensile strength of the CM, but attempts to PCM with the polymer matrix of this type shows that the adhesion strength tends to decrease to the operation of the water coating and high humidity environments.

The experimental results performed on samples maintained under hydrostatic conditions shows specific behavior of the PCM polyamide in terms of change in adherence. Thus the samples kept in higrostat at a temperature of 60°C and relative humidity 95-100% were detached from the substrate after 520 hours exhibition and those kept in increased humid weather conditions (outside in the months of October to May) for 8 months have not presented changes to the initial adhesion which remains equal to 40MPa.

2.2. Research on the hardness of PCM reinforced with glass microspheres

PCM hardness in many cases is determined to relate a number of properties that are difficult to determine. Thus hardness can be used to estimate the moisture content gradient and its penetration depth [11, p.102-103].

Processing of data obtained in the result of experiments conducted in accordance with the schedule in table 1, yielded the following regression equation which in coded coordinates highlights the dependence of hardness estimated by Shore D depending on the content of constituents of PCM of polyamidepoxy matrix (30% oligomer epoxy the remaining Polyamide 12 percentage volume):

$$H.ShoreD/15 = 82,0 + 0,125x_1 + 1,375x_2 + 0,25x_3 - \\ -0,25x_1x_2 + 1,0x_2^2 + 0,25x_2x_3 - 0,25x_3^2, \quad (4)$$

where H Shore D15 is the hardness after Shore estimated with durometer type D (15-time, in seconds, after which the reading was done), x_1, x_2 and x_3 is the volume percentage of components in coded coordinates, respectively MoS_2, glass microspheres and basalt microfibers.

Using STATGRAPHICS program features and the outcome of optimizing the response factor corresponding to the H Shore D/15 = 84,72, we find the following percentages of constituents: MoS_2 = -0,9 (9); glass microspheres =+ 0,996; basalt microfibers = +1,0.

In the synthesis of research of designed PCM hardness was found that in the case of PCM polyamidepoxy heavy reinforced with glass microspheres, introduction of particles hardness of the composites produced, while adding the glass microspheres increased the hardness reaching the maximum value at the level of 0,99 in the coded coordinates that in natural coordinates corresponds to the quantity of 29,9% of the total volume.The reinforcement with basalt microfibers also resulted in increased hardness, achieving the maximum hardness for the high level (+1 – in the coded of molybdenum disulphide decreased the

coordinates and 6% - natural coordinates. It should be noted that the increase of the percentage of glass microspheres of more than 30% does not contribute to increase of hardness, while the zone of the maximum for glass microfibers is outside of the carried out experiment.

2.3. Study the degree of hydrophilicity / hydrophobicity of PCM intensive reinforced with glass microspheres

Researchers' interest opposite the CM interaction problems with different liquids is motivated by the practical importance of the behavior of those materials in real operating conditions. The sorption capacity for water of the PCM, which includes the ability to both the absorption and adsorption, has a mixed significance for refurbished parts with such materials. The undesirable aspect, in the first place, is related to the degree of liquid sorption influence on the dimensional stability of the covered surfaces with PCM [4, pp. 108-110], and the desired aspect is that higher sorption capacity contributes to the incorporation by outside diffusion of some substances favorable to tribological process in a contact area of conjunctive surfaces.

Some authors have proposed special procedures to enhance porosity of superficial coating of PCM used to offset the surfaces wear of tribologic couplings [2]. Also liquids sorption rate by PCM is an important parameter that talks about the level of improvement of the application process and formation of polymeric coatings [3, p.89-93].

It is obvious that knowledge of the kinetics of sorption processes of liquids in PCM provides valuable information on the behavior of refurbished parts in inclemencies of weather conditions, poor lubrication etc. Thus, in the following, are presented Kinetic sorption processes of water and oil to the series of materials prepared by enhanced adding of hollow glass microspheres.

The result of processing experimental data on the evolution of the rate of sorption of water by coatings of PCM of polyamidepoxy matrix studied were obtained the results described by the following regression equation:

$$W_{water} = 1,6333 + 0,0025x_1 + 0,1312x_2 + 0,0412x_3 + 0,0058x_1^2 - \\ -0,0775x_1x_2 - 0,0025x_1x_3 + 0,0533x_2^2 + 0,005x_2x_3 - 0,0317x_3^2, \quad (5)$$

where W_{water} is the water sorption capacity expressed in per cents; x_1, x_2 and x_3 are percentages of the components in the coded coordinates, respectively MoS_2, glass microspheres and basalt microfibers.

Similar research conducted on the second group of samples that have been immersed in SAE oil 15W-40 at the temperature (20 ± 2)°C showed similar behavior to the oil-immersed with those submerged in water. After statistical processing of the experimental data the following regression equation was obtained:

$$W_{oil20} = 1,597 - 0,002x_1 + 0,129x_2 + 0,049x_3 - 0,01x_1^2 - \\ -0,075x_1x_2 - 0,01x_1x_3 + 0,089x_2^2 + 0,02x_2x_3 - 0,047x_3^2, \quad (6)$$

where W_{oil} is the oil sorption capacity at 20°C expressed as a percentage, x_1, x_2 and x_3 represents the percentage of components coded coordinates, respectively MoS_2, glass microspheres and microfibers basalt.

Analysis of equation 6 shows that the glass microspheres have a dominant influence on the absorption capacity of the oil. Basalt microfibrils also increase absorption of oil but only to a halve of it and MO_2, practically does not influence the oil sorption.

Optimization of response factor, which corresponds to the value of W_{oil20}. = 1,901, ascertains the following percentage of constituents for maximum oil sorption SAE15W40 maintained at 20°C: MoS_2 = -0,99988; glass microspheres = +1; basalt microfibers = + 0,6494.

The test results of the two groups of samples, namely samples immersed in water and those oil-immersed, it was found that the optimum composition that ensures the maximum rate of sorption of water (1,92%) and oil (1,9%), are within the boundaries: +1 glass microspheres, basalt microfibers +0,65 ...+ 0,77, and molybdenum disulfide -1 (in coded coordinates) corresponding to the natural coordinates: glass microspheres - 30%, basal microfibers - 5,3 ... 5,54% and molybdenum disulfide - 2%. (seetable 2).

Tests carried out on samples made of the constitution PPCM: glass microspheres - 30%, basalt microfibers – 5,3 ... 5,54%, molybdenum disulfide - 2%, the remainder PA12 immersed in water at 20°C and the oil SAE15W40 temperatures 20, 40, 60 and 80°C showed that the temperature of the medium in which the samples are immersed, practically does not influence the rate of sorption of oil to the samples made of the polyamide in the state of delivery, while samples with heavy reinforced glass microspheres have a slow growth of oil sorption with increasing of medium temperature. Probably this is due to the presence of glass microspheres which are some of the oil storage cavities.

Table 2. Rates of sorption of various lubricants to the PCM according to the temperature of the immersion medium.

Immersion time, hours	Immersion medium																			
	water		SAE 15W40								water		SAE 15W40							
	heat treated us										annealed									
	20°C		20°C		40°C		60°C		80°C		20°C		20°C		40°C		60°C		80°C	
	PA12	PPMP	PA12	PPMP	PA12	PPMP	PA12	PPMP	PA12	PPMP	PA12	PPMP	PA12	PPMP	PA12	PPMP	PA12	PPMP	PA12	PPMP
12	1,34	1,48	1,30	1,62	1,34	1,66	1,38	1,68	1,38	1,70	0,80	0,80	0,00	0,20	0,00	0,32	0,08	0,38	0,32	0,38
24	1,48	1,88	1,37	1,88	1,42	1,90	1,42	1,92	1,42	1,92	0,90	0,88	0,00	0,20	0,00	0,32	0,08	0,39	0,32	0,40
36	1,52	1,92	1,42	1,90	1,46	1,91	1,46	1,92	1,46	1,92	1,00	1,18	0,00	0,20	0,00	0,32	0,08	0,39	0,32	0,40
48	1,52	1,92	1,42	1,90	1,46	1,91	1,46	1,92	1,48	1,92	1,00	1,18	0,00	0,20	0,00	0,32	0,08	0,39	0,32	0,40
60	1,52	1,92	1,42	1,90	1,46	1,91	1,46	1,92	1,48	1,92	1,00	1,18	0,00	0,20	0,00	0,32	0,08	0,39	0,32	0,40
72	1,52	1,92	1,42	1,90	1,46	1,91	1,46	1,92	1,48	1,92	1,00	1,18	0,00	0,20	0,00	0,32	0,08	0,39	0,32	0,40

Legend: PA12 - polyamide 12; PPCM – polymer composite material of PA 12 matrix reinforced with: MoS_2 -2%; BII - CM -30%; MF Basalt -5,5%.

The assumption made is supported by the second set of experiments and namely tests carried out on samples that are made of the same material and the same technological schemes but which have undergone extra heat treatment by heating in an oil bath at a temperature of 180°C, kept at this temperature for 30 ± 5 min and cooled with oil bath. Finally, it should be noted that the effects described in this section can serve prerequisites for choosing constitution of CM used to renovate worn areas of tribological joints of bearing type. It has been shown that intensive alloying CM with hollow glass microspheres creates favorable conditions for storing lubricants in microcavities formed by respective materials.

2.4. Tribological behavior PCM reinforced with hollow glass microspheres

2.4.1. Studies on tribological properties of PCM-reinforced with hollow glass microspheres tested in terms of friction without lubrication

It is obvious that at the choice of materials for tribological couples renovation it is insisted on a coefficient of friction of the materials, which make the couple, as small as possible. For this reason, the purpose of carried out tests on the family of PCM in this subchapter is to establish PCM constitution that would ensure the lowest coefficient of friction, and that would guarantee and other physical and mechanical important properties for maintaining a sustainable refurbished joints technical requirements imposed by the regulations in force.

Tests carried out on tribometer UMT2, revealed different tribological behavior of the family CM of polyamide matrix and polyamidepoxy depending on the percentage of reinforcement with molybdenum disulfide, hollow glass microspheres and basalt microfibers (Fig. 3).

Regression equations (7) and (8), in the coded coordinates, express PCM development of the coefficient of friction of the polyamide matrix P12 and the matrix of polyamidepoxy hybrid mixture.

$$K_{PPMC_{dry.}} = 0,187 - 0,012x_1 - 0,009x_2 - 0,004x_3 - 0,006x_1^2 + \\ +0,001x_1x_2 - 0,011x_1x_3 + 0,001x_2^2 - 0,003x_2x_3 - 0,006x_3^2, \quad (7)$$

$$K_{PPECM_{dry.}} = 0,188 - 0,018x_1 - 0,009x_2 - 0,001x_3 + \\ +0,001x_1^2 + 0,001x_1x_2 - 0,006x_2^2 - 0,004x_2x_3, \quad (8)$$

From the analysis of equations (7) and (8) results that, for both PCM families, all reinforcing agents contribute to the reduction of the coefficient

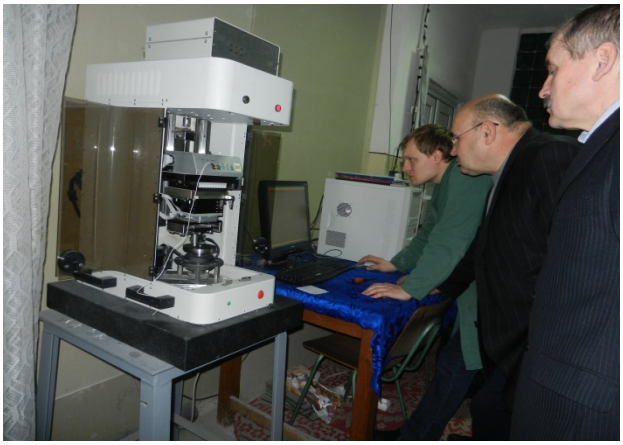

Figure 3. Aspects from the measurement of the coefficient of friction with the universal tribotester UMT2 (CETR ®, USA) with pin-on-disk configuration: *1 - dual sensor for friction and load, 2 -suspension, 3 - pin support, 4 - pin, 5-disc, 6 – table- support for disc.*

of friction of the composite polyamidepoxy (b_1, b_2 and b_3 vary from 0 having negative values). Both in the case of PCM of the polyamide matrix and in that of poliamidepoxy matrix mostly influences the coefficient of friction the desulphurised Mo followed by the glass microspheres and, finally, the basalt microfibers ($|b_1| > |b_2| > |b_3|$).Experiments carried out found that the optimal values of both PCM families are quite close (see table 3). These values, when optimizing the purposes of determining the minimum values of the coefficient of friction, is: for the PCM family of polyamide matrix – 0,14, and for PCM of polyamidepoxy matrix - 0,146. For the case of optimizing with the purpose of maximizing the coefficient of friction for PCM of polyamide matrix is equal to 0,209 and for family PCM of polyamidepoxy matrix is 0,22. These values are obtained by processing the regression equations (7) and (8).

Table 3. Optimal values of the friction coefficient depending on the constitution for PPCM and PPECM tested under dry friction.

Factor	Optimum values							
	Minimize				Maximize			
	PPCM		PPECM		PPCM		PPECM	
	code	real, %	code	real %	code	real, %	code	real, %
MoS_2	*+1*	*5*	*+0,92*	*4,84*	*-1*	*1*	*-1*	*1*
Glass Microspheres	*+1*	*30*	*+1*	*30*	*-1*	*10*	*-0,5*	*15*
Basalt Microfibres	*+0,98*	*5,96*	*+1*	*6*	*+0,72*	*5,44*	*-1*	*2*
$K_{optimum}$	0,14		0,146		0,209		0,22	

Based on the results of tribology tests, performed in this chapter, it can be concluded that the friction resistance of the PCM of hybrid mixture of polyamidepoxy matrix is essentially on the same domain as the PCM of polyamide matrix (K_{ppecm} = 0,146 and Kppcm = 0,14). It is possible to decrease the coefficient of friction with increasing percentage of glass microspheres and basalt microfibers as the minimum values for the coefficient of friction are at the boundary of the experiment. At the same time the increase of the percentage of hollow glass microspheres is not recommended because according to the results obtained in section 2.1 the increased percentage of glass microspheres impairs the adhesion capacity of the PCM.

2.4.2. Studies on tribological properties of PCM-reinforced with glass microspheres tested in various lubrication conditions

Wear, being defined as a process of destruction of the surface layer of a solid body at mechanical interaction with another solid body, is greatly influenced by the medium in which the friction occurs and tribological coupling superficial layers ability to store and maintain, in the area of the contact for a certain period of time, the specific agent for the operating medium.

The research conducted on aspects of tribology of couples operated in conditions of lubrication under low-capacity led to the use of some materials with enhanced properties of storage and retention of lubricant in the contact area [2 p 68-75, 6, 7].

Experimental studies conducted at the Department of Machine and graphics at the University of the Lower Danube Galati on lubrication with low-capacity fluid lubrications have indicated specific processes in superficial layers of tribological semicouples ,optimal intervals being established for speeds, loads, concentrations of filler materials, etc. in the case of PCM. [8-10].

In the following the experimental results are

presented carried out in order to determine the friction coefficient of PCM in conditions of contamination of the contact area with water, oil of type SAE15W40 and greases of type LITOL 24, STAS 21150-87 all for the cases PIN with the end covered with PCM - ordinary quality carbon steel disc non heat treated (in state of delivery).

A comparative analysis of the obtained results shows that the variation of the friction coefficient values with respect to the friction coefficient for the dry lubrication is different (see table 4).

Thus it is noted that the coefficient of friction of PCM-intensively reinforced with hollow glass

Table 4. Comparative data on the values of the coefficient of friction for various lubrication conditions.

Lubricant type and lubrication character	**Coefficient of friction**			**Reported coefficient of friction**				
	PA12	PPCM	PPECM	KPPCM/up	KPPECM/ up	KPPECM/ up	KPPCM/PP ECM	KPPECM/P A12
water (a)	0,11	0,107	0,091	0,764	0,650	0,623	0,850	0,827
water (l)	0,12	0,123	0,112	0,879	0,800	0,767	0,911	0,933
oil (a)	0,02	0,016	0,010	0,114	0,071	0,068	0,625	0,500
oil (l)	0,04	0,035	0,025	0,250	0,179	0,171	0,714	0,625
LITOL (a)	0,03	0,025	0,024	0,179	0,171	0,164	0,960	0,800
LITOL (l)	0,1	0,063	0,042	0,450	0,300	0,288	0,667	0,420
drying	0,18	0,14	0,146				1,043	0,811

Legend: Kppcm/up - the ratio of the coefficient of friction of PPCM tested under lubrication and friction coefficient of PPCM tested under dry friction; Kppecm/up - the ratio of the coefficient of friction of PPECM tested under lubrication and coefficient of friction of PPCM tested under dry friction; Kppecm/up - the ratio of the coefficient of friction of PECM tested under lubrication and friction coefficient of PPECM tested under dry friction; Kppecm / ppcm - the ratio of the coefficient of friction of PPCM and the PPECM tested under lubrication; Kppecm/PA12 - the ratio of the coefficient of friction of the PPECM and that of polyamide matrix (PA12).

microfibers of both polyamide matrix and the matrix of polyamidepoxy mixture, is reduced in comparison with the reference material.

In the case of dry friction, samples of PPCM have a coefficient of friction of 1,28 times less than the control samples (PA12 in state of delivery condition) and PPECM samples of 1,23 times lower (Kppecm/PA12 = 0,811) . This can be explained by the fact that during the friction under dry regime thermochemical processes take place specific to each material separately.

The strongest reduction of the coefficient of friction for PPECM tested under various conditions of lubrication, relative to the control material (PA 12) refers to samples tested in limit lubrication conditions with LITOL24 – 2,38 times smaller (Kppecm/PA12 = 0,420) and those tested under conditions of abundant lubrication with oil - 2 times lower (Kppecm/PA12 = 0,5), followed by samples tested under boundary lubrication with oil – 1,6 times lower (Kppecm/PA12 = 0,625) and abundant lubrication conditions with LITOL24 – 1,25 times lower (Kppecm/PA12 = 0,8).

For sliding bearings refurbished with PCM a special importance has, namely the behavior at wear of the aging joints of tribological couples behavior under dry friction and lubricating with greases under boundary limit. This is explained by the fact that the mentioned conditions are specific to joints of bearing type of agricultural machinery and related industries. Thus, the good behavior at wear of the PPECM in conditions of lubrication with LITOL24 type lubricating greases, particularly under limit regim, as well as a rather good behavior in conditions of dry friction, argues fully the perspective use of PPECM as compensation material of wear to renovate the joints of bearing type operated under poor lubrication conditions.

Using the conditions of compromise, based on the weight of the influence of various factors on the coefficient of friction, for restoring worn parts constituting the bearing type joints PPECM is recommended with the following constitution: MoS_2 - 5% + hollow glass microspheres - 30% + basalt chopped microfibers - 5% the rest of the mixture of epoxy oligomer PA12 in the volume ratio of 7/3.

2.5. Research on durability of bearing type joints renovated with PCM intensively reinforced with hollow glass microspheres

Sliding bearings composed of bush made of carbon steel brand 35 in state of delivery and spindle of carbon steel coated with PPECM (MoS_2 -5% +hollow glass microsphers -30% + basalt chopped microfibers – 5%, the rest a mixture of PA 12 and epoxy oligomer in volume ratio of 7/3 were subjected to tests.

Evolution of adjusting change of these tribological couplings tested under conditions of dry friction and lubrication under limit regim with LITOL 24 limit, is convenient to follow in figure 4.

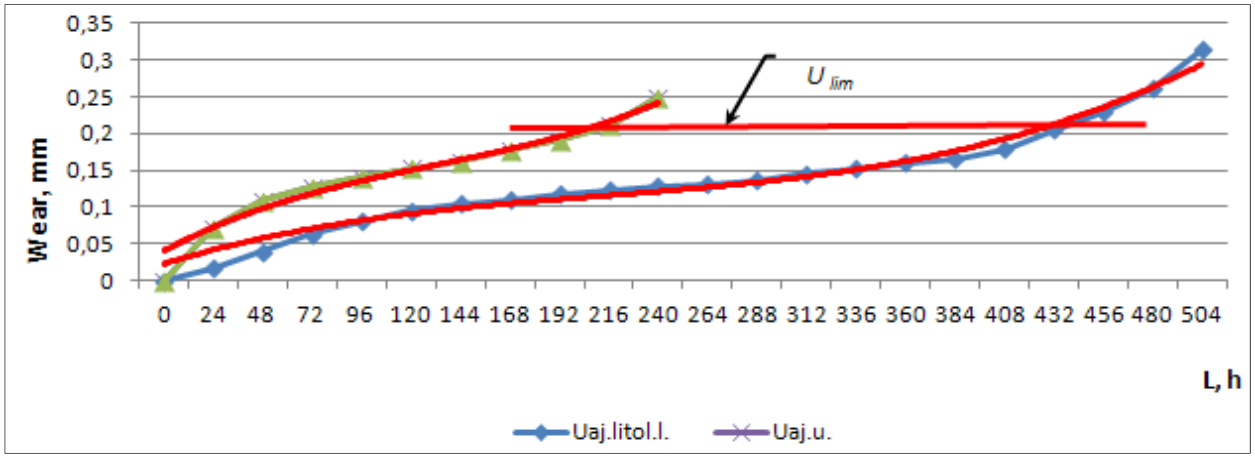

Figure 4. Evolution of wear of tribological co couplings adjustment Ø40H8/e7 tested under dry friction and boundary lubrication with LITOL24 STAS 21150-87: *Test conditions: accelerated tests under cyclic oscillating regim, p = 3,5 MPa, n = 1800 min^{-1} (v = 3,8 m / s, the measurements were carried out at parts temperature of 20 ± 2°C and air relative humidity 60 ... 70%.*

Slower wear of joints tested under boundary lubrication with LITOL can be explained by a few aspects of major importance. On the one hand, can result the obtained tribological characteristics can be the result of increased resistance to wear due to the addition of Mo disulfide, and increased resistance to deformation due to the addition of micro basalt microfibers and glass microspheres, embedded reliably in a polyamidepoxy matrix due to the presence of epoxy oligomer.

On the other hand, the microcavities caused by glass microspheres, provides a more pronounced penetration layer of grease in the superficial layer of semicoupling with PPECM, penetration which increases concomitant with the warming of the contact area. This situation amplifies the storage capacity of the surface layer with heated grease molecules and the ability to maintain for a longer period the grease from the microcavities of the contact area.

The results of the durability tests, carried out by accelerated tests on an exhausted sample consisting of 25 sliding bearing renovated with PPECM with Ø40H8/e7 are shown in figures 5 and 6. The objective of these tests is to simulate the operation of sliding bearings tested in its operating medium. To do this, on the bearings included in the study were applied stress quasi - identical to those appearing in the agricultural machinery during operation. In these tests, the tests were performed up to exhaustion of exploitation resource (appearance of catastrophic play). Sustainability was estimated by resource percentage range of 80 to 90% - values accepted by the technical regulations on farm equipment.

Figure 5 shows that the variation of the resource percentage range of $\gamma = 0,8$ to $\gamma = 0,9$, for bearings tested without lubrication, is 5 hours being within the range 245,5 and 249,5 hours. It is noteworthy that with a probability of 99,9% all of the pieces studied, will operate up to 240 working hours of guaranteed resource continuously.

Plain bearings tested under boundary lubrication with lubricating LITOL24 presents a durability net superior to bearings tested under dry friction. Thus the data presented in figure 6 permit to conclud that for $\gamma = 0,8$ resource percentage range is 434,6 hours and 430,4 hours respectively for $\gamma = 0,9$ hours. In addition, it is found that, with a probability of 99,9%, all parts included in the study have a durability of at least 420 hours.

These results correlate with the data presented in the previous sections and can be explained by the effect of anti-friction of the layer of PPECM.

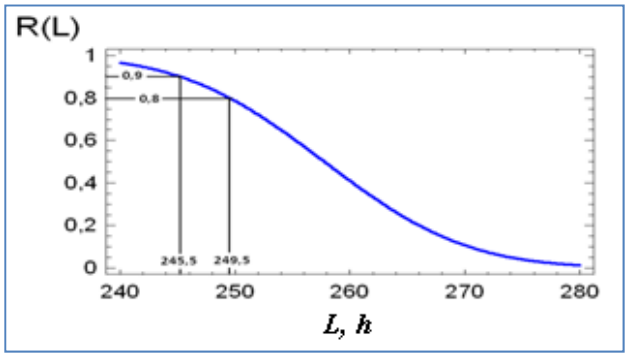

Figure 5. Sustainability percentage range of 80 to 90% of metallpolimers Ø40H8/e7 joints tested under dry friction: *Conditions: accelerated tests under cyclic oscillating, p = 3,5 MPa, n = 1800 min^{-1} (v = 3.8 m/s), measurements were carried out at parts temperature of 20 ± 2°C and air relative humidity of 60 ... 70%.*

After polymerization of the CM, on the surface of the coated part a layer of microdisperse particles of glass microspheres, basalt microfibers and Mo disulfide is formed. In the initial phase of lubricating with greases the later enter in the microcavities on the surfaces of junction parts. In the process of friction, some of the lubricant particles are transferred to microirregularities onto the surface of junction part and the other part into the microcavities on the surface of the covered part storing into them.

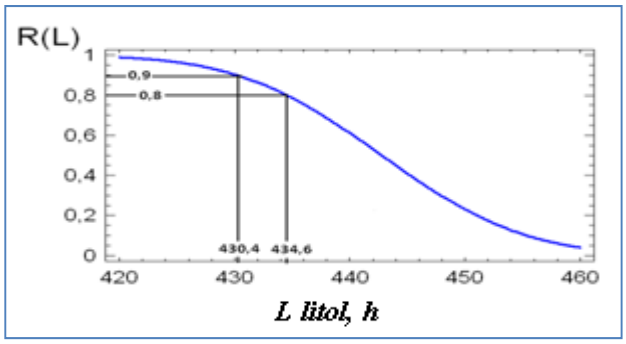

Figure 6. Sustainability percentage range of 80 to 90% of metallpolimers couplings Ø40H8/e7 tested under boundary lubrication with LITOL24: *Conditions: accelerated tests under cyclic oscillating regim, p = 3.5 MPa, n = 1800 min^{-1} (v = 3,8 m/s); measurements were made at parts temperature of 20 ± 2°C and air relative humidity 60 --- 70%.*

In the wear process, the particles of lubricant penetrated into surface microcavities are oriented in parallel to the direction of movement, forming a smooth sliding microfilm. This microfilm is maintained a rather long period due to the amount of lubricant in the cavities formed continuously as a result of appearance of new micropores caused by damage of the glass microspheres.

Here it should be noted that the dispersed particles of the Mo disulphate, with a capacity of solid lubricants also continuously appear in the contact area and they have an influence on the tribological processes of the area.

Since the test bench is designed in such a way that each engine speed to provide an oscillating cycle (on the shaft is installed a cam which, at each rotation, unbalances the shaft on which the bearing is installed). Thus, the shaft speed of 1800min^{-1}, is established that the limit state of bearings operated in the regime of dry friction with a probability of 90% occurs after 26528730 cycles, and of those tested under boundary lubrication regime with LITOL24 - after 46509024 cycles.

Since the law of wear mechanism, followed in previous researches on the evolution of changing parts size ranging and comprehensive of metalpolimer tribocoupplings tested and of that followed in the accelerated reliability test has the same shape (NLD) the obtained results can be validated and compared with operational tests performed on natural components.

3. CONCLUSIONS

1. Experiments carried out on the adhesion of PCM intensively reinforced with hollow glass microspheres confirm that the adhesion of PCM to the matrix of a mixture of polyamide and epoxy oligomers contribute to the increase of adhesion as compared with PCM analogue but with the polyamide matrix in the delivery condition. It has been shown that the addition of epoxy oligomer in a proportion of 30% of the matrix material increases the adhesion of 1,63 times.

2. It was argued the optimal constitution of PPECM on the basis of adhesion tests, hardness, degree of hydrophilicity / hydrophobicity and resistance to wear. It has been shown experimentally that the reinforcement of polyamidepoxy PCM with hollow glass microspheres in an amount up to 30%, practically does not influence the adherence and its stability on carbon steel substrates and toughness, on the contrary - increases, requiring the maximum values in the case of reinforcement with the glass microspheres at the level of 29,9%.

3. On the basis of synthesis of hardness research of designed PPCM it was found that in the case of reinforcement with the glass microspheres, the introduction of the molybdenum disulfide particles decreased the hardness of the composites produced,

while the addition of glass microspheres, on the contrary, increased the hardness, reaching a maximum value at the level of 29,9% of the total volume. The reinforcing with basalt microfibers also resulted in increased hardness, achieving the maximum toughness for the level of 6% of the total volume.

4. It has been shown that intensive alloying of CM with hollow glass microspheres creates favorable conditions for storing lubricants in microcavities formed by respective materials. It was found that the optimum composition that ensures the maximum rate of sorption of water (1,92%) and oil (1,9%) is within the: glass microspheres - 30%, basalt microfibers – 5,3... 5,54% and molybdenum disulfide - 2%.

5. Comparative tests carried out at different temperatures showed that the temperature of the medium in which samples are immersed practically does not influence the rate of oil sorption by the samples made of polyamide in a state of delivery, while samples with heavy reinforced glass microspheres have a slow increase of the oil sorption with increasing of medium temperature.

6. Tribological characterization of laboratory samples of PPECM intensively reinforced with glass microspheres tested under different conditions of friction confirms the assumption that hollow glass microspheres causes less friction in the polymer-metal contact under all conditions of lubrication thanks to storage capacity and maintaining it a longer period of time in the contact area.

7. Based on the monitoring of the friction coefficient and wear it was revealed that:

- in the case of dry friction, samples of PPCM have a coefficient of friction of 1,28 or lower and PPECM samples of 1,23 times less than the control samples (PA 12 in the state of delivery) with a coefficient of reported friction $K_{ppecm}/PA12 = 0,811$;
- in the case of friction under boundary lubrication, the friction coefficient of the PPECM in relation to the material sample (PA 12 in the state of delivery) is 1.6 times lower for the conditions of oil lubrication and 2,38 times lower for lubrication conditions with LITOL 24;
- in the case of friction in conditions of abundant lubrication, the friction coefficient of the PPECM in relation to the material sample (PA 12 in the state of delivery) is 2 times lower for the conditions of lubrication with oil and 1,25 times lower for the conditions of lubricating with LITOL 24.

8. Durability test results, achieved by accelerated tests under boundary lubrication conditions with lubricating LITOL 24, demonstrated a net superior durability of PPECM samples in relation to those tested under dry friction. Thus it was established, with a probability of 99,9% that all parts under study have a durability of at least 420 hours, while those tested under dry friction only 240 continuously working hours.

References

1. Malai L., Marian Gr. *Alegerea şi optimizarea constituției MC polimerice folosite la renovarea îmbinărilor de tip lagăr. În: Ştiința Agricolă. 2011, nr. 2, pp. 50 – 53. ISSN1857-0003.*

2. Țapu V. *Sporirea disponibilității şi mentenabilității îmbinărilor cu joc renovate cu materiale compozite polimerice: Teza de dr. în tehnică: 05.20.03. – Chişinău, 2011, 132 p.*

3. Marian Gr., Malai L., Gorobeț V. *Cercetări cu privire la durabilitatea îmbinărilor de tip lagăr renovate cu materiale compozite polimerice ranforsate intensiv cu microfibre de sticlă. În: Ştiința Agricolă nr. 2, Chişinău, pp. 50 – 53. ISSN1857-0003.*

4. Marian G. *Contribuții teoretico-experimentale la studiul fiabilității pieselor şi îmbinărilor utilajului agricol recondiționate cu compozite pe bază de polimeri: Teza de doctor habilitat în tehnică: 05.20.03. Chişinău, 2005. 252 p.*

5. ***Marian G.*** *Vostanovlenie posadochnyh uzlov elektricheskih mashin poroshkoobraznymi polimernymi kompoziczizami. Teza de doctor habilitat în tehnică: 05.20.03. Chişinău, 163 p.*

6. Frêne J., Nicolas D., Deguerece B., Berthe D., Godet M. *Lubrification hydrodynamique. Paliers et butées, Edition Eyrolles, Paris, France, 1990.*

7. Tochilnikov D.G., Krasnyj V.A., Priemskij L.D., Ginzburg B.M., Bulatov V.P. *Application of polymeric coatings to increase of wear resistance bearing linear operating surface at insufficient lubrication, Soviet Journal of Friction and Wear, 13, 1992, pp 689-694.*

8. Deleanu L., Birsan I.G., Andrei G., Rîpă M., Badea P. *2007, PTFE Composites and Water Lubrication. I. Tribological Characterisation, Materiale Plastice 44, (1), pp. 66-71.*

9. Ciortan S., Rîpă M., Chiculiță S., Spânu C. *Shear Stability as Oils' Performance Indicator, The annals of University "Dunărea De Jos" of Galați, Fascicle VIII, Tribology, 2008 (XIV), pp. 175-178.*

10. Preda A., Rîpă M., Miculescu F., Dulea G. *Structure Effects Over Behavior of Graphite Gray Iron in Running, The Annals of "Dunarea de Jos" University of Galati. Fascicle IX Metallurgy and Materials Science, No. 2 – 2008, pp. 126-130.*

11. Nel'son U.E. *Tehnologiza plastmass na osnove poliamidov. Himiya, 1989, 256 s.*

Recommended for publication: 22.01.2013.

OPTIMAL SYNTHESIS AFTER GEOMETRY IN ANTENNA TECHNIQUE

[1]PhD, associate professor M. Perebinos, [2]PhD I. Andries
[1]Technical University of Moldova, Chisinau
[2]State University of Moldova, Chisinau

1. INTRODUCTION

1.1. Antenna optimal synthesis after geometry

The antenna synthesis problem, generally speaking, is a problem of finding such a spatial distribution of electromagnetic field sources, that generate the desired radiation pattern. It means the determination of the *geometry structure* of a radiating system, as well as the *current distribution* on this structure.

The basic electrodynamic relation, connecting the involved functions is the integral equation of the first kind

$$\hat{A}z = f, \qquad (1)$$

where $z = z(x), x \in G$ is the current distribution in the region *G,* occupied by antenna; $f = f(\omega), \omega \in \Omega$ is antenna pattern as a function of spherical angles $\{\theta, \varphi\}$. The integral operator $\hat{A}$ is determined by the antenna geometry *G.* Equation (1) is just the equation that is traditionally used as the model of antenna synthesis problem, being reduced to a standard mathematically abstracted *inverse problem for current distribution* along the fixed geometry and solved then by Tihonov's regularization methods [1-3]. However, the current distribution can't be an independently variating function physically. As such functions can be only antenna geometry and excitation function, i.e. incident electromagnetic field or voltage of $\delta -$ functional generator. The equation (1) does not contain the excitation function and thus, the based on it model must be treated physically incomplete. The result is that the practical realization of the obtained current distribution remains to be a separate not at all simple engineering problem. As to *optimal* antenna synthesis, some formulations of quasi-optimal or optimal synthesis were proposed [3], but all of them were obtained within the framework of regularization method and are like a many-parametric variation method, which is not properly speaking an optimization method. Furthermore, in view of mathematical difficulties, the deviation of synthesized pattern f from the desired one f_0 is considered in the least mean square sense (L_2 norm), which is not only one of practical importance. The type of closeness to desired function must be an engineering decision since it will govern the performance of the antenna being synthesized. From the practical standpoint, more important is the closeness estimation in sense of difference $/ f - f_0 /$ |for all directions (L_∞, norm). As a deficiency of the based on equation (1) approach also must be considered the unjustified difficulties, arising via necessity to carry out the regularization of mathematically instable inverse problem

1.2. A new statement of antenna optimal synthesis 1y geometry problem

As it was pointed above, the relation (1) is not enough for optimal synthesis by geometry problem formulation because it does not contains the mechanism of antenna excitation that is why we first of all complete it with integral equation of the type

$$\hat{B}z = \varphi, \qquad (2)$$

It explicitly describes the relationship between current distribution function $z = z(x), x \in G$ and excitation operator function $\varphi = \varphi(x), x \in G$. The integral operator $\hat{B}$ is determined by the physical part of problem and the geometrical form. In case of thin wire antennas (2) may be the well-known Hallen's or Poclington's equation [4]. In general case it is an integral relation between incident electromagnetic field and induced current distribution.

The system of equations (1) - (2) is thus physically complete, since describes both the excitation and radiation processes, including geometry. Basing on it we can correctly formulate different statements of antenna optimal synthesis problem: optimal pattern synthesis by geometry, optimal pattern synthesis by excitation, combined statements.

Consider further the optimal synthesis by geometry. Let $\rho_i(t)$ be a set of continuous parametric functions describing the geometric form - axial line for thin wire structures, contour of revolution for rotational symmetry shells. The problem is to find a set of $\rho_i(t)$ such that for a given excitation mechanism the corresponding antenna pattern will possess desired characteristics. To give it a standard form of optimal

control problem the following system of differential equations is introduced

$$\begin{cases} \dfrac{d\rho_i}{dt} = u_i(t), \alpha \le t \le \beta; \\ \rho_i(\alpha) = \rho_i^0, i = 1,2,... \end{cases} \quad (3)$$

This system plays part of state equations dynamical controi system respect to functions $\rho_i(t)$, as the state or phase variables. Totality of quantities $\{u_i(t), \rho_i^0\}$ is declared as control, since it uniquely determines the functions $\rho_i(t)$, i.e. the geometrical form of radiating system. Knowing $\rho_i(t)$, one can derived all the electrodynamtc characteristics, using equations (1) - (2) in direct calculations. From the optimal control theory point of view, the operator equations (l) - (2) play role of the bond equations. Note that they are integral equations, but no inverse problem arises here. The optimal synthesis problem is formulated thus under the scheme: on the multitude of system (3) solutions to find the extremum of functional F_0 under conditions $F_k \le 0$, or

$$\begin{cases} F_0[u_i(t), \rho_i^0] \to extremum; \\ F_k[u_i(t), \rho_i^0] \le 0, k = 1,2,... \end{cases} \quad (4)$$

As a quality functional F_0 any expressions derived from synthesized and desired pattern can be chosen. The restrictions $F_k \le 0$ also can be of any kind concerning the pattern, as we D as the current distribution or geometricaL dimensions. Concrete expressions of F_0, F_k bond equations (1)-(2) and state equations (3) allow us to express the variations of these functionalize on geometrical form by the variations on control $\{u_i(t), \rho_i^0\}$. Thus, different concrete problems can be resolved in strict accordance with engineering desires: minimization of sideiobes and main beam area by arbitrary geometrical restrictions, beam-peak maximization by any restrictions on pattern and s.a.

The formulated problem of optimal control can be easy reduced to a straight non-linear problem of mathematical programming in functional space and numerically solved using the consecutive linearization method [5]. this approach both closeness estimation between synthesised and desired pattern can be admitted: in L_2 norm and in L_∞ norm.

2. OPTIMAL SYNTHESYS OF ROTATIONAL SYMMETRY SHELLS

2.1. Problem formulation

Consider for certainty the rotational symmetry problem of excitation of a conducting shell magnetic dipole irradiator as shown Figure 1. The non-zero field components in this case of E - polarization are E_φ, H_r, H_z. The shell is described by rotated contour Γ in vector-parametrical form

$$\vec{r}(t) = \vec{i}_\rho \rho(t) + \vec{i}_z \xi(t), \alpha \le t \le \beta. \quad (4)$$

The pattern of such radiating system is

$$f(\omega) = f^{(i)}(\omega) + f^{(s)}(\omega), \omega \in \{\vartheta, \varphi\} \quad (5)$$

where $f^{(i)}(\omega)$ is the known pattern of irradiator, $f^{(s)}(\omega)$ the pattern of induced on shell current *distribution* $j(t)$

$$f^{(s)}(\omega) = \int_\alpha^\beta \Phi[\rho(t), \xi(t), \dot{\rho}(t), \dot{\xi}(t), \omega] j(t) dt. \quad (6)$$

Here $\Phi[...]$ is a known complex function and $j(t)$ is the solution of integral equation [6]:

$$\int_\alpha^\beta K(t,\tau) j(t) dt = \hat{\varphi}(\tau), \alpha \le \tau \le \beta. \quad (7)$$

$$K(t,\tau) = i\rho(t) s(t) \sqrt{\dot{\rho}^2(t) + \dot{\xi}^2(t)} \int_a^b \frac{e^{-ikL}}{L} \cos\varphi d\varphi, \quad (8)$$

$$L = \{\rho^2(t) + \rho^2(\tau) - \rho(t)\rho(\tau)\cos\varphi + [\xi(t) - \xi(\tau)]^2\}^{1/2}, \quad (9)$$

where $k = 2\pi/\lambda$ is the wave number, λ - wave length. The excitation function $\hat{\varphi}(\tau)$ for magnetic dipole (round current frame) is

$$\hat{\varphi}(\tau) = \frac{\rho(t)}{R_0^2}\left(k - \frac{i}{R_0}\right) e^{-ikR_0}, \quad (10)$$

$$R_0 = \{\rho^2(t) + [\xi(\tau) - H]^2\}^{1/2}, \quad (11)$$

where H is the coordinate z value of dipole. The function $s(t)$ in (8) is determined by the edge condition for $\boldsymbol{E}$ - polarization [6]

$$s(t) = \frac{1}{\sqrt{(t-\alpha)(\beta-t)}}. \quad (12)$$

From expressions (5)-(11) it is seen that adjusting the contour Γ, i.e. variating the functions $\rho(t), \xi(t)$ provides the variation of the pattern $f(\omega)$. Naturally arises the possibility of choosing such a

contour Γ, that $f(\omega)$ would be optimal in some sense.

Let us discuss the kind of conditions and restrictions that may occur in problem of optimal synthesis by geometry from engineering standpoint. First group of restrictions is concerned to geometric structure. For example, the inequalities

$$\max_t / \rho(t) / \le K_\rho, \max_t / \xi(t) / \le K_\xi, \quad (13)$$

$$\max_t / \dot{\rho}(t) / \le K_{\dot\rho}, \max_t / \dot{\xi}(t) / \le K_{\dot\xi}, \quad (14)$$

restrict the spatial position and the curvature of the contour Γ correspondingly. Coefficients K_ρ, K_ξ, $K_{\dot\rho}$, $K_{\dot\xi}$ are the given quantities. It assumed that $\rho(t), \xi(t)$ have continuous derivate not turning into zero

$$\begin{cases} \rho^-(t) \le \rho(t) \le \rho^+(t), \\ \xi^-(t) \le \xi(t) \le \xi^+(t), \alpha \le t \le \beta \end{cases} \quad (15)$$

keep the contour Γ in some space corridor limited by curves $\{\rho^-(t), \xi^-(t)\}$ and $\{\rho^+(t), \xi^+(t)\}$.

The end points α, β of contour Γ can be fixed or not fixed. For the free end point the restrictions on its possible position should be specified

$$\begin{cases} \rho^-(\alpha) \le \rho(\alpha) \le \rho^+(\alpha), \\ \xi^-(\alpha) \le \xi(\alpha) \le \xi^+(\alpha). \end{cases} \quad (16)$$

At last, to avoid electrical contact between the conducting shell and the irradiator the minimum distance (11) between them must be required to be more then or equal to a given quantity $\boldsymbol{K_H > 0}$

$$\min_t R_0(t) \ge K_H, \alpha \le t \le \beta. \quad (17)$$

The second group of restrictions is related to antenna pattern form. They can be of a large diversity and be applied to a part ofpattern coinciding with main beam area Ω_M or with sidelobes area Ω_S as well as to the total pattern. The more natural for practice are the restriction

$$\max / f(\omega) / < K_S, \omega \in \Omega_S, \quad (18)$$

$$\max / f(\omega) / > K_M, \omega \in \Omega_M, \quad (19)$$

where K_S , K_M are the given quantities. Last restriction can be substituted for more rigorous one

$$\max // f(\omega) / - f_0(\omega) / < K_0, \omega \in \Omega_M, \quad (20)$$

where $f_0(\omega)$ is the needing function. The restrictions can be also applied to different functions on pattern such as directivity or antenna gain.

As quality functionals which must be minimized we can choose one from foHowing expressions

$$F_0 = \int_{\Omega_M} | f(\omega) |^2 d\omega, \quad (21)$$

$$F_0 = \int_{\Omega_S} || f(\omega) - f_0(\omega) |^2 d\omega, \quad (22)$$

$$F_0 = \max_{\omega \in \Omega_M} || f(\omega) | - f_0(\omega) \quad (23)$$

The physical sense ofthem is obvious.

Finally formulate a possible statement of pattern optimal synthesis for geometry. On the totality of solutions of the differential equations system

$$\begin{cases} \dfrac{d\rho}{dt} = u(t), \\ \rho(\alpha) = \rho^0, \end{cases} \quad \begin{cases} \dfrac{d\xi}{dt} = v(t), \\ \xi(\alpha) = \xi^0, \end{cases} \alpha \le t \le \beta, \quad (24)$$

with $\rho(t), \xi(t)$ being the components of vector-parametrical form of contour Γ, to minimize the functional

$$F_0[u, v, \rho^0, \xi^0] = \int_{\Omega_S} | f(\omega, u, v, \rho^0, \xi^0) |^2 d\omega, \quad (25)$$

under the conditions:

$$F_1[u, v, \rho^0, \xi^0] = K_M - \max_{\omega \in \Omega_M} | f(\omega, u, v, \rho^0, \xi^0) | \le 0, \quad (26)$$

$$F_2[u, v, \rho^0, \xi^0] = \rho(\beta) - \rho^1 = 0, \quad (27)$$

$$F_3[u, v, \rho^0, \xi^0] = \xi(\beta) - \xi^1 = 0, \quad (28)$$

$$F_4[u, v, \rho^0, \xi^0] = \max_t \rho(t) - K_\rho \le 0, \quad (29)$$

$$F_5[u, v, \rho^0, \xi^0] = -\max_t \rho(t) < 0, \quad (30)$$

$$F_6[u, v, \rho^0, \xi^0] = \max_t | \xi(t) | - K_\xi \le 0, \quad (31)$$

$$F_7[u, v, \rho^0, \xi^0] = -\min_t R_0(t) + K_1 \le 0 \quad (32)$$

if $\{u, v, \rho^0, \xi^0\} \in \Delta$, where Δ is determined by the conditions

$$\begin{cases} | u(t) | \le K_{\dot\rho}, \\ | \rho^0 | \le K_{\rho^0}, \end{cases} \quad \begin{cases} | v(t) | \le K_{\dot\xi}, \\ | \xi^0 | \le K_{\xi^0}, \end{cases} \quad (33)$$

The so formulated optimal synthesis problem in form of optimal control problem can be reduced to a non-linear problem of mathematical programming in functional space. For numerical solution the sequential linearization method [7] is used.

2.2. Calculation of functionals variations

The explicit form of functionals F_i allows relatively easy to deduce the expressions for δF_i in form of a linear functional on all components of variation of trajectory $\{\delta u, \delta v, \delta\rho^0, \delta\xi^0, \delta\rho, \delta\xi, \delta j, \delta f\}$. These expressions must be transformed by substitution the terms with $\delta\rho, \delta\xi, \delta j, \delta f$ for others equal them and containing only the variations of control $\{\delta u, \delta v, \delta\rho^0, \delta\xi^0\}$ This is possible since the variations $\delta\rho, \delta\xi, \delta j, \delta f$ are completely determined through $\{\delta u, \delta v, \delta\rho^0, \delta\xi^0\}$ by virtue of:

- "*Equations in variations*"

$$\begin{cases} \dfrac{d\delta\rho}{dt} = \delta u(t), \\ \delta\rho(\alpha) = \delta\rho^0, \end{cases} \quad \begin{cases} \dfrac{d\delta\xi}{dt} = \delta v(t), \\ \delta\xi(\alpha) = \delta\xi^0, \end{cases} \quad \alpha \le t \le \beta, \tag{34}$$

$$\delta f^S(\omega) = \int_\alpha^\beta \Phi(t,\omega)\delta j(t)dt + \int_\alpha^\beta \Phi_\rho(t,\omega) j(t)\delta\rho(t)dt +$$
$$+ \int_\alpha^\beta \Phi_\xi(t,\omega) j(t)\delta\xi(t)dt + \int_\alpha^\beta \Phi_u(t,\omega) j(t)\delta u(t)dt + \tag{35}$$
$$+ \int_\alpha^\beta \Phi_v(t,\omega) j(t)\delta v(t)dt$$

- "*Lagrangian identity*"

$$\int_\alpha^\beta \left\{ (\Psi_\rho \frac{d\delta\rho}{dt}) + (\Psi_\xi \frac{d\delta\xi}{dt}) + (\frac{d\Psi_\rho}{dt}\delta\rho) + (\frac{d\Psi_\rho}{dt}\delta\rho) \right\} dt = \tag{36}$$
$$= (\Psi_\rho \delta\rho)\Big|_\alpha^\beta + (\Psi_\xi \delta\xi)\Big|_\alpha^\beta,$$

- "*Integral equation in variations*"

$$\int_\alpha^\beta \{K(t,\tau)\delta j(t) + Q_1(t,\tau)\delta\rho(t) + Q_2(t,\tau)\delta\xi(t)\}dt +$$
$$+ Q_3(\tau)\delta\rho(\tau) + Q_4(\tau)\delta\xi(\tau) +$$
$$\int_\alpha^\beta \{Q_5(t,\tau)\delta u(\tau) + Q_6(t,\tau)\delta v(\tau)\}dt - \tag{37}$$
$$- P_\rho(\tau)\delta\rho - P_\xi(\tau)\delta\xi = 0, \alpha \le \tau \le \beta,$$

which is obtained by variation (7) under procedure analogous that described in [8]. Here ω belongs the range of definition for $f(\omega)$ and

$Q_i, i = 1,2,3,4,5,6, P_\rho, P_\xi$ are

$$Q_1(t,\tau) = K_{\rho_t}(t,\tau) j(t),$$
$$Q_2(t,\tau) = K_{\xi_t}(t,\tau) j(t),$$
$$Q_3(\tau) = \int_\alpha^\beta K_{\rho_\tau}(t,\tau) j(t)dt,$$
$$Q_4(\tau) = \int_\alpha^\beta K_{\xi_\tau}(t,\tau) j(t)dt,$$
$$Q_5(t,\tau) = K_u(t,\tau) j(t), \tag{38}$$
$$Q_6(t,\tau) = K_v(t,\tau) j(t),$$
$$P_\rho(\tau) = \varphi_{\rho_\tau}(\tau),$$
$$P_\xi(\tau) = \varphi_{\xi_\tau}(\tau),$$

where the indices $\rho_t, \rho_\tau, \xi_t, \xi_\tau$ mean partial derivates with respect to corresponding function in kernel $K(t,\tau)$ or in right part of $\varphi_{\rho_\tau}(\tau)$.

The technique of calculation the functional derivates is more convenient to demonstrate for the functional (25) as an example. In this case the calculations embrace all typical chain elements of dependences and are realized in following order:

- Having $\{u, v, \rho^0, \xi^0\}$ calculate $\rho(t), \xi(t)$ from (24);
- Solving (7) than determine $j(t)$;
- Further calculate $f(\omega)$ using (5) and;
- Finally functional $F[u, v, \rho^0, \xi^0]$ using (25).

The calculations of functional variations are realized in invers order:

1. First, the straight variation of (25) gives

$$\delta F_0[u,v,\rho^0,\xi^0] = \int_{\Omega_S} \{\bar{f}(\omega)\delta f(\omega) + f(\omega)\delta\bar{f}(\omega)\}d\omega \tag{39}$$

Obviously, if is enough in the following to express through $\delta u, \delta v, \delta\rho^0, \delta\xi^0$ only the first term in (39), since the second one is obtained by analogy with it.

2. Variating (5), we obtain the equation in variations $(\delta f(\omega) = 0)$

$$\delta f(\omega) = \int_\alpha^\beta \Phi(t,\omega)\delta j(t)dt + \int_\alpha^\beta \Phi_\rho(t,\omega) j(t)\delta\rho(t)dt +$$
$$+ \int_\alpha^\beta \Phi_\xi(t,\omega) j(t)\delta\xi(t)dt + \int_\alpha^\beta \Phi_u(t,\omega) j(t)\delta u(t)dt + \tag{40}$$
$$+ \int_\alpha^\beta \Phi_v(t,\omega) j(t)\delta v(t)dt$$

We are interesting though in integral on $\bar{f}(\omega)\delta f(\omega)$. It is obviously that

$$\int_{\Omega_S} \bar{f}(\omega)\delta f(\omega)d\omega = \int_\alpha^\beta \hat{\Phi}(t)\delta j(t)dt + \int_\alpha^\beta \hat{\Phi}_\rho(t)\delta\rho(t)dt + \\ + \int_\alpha^\beta \hat{\Phi}_\xi(t)\delta\xi(t)dt + \int_\alpha^\beta \hat{\Phi}_u(t)\delta u(t)dt + \int_\alpha^\beta \hat{\Phi}_v(t)\delta v(t)dt, \quad (41)$$

where

$$\hat{\Phi}(t) = \int_{\Omega_S} \bar{f}(\omega)\Phi(t,\omega)\, j(t)d\omega, \text{ and s.o.}$$

3. The following step is to transform $\int_\alpha^\beta \hat{\Phi}(t)\delta j(t)dt$ into integral on $\delta\rho, \delta\xi, \delta u, \delta v$. It is achieved by using the "integral equation in variations" (37). Multiplying (37) by a function $P(t)$, which will be defined bellow, integrating on *t,* changing the order of integration, denoting *t* through τ and vice versa, we obtain the expression

$$\int_\alpha^\beta R_0(\tau)\delta j(\tau)d\tau + \int_\alpha^\beta R_\rho(\tau)\delta\rho(\tau)d\tau + \\ \int_\alpha^\beta R_\xi(\tau)\delta\xi(\tau)d\tau + \int_\alpha^\beta R_u(\tau)\delta u(\tau)d\tau + \quad (42) \\ + \int_\alpha^\beta R_v(\tau)\delta v(\tau)d\tau = 0,$$

which we name the "*Lagrangian identity*" for integral equation in variations (37). Here

$$R_0(\tau) = \int_\alpha^\beta K^*(t,\tau)P(t)dt, K^*(t,\tau) = \overline{K}(\tau,t), \\ R_\rho(\tau) = \int_\alpha^\beta Q_1(t,\tau)P(t)dt + Q_3(\tau)P(\tau) - P_\rho(\tau)P(\tau), \\ R_\xi(\tau) = \int_\alpha^\beta Q_2(t,\tau)P(t)dt + Q_4(\tau)P(\tau) - P_\xi(\tau)P(\tau), \quad (43) \\ R_u(\tau) = \int_\alpha^\beta Q_5(t,\tau)P(t)dt, R_v(\tau) = \int_\alpha^\beta Q_6(t,\tau)P(t)dt.$$

Now concretize the choice of $P(t)$ talking it as a solution of integral equation

$$\int_\alpha^\beta K^*(t,\tau)P(t)dt = \Phi(\tau), \alpha \le \tau \le \beta. \quad (44)$$

Then (42) obviously gives the expression of integral on $\delta j(t)$ to be found, through the integrals on $\delta\rho, \delta\xi$ and $\delta u, \delta v$

$$\int_\alpha^\beta \hat{\Phi}(t)\delta j(t)dt = -\int_\alpha^\beta R_\rho(\tau)\delta\rho(\tau)d\tau - \\ - \int_\alpha^\beta R_\xi(\tau)\delta\xi(\tau)d\tau - \int_\alpha^\beta R_u(\tau)\delta u(\tau)d\tau - \quad (45) \\ - \int_\alpha^\beta R_v(\tau)\delta v(\tau)d\tau.$$

Making the substitution of $\int_\alpha^\beta \hat{\Phi}(t)\delta j(t)dt$ for that from (41) we obtain

$$\int_{\Omega_S} f(\omega)\delta f(\omega)d\omega = \int_\alpha^\beta \hat{R}_\rho(\tau)\delta\rho(\tau)d\tau + \\ \int_\alpha^\beta \hat{R}_\xi(\tau)\delta\xi(\tau)d\tau + \int_\alpha^\beta \hat{R}_u(\tau)\delta u(\tau)d\tau + \quad (46) \\ + \int_\alpha^\beta \hat{R}_v(\tau)\delta v(\tau)d\tau,$$

where

$$\hat{R}_\rho(\tau) = \hat{\Phi}_\rho(\tau) - R(\tau), \text{ and s.o.}$$

In the same way for $\int_{\Omega_S} f(\omega)\overline{\delta f(\omega)}d\omega$ we obtain

$$\int_{\Omega_S} f(\omega)\overline{\delta f(\omega)}d\omega = \int_\alpha^\beta \hat{R}^*_\rho(\tau)\delta\rho(\tau)d\tau + \\ \int_\alpha^\beta \hat{R}^*_\xi(\tau)\delta\xi(\tau)d\tau + \int_\alpha^\beta \hat{R}^*_u(\tau)\delta u(\tau)d\tau + \quad (47) \\ + \int_\alpha^\beta \hat{R}^*_v(\tau)\delta v(\tau)d\tau,$$

Here $\hat{R}^*_\rho(\tau) = \overline{\hat{R}^*_\rho(\tau)}$ and s.o. From (46), (47) and (39) we have

$$\delta F[\delta u, \delta v, \delta\rho^0, \delta\xi^0] = \int_\alpha^\beta R(\tau)\delta\rho(\tau)d\tau + \\ + \int_\alpha^\beta \Xi(\tau)\delta\xi(\tau)d\tau + \int_\alpha^\beta U(\tau)\delta u(\tau)d\tau + \quad (48) \\ + \int_\alpha^\beta V(\tau)\delta v(\tau)d\tau,$$

where

$$R(\tau) = 2\,\mathrm{Re}\,\hat{R}_\rho(\tau), \Xi(\tau) = 2\,\mathrm{Re}\,\hat{R}_\xi(\tau), \\ U(\tau) = 2\,\mathrm{Re}\,\hat{R}_u(\tau), V(\tau) = 2\,\mathrm{Re}\,\hat{R}_v(\tau), \quad (49)$$

4. The final step of transformations consists in expressing integrals with $\delta\rho, \delta\xi$ through integrals on $\delta u, \delta v, \delta\rho^0, \delta\xi^0$.

Using the equation in variations (34), Lagrangian identity (36) and specifying functions $\Psi_\rho(t), \Psi_\xi(t)$ as the solutions of the systems

$$\begin{cases} \dfrac{d\Psi_\rho(t)}{dt} = -R(t), \\ \Psi_\rho(\alpha) = 0, \end{cases} \quad \begin{cases} \dfrac{d\Psi_\xi(t)}{dt} = -\Xi(t), \\ \Psi_\xi(\alpha) = 0, \end{cases} \tag{50}$$

on the interval $\alpha \le t \le \beta$ obtain the final expression for δF

$$\delta F[\delta u, \delta v, \delta\rho^0, \delta\xi^0] = \int_\alpha^\beta W_u(\tau)\delta u(\tau)d\tau + \int_\alpha^\beta W_v(\tau)\delta v(\tau)d\tau + a\delta\rho^0 + b\delta\xi^0, \tag{51}$$

where

$$\begin{cases} W_u(t) = \Psi_\rho(t) + U(t), \\ a = \Psi_\rho(\alpha) \end{cases} \quad \begin{cases} W_v(t) = \Psi_\xi(t) + V(t), \\ b = \Psi_\xi(\alpha) \end{cases} \tag{52}$$

All calculations are making of course on a not "perturbed trajectory" $\{u, v, \rho^0, \xi^0, j, f\}$.

The derivatives evaluation for other functional being by Freshe differentiable are making by the some scheme.

As to functionals being only by Gato differentiable (by directions in functional space) the approximation described in [5,8] is used. The main elements of this approximation are directional derivatives of functionals like

$$F[u, v, \rho^0, \xi^0] = |f(\omega^*)|, \tag{53}$$

where ω^* is a point in range of definition of $f(\omega^*)$. The evaluation of derivatives for such functional differs from above described scheme only in that the equation (44) must be solved with the right part of the form

$$A(t) \to \frac{f(\omega^*)}{|f(\omega^*)|} F(t, \omega^*), \tag{54}$$

The solvability of formulated problem of mathematical programming in functional space is proofing by references to theorems of extremum theory. That is about existence. As to uniqueness, in similar problems it is not essential: even if the solution is not unique, we satisfy with any optimal one.

3. NUMERICAL RESULTS

The formulated problem was numerically solved using the programme, described in detail in [7]. Its adaptation is connected with discrete approximation of the continuous problem. As a result a set of FORTRAN programmes was elaborated which allows to synthesize the radiating surfaces of revolution by any conditions on geometry form and on antenna pattern.

Figure 1, a shows the geometry. As a primary radiator a magnetic dipole is chosen, but it is not a serious restriction since any excitation with axial symmetry can be used. The function $\varphi(\tau)$ in right part of (7) will be changed only. Figure 1,b – pattern, Figure 1,c - geometry.

In **Figure 2** are represented the results of synthesis a surface having the pattern of a disk. So, the main bim is demanded to be in range $\Omega_M = [20^0, 80^0]$. The end points of contour Γ are fixed at $\{\rho(\alpha), \xi(\alpha)\} = (0;0)$; $\{\rho(\beta), \xi(\beta)\} = (1;0)$. So as the control is the set $\{u(t), v(t)\}$. Initial control $\{u^0(t), v^0(t)\}$ satisfies (30) and initial geometric form is a cone with cone angle **45°**. The synthesized surface is very close to that of a disk and synthesized pattern is also close to a disk pattern. The result was achieved on 11-s iteration of the sequential linearization method.

As the second example (**Figure 3**) was chosen the problem (23)-(33) with fixed end points of contour Γ. The purpose was to synthesize the surface with pattern in region $\Omega_M = [150^0, 170^0]$ Initial control $\{u^0(t), v^0(t)\}'$ satisfies (30). In **Figure 3a** and **Figure 3b** are represented the pattern and the corresponding contours Γ after 1-t, 6-s and 12-s iteration. The synthesized pattern satisfies the conditions and the synthesized surface has a smooth character so that easy can be reproduced technically.

In **Figure 4** are represented the results of contour synthesis with free end point $|\rho(\alpha), \xi(\alpha)\}$. The control in this case is $\{u^0(t), v^0(t), \rho^0, \xi^0\}$ The desired pattern must be in region $\Omega_M = [4^0, 24^0]$ The initial control satisfies (33). In **Figure 4a** and **Figure 4b** are represented the patterns and contours after 1-t, 10-s and 12-s iteration correspondingly. The obtained surface as in previous case is smooth enough. The represented results demonstrate the wide possibilities of the proposed here technique for solving the antenna pattern optimal synthesis for geometry problem.

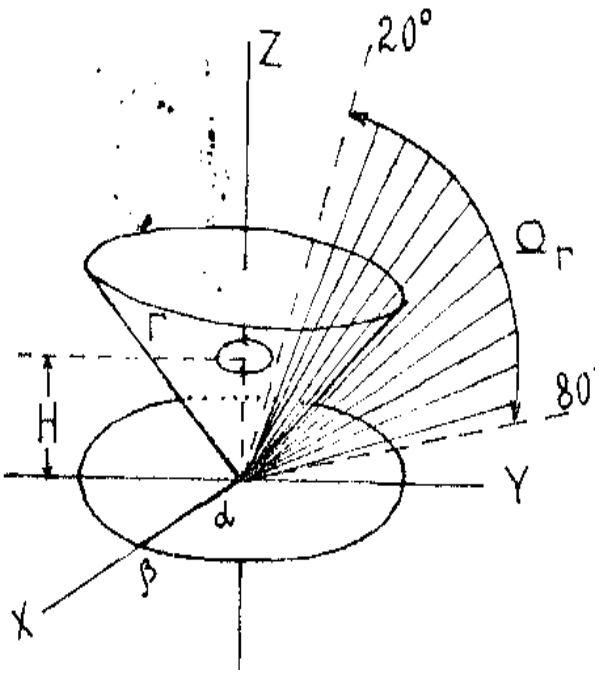

a.

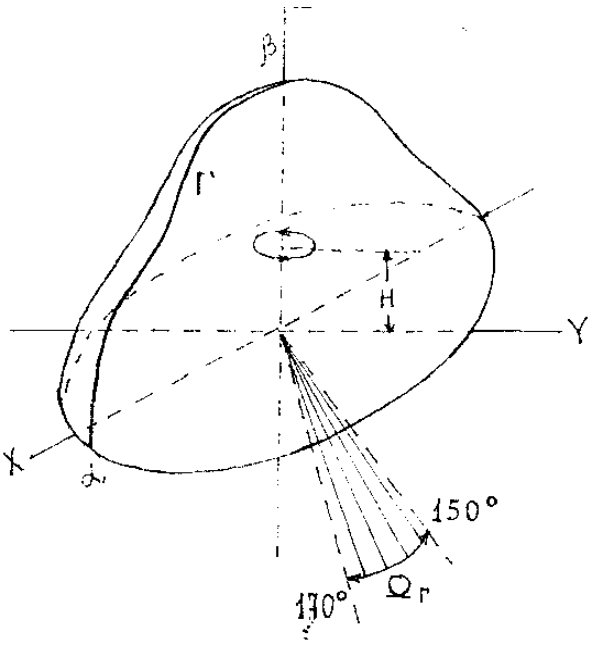

Figure 2. The results of synthesys a surface having a pattern of a disk.

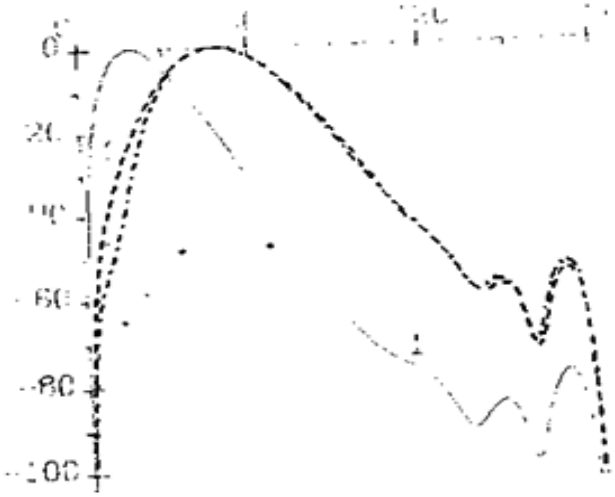

b.

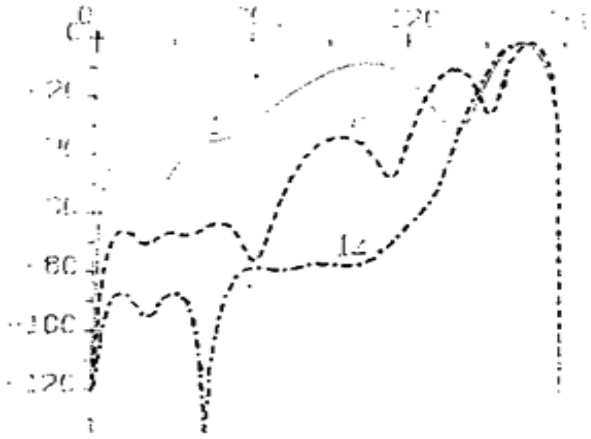

a.

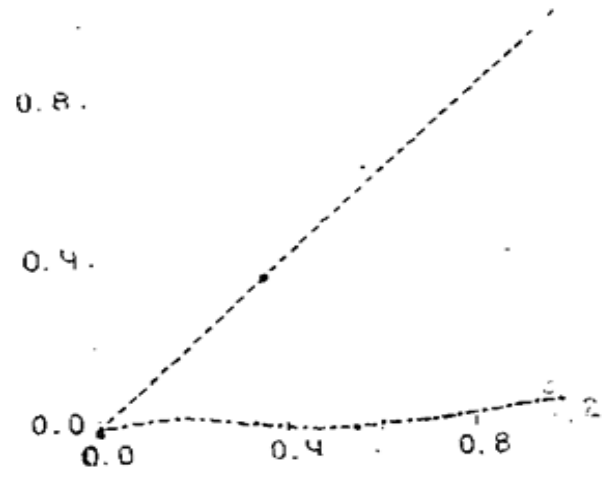

c.

Figure 1. Initial surface area has been used the surface area of the cone: *a – magnetic dipole; b – pattern; c - geometry*.

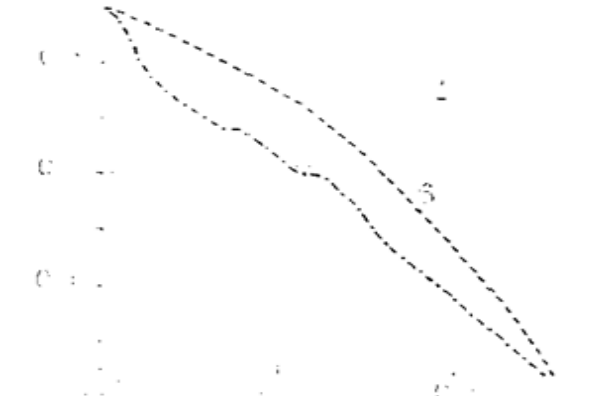

b.

Figure 3. Magnetic dipole under the surface with fixed point of the coutour Γ : *a – pattern; b – geometry.*

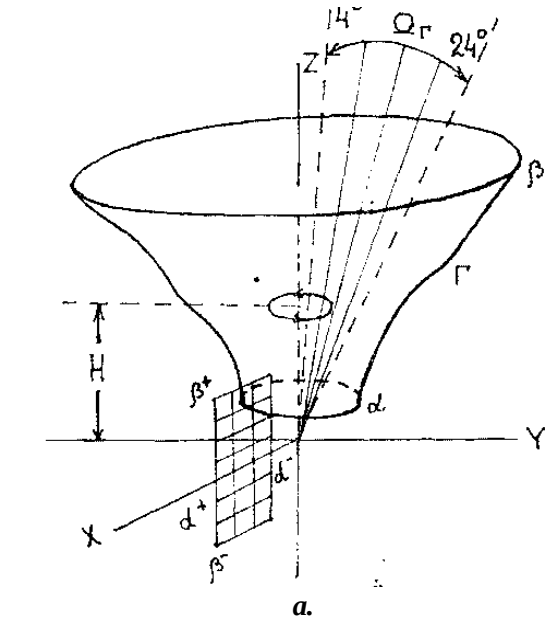

a.

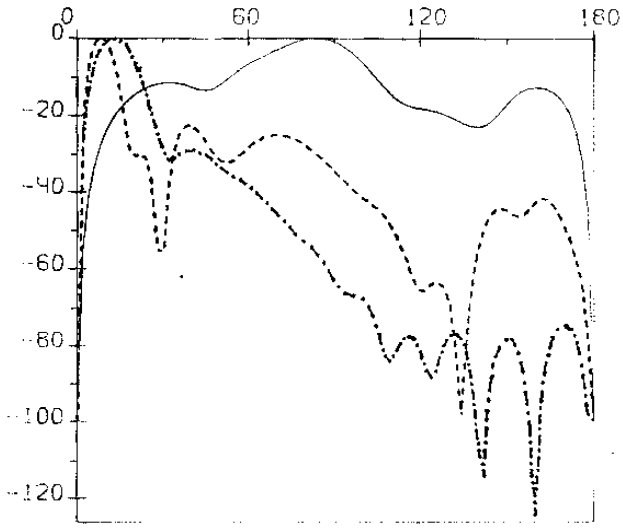

b.

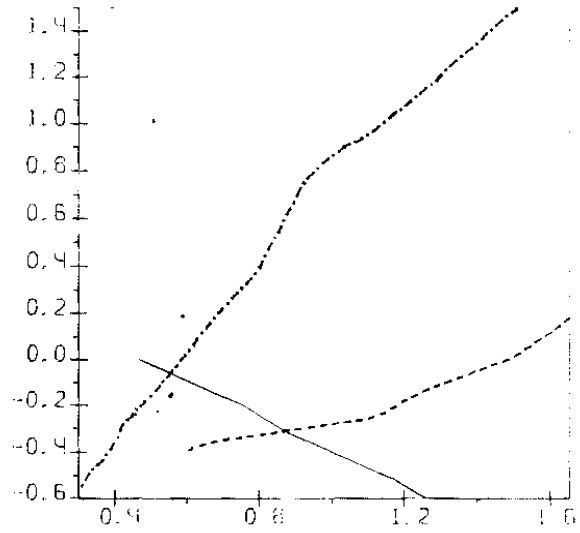

c.

Figure 4. *a - geometry with free end point of contour Γ ; the results of synthesys a surface: b – pattern; b - geometry.*

Bibliography

1. ***L.D.Bahrah, S.B.Cremenetcky.*** *Synthesis of Radiating Systems. Moscow: Sovradio, 1974 (in Russian).*
2. ***A.N.Tihonov, V.I.Dmitriev.*** *About methods of solving the inverse antenna theory problem", Numerical Methods ami Programming, vol. 13, pp. 209-214, 1969. Moscow: Moscow University (in Russian).*
3. ***V.I.Dmitriev, E.V.Zaharov, A.S.Ilinsky, A.G.Sveshnicov.*** *The inverse problems of electrodynamics, in Incorrect Problems in Natural Sciences, A.N.Tihonov and A.V.Goncharsky, Ed-s. Moscow: Moscow University, 1987 (in Russian).*
4. ***K.K.Mei.*** *On the integral equations of thin wire antennas", IEEE, vol. AP-13, no. 3, pp. 374-378, 1965.*
5. ***R.P.Fedorenco.*** *Approximate Solution of Optimal Control Problems. Moscow: Nauka, 1978 (in Russian).*
6. ***E.V.Zaharov, Yu.V.Pirnenov.*** *Numeric Analysis in Radio Waves Diffraction. Moscow: Radio i Sviazi, 1982 (in Russian).*
7. ***R.P.Fedorenco.*** *About an algorithm of solving the mathematical programming problems", J. Comput. Math. and Math. Phys., vol. 22, pp. 1331-1343, 1982 (in Russian).*
8. ***M.F.Perebinos, R.P.Fedorenco.*** *The mathematical programming methods in antenna optimal synthesis, Comput. Math. and Math. Phys., vol. 26, pp. 711-722, 1986 (in Russian).*

Recommended for publication: 17.01.2013.

STRUCTURAL COMPOSITION OF RED WINES DETERMINED BY THE COLOR OF BOTTLE

PhD, lecturer V. Popov, S. Ursu, A. Gherța
Technical University of Moldova

INTRODUCTION

Red wines occupy a preponderant part of the total wine production. White wines are distinguished not only by colour, taste and aroma, but also by physic-chemical properties, physiological action on the human body.

Young red wine colour is usually intense, but at the stage of maturation and aging is also diminished in intensity leading to shades of peel of onion. Physico -chemical methods of analysis make it possible to measure the instrumental intensity and hue of the wine. The evolution of wine red colour quality largely depends on the conditions of storage of wines. The factors that ensure the conditions of wines storage, particularly red ones are: temperature, humidity, ventilation, vibration, the colour of the bottle in which the wine is kept.

Glass bottle is the best known and all at once most appreciated packaging for wine. Glass bottles presents a series of advantages namely that they are chemically inert, non - impermeable and hygienic, resistant to high pressures, recyclable and relatively inexpensive. The disadvantages I could notice: fragility, high weight. There are several types of bottles as: bordeaux, porto, jidvei, murfatlar, rhein, tokay.

Color tints of the bottles are: white, white with yellowish tinge, green and brown. The darker coloured tint resists UV rays, especially between 360-440 nm and are used in bottles in high-quality wines as well as in sparkling and white wines. The colour of the container can greatly influence the consumer choice, but it may have some influence on the quality of wine.

1. MATERIALS AND METHODS

The aim of the study was to investigate the structural changes of the red wines stored in bottles of different colours under similar conditions.

As the research object were untreated red wines Merlot and Rară Neagră (Rare Black) produced in the southern zone of Moldova, Cahul. The wines have been produced by the classical technology of red wine production.

To determine the physic - chemical indexes of untreated red wines Merlot and Rară Neagră (Rare Black) have used modern methods, in accordance with the standards in force, as well as recommended by O.I.V. Specific and stable chromatic indexes were determined by spectrophotometric method of analysis.

Initially, the wines were sulfitated up to a concentration of 100 mg/l of SO_2, and maintained at a temperature of t = 0 °C for 3 days, then filtered and bottled.

Red wines Merlot and Rară Neagră (Rare Black) were kept in bottles of transparent white and green within 90 days, at a temperature of 14-16°C.

2. RESULTS AND DISCUSSION

During the retention samples of the red wines Merlot and Rară Neagră (Rare black) in white transparent and green bottles were determined the following specific and stable chromatic indexes: the content of: the total phenolic substances, polyphenol index (I. P. T.) total and ionized anthocyanins); the intensity and hue of colour.

Table 1. The influence of bottle colour on the evolution of the content of total phenolic substances and I. P. T. in red wines Merlot Rară Neagră (Rare Black).

Name of wine	Initially		Wine treated		Green bottle		White bottle	
	Total phenolic substances, mg/l	I.P.T.	Total phenolic substances, mg/l	I.P.T.	Total phenolic substances, mg/l	I.P.T.	Total phenolic substances, mg/l	I.P.T.
Merlot	2534	42,62	2436	41,12	2371	38,12	2153	36,12
Rară Neagră	1682	31,9	1640	30,2	1601	29,2	1512	29,05

According to data in the chart 1 shows that keeping wines in white bottles is contributing to a higher decrease of phenolic substances than in green bottles. The lowest concentration of phenolic substances of 1512 mg/l and the value of I. P. T. by 29,05 was registered for wine sample Rară Neagră (Rare Black) maintained in white bottle .

The results obtained are in complete correlation with the data in the specialized literature [1, 3] that white glass with high transparency allow visible light radiation to destroy the colouring of red wines while coloured glass bottle retains some of these radiations.

Diminutive changes are recorded and on the content visible and ionized anthocyanins for both types of red wines samples, the results are presented in figurile1 and 2. According to the processing results we found that anthocyanins have diminished on the average by 34% to wines kept in green bottles and roughly 48% for those in the white transparent bottles, compared to the original values recorded.

Lowering the concentration of ionized anthocyanins is attested by the minimum value of 14 mg/l in Rară Neagră (Rare Black) wine kept in white bottles, while in the green bottle it is 18 mg/l.

The white transparent glass favours rapid degradation of anthocyanins due to their irreversible oxidation as red wine afterwards change the colour [1].

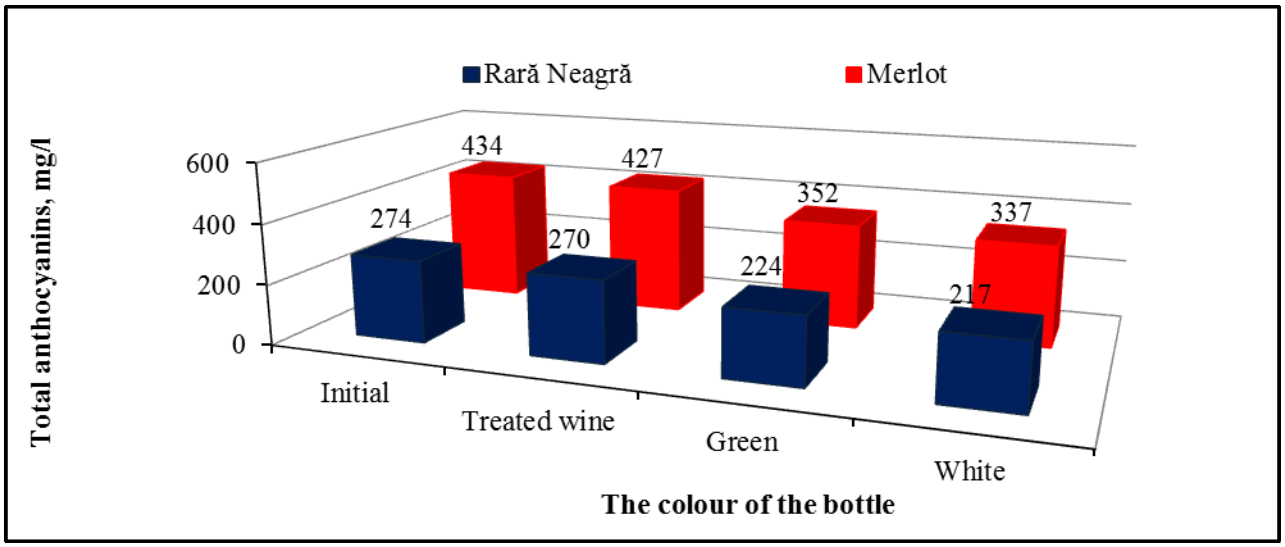

Figure 1. The variation of total anthocyanins in Merlot and Rară Neagră (Rare Black) wines, depending on the colour of the bottle.

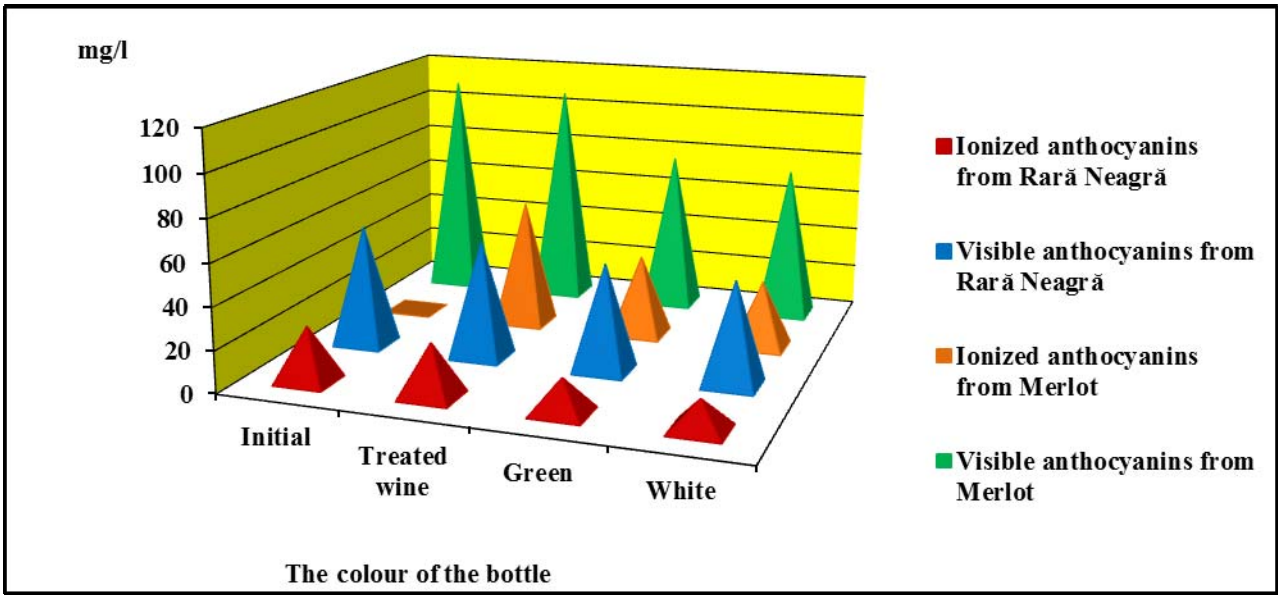

Figura 2. Modification of the ionized and visible anthocyanins in Merlot and Rară Neagră (Rare Black) wines, depending on the colour of the bottle

Table 2. Influence of the bottle colour on the evolution value of colorant intensity and the hue of colour in Merlot and Rară Neagră (Rare Black).

Name of wine	Initially		Wine treated		Green bottle		White bottle	
	Colouring intensity, u.a.	Colour tint, u.a.	Colouring intensity, u.a.	Colour tint, u.a.	Colouring intensity, u.a.	Colour tint, u.a.	Colouring intensity, u.a.	Colour tint, u.a.
Merlot	1,37	0,54	1,25	0,56	1,2	0,63	1,01	0,69
Rară Neagră	1,1	0,43	0,95	0,44	0,7	0,51	0,6	0,59

Distinct changes are recorded and on the evolution of stable chromatic indexes keep samples of red in white wines in white and green bottles. The results obtained are shown in table 2. As a result of keeping the wine in white bottles are observed an increase in the colour hue up to 0,69 u.a. and 0,59 u.a. respectively for Merlot and Rară Neagră (Rare Black), which denotes a decrease of the colouring intensity.

Colouring intensity decreased on average by 36.1% and respectively 26.3% for Rară Neagră (Rare Black) and Merlot wines kept in white bottles and respectively by 35.1% and 13.0% for samples of Rară Neagră (Black Rare) and Merlot kept in green bottles.

Value increasing of the colour hue occurs on average by 18% for wines kept in green bottles and by 32% for samples kept in white transparent bottles.

CONCLUSIONS

Keeping red wines Merlot and Rară Neagră (Rare Black) in green bottles maintain its chromatic qualities longer in comparison with red wines kept in white transparent as white glass allows transmitting ultraviolet rays, which have the aggressive effect on the colour of the wine, favouring its rapid degradation due to oxidation of tannins, compounds that restore smoothness, colour and softness of wine.

BIBLIOGRAPHIC REFERENCES

1. Cotea V. D., Zănoagă C., Cotea V. V. *Tratat de Oenochimie. Volumul I. Bucureşti: Editura Academiei Române, 2009. 684 p.*

2. Jacobson J. L. *Introduction to Wine Laboratory Practices and Procedures. USA: Springer, 2006. 375 p*

3. Musteață Gr., Popov V., Ursu S., Costețchi T. *The variation of oxidation-reduction potential in red wines. In: Meridian Ingineresc, 2010, nr. 4, p. 31-33. ISSN 1683-853X*

4. Musteață Gr., Popov V., Ursu S., Costețchi T. *Modificările proprietăților antioxidante ale vinurilor roşii sub influența tratărilor termice. In: Ştiința agricolă, 2011, nr. 1, p. 18-22. ISSN 1857-0003*

5. Musteață Gr., Popov V., Ursu S., Velicu A. *Oportunități de păstrare şi maturare a vinurilor roşii. In: Meridian Ingineresc, 2012, nr. 3, p. 17 - 21. ISSN 1683-853X*

6. Musteață Gr., Popov V., Ursu S. *Variația potențialului oxido-reducător în vinurile roşii. In: Agricultura Moldovei, 2011, nr. 6-7, p. 28-30. ISSN 0582-5229*

7. Ursu S. *Phenolic compounds in grapes. In: Meridian Ingineresc, 2010, nr. 4, p. 78-83. ISSN 1683-853X*

8. Ursu S. *Acțiunea procesului de fermentare - macerare asupra capacităților reducătoare a vinului roşu Pinot Noir. In: Meridian Ingineresc, 2013, nr. 1, p.26-29. ISSN 1683-853X*

9. Ursu S., Musteață Gr. *Intensificarea proprietăților sanogenice în vinuri. În: Conferința Tehnico-Ştiințifică a Colaboratorilor, Doctoranzilor şi Studenților. Chişinău: Universitatea Tehnică a Moldovei, 17-19 noiembrie 2010, vol. II, p. 122-123.*

10. Taran N., Soldatenco E., Morari B. *Studiul componenței substanțelor fenolice în vinurile materie primă pentru spumante roşii în dependență de procedeele utilizate. În: Culegerea conferinței ştiințifico-practică cu participare internațională „Vinul în mileniul III – probleme actuale în vinificație" 24 – 26 noiembrie 2011 Chişinău, p. 108-110.*

11. Țârdea C. *Chimia şi analiza vinului. Iaşi: Editura „ION IONESCU DE LA BRAD", 2007. 1398 p.*

Recommended for publication: 15.02.2013.

CALCULATION ERRORS OF THE PLATES USING FINITE ELEMENT METHOD

S. Galbinean, Postgrad.
Technical University of Moldova

INTRODUCTION

The finite element method (FEM) is currently the most used numerical method of calculation It is very effective for studying various problems from different areas of engineering. FEM, usually leads to solving a system of algebraic equations with a large number of unknowns, so it is closely related to computer use. One of the basic problems of MEF is the difficulties of calculating the plates with different conditions on boundary. The problem is actual and were not proposed any solutions to solve it.

Below are studied rectangular plates with different ways of bearing edge and are estimated the errors occurring in their modeling by finite element method.

CALCULATION OF THE PLATE WITH DIFFERENT CONDITIONS ON BOUNDARY

To solve the problem for rectangular plates with various types of supports we use the solution proposed by L. Levy, considering the two opposite sides simply supported. If simply supported sides are $x = 0$ and $x = a$ (fig. 1), the deflection $w(x, y)$ can be expressed with relation

$$w(x,y) = \sum_{m=1}^{\infty} Y_m(y) \sin\frac{m\pi x}{a}. \qquad (1)$$

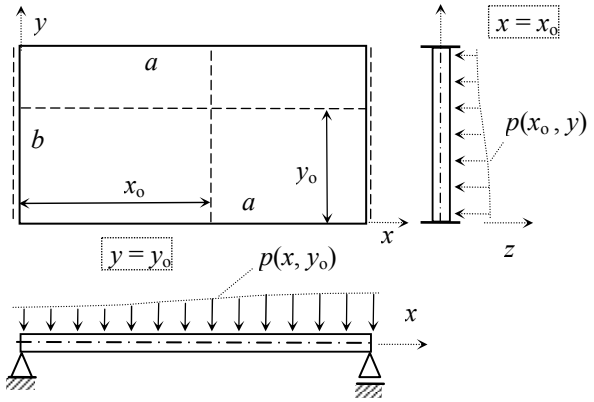

Figure 1. Plate having two opposite sides ($x = 0$; $x = a$) simply supported and the other two of any kind.

The load p(x,y) is presented in Fourier series of the same form

$$p(x,y) = \sum_m p_m(y) \sin \alpha_m x, \qquad (2)$$

where,

$$p_m(y) = \frac{2}{a}\int_0^a p(x,y)\sin(\alpha_m x)\,dx, \qquad (3)$$

and

$$\alpha_m = m\pi / a \ . \qquad (4)$$

Frequently we meet two cases::

1) uniformly distributed load,

$$p_m(y) = \frac{4p}{m\pi} = const. \ , \ m = 1, 3, 5, \ldots \ ; \qquad (5)$$

2) hydrostatic load distributed according to the law $p(x, y) = px/a$,

$$p_m(y) = \frac{2p}{m\pi}(-1)^{m+1} = const., \qquad (6)$$

$m = 1, 2, 3, \ldots$.

According to the classical theory of Kirchhoff's plates, the differential equation of deflection has the form

$$\frac{\partial^4 w}{\partial x^4} + 2\frac{\partial^4 w}{\partial x^2 \partial y^2} + \frac{\partial^4 w}{\partial y^4} = \frac{p}{D}. \qquad (7)$$

Substituting relation (1) and (2) in the differential equation of the plate (7) we obtain:

$$Y_m'''' - 2\alpha_m^2 Y_m'' + \alpha_m^4 Y_m = p_m / D, \qquad (8)$$

which is a fourth order differential equation with constant coefficients. Noting with Y_m^{part} the particular solution of the equation (8) and considering that the roots $r_{1,\,2,\,3,\,4} = \pm\,\alpha_m\, y$ of its characteristic equation of the homogeneous equation are real, $r_{1,\,2,\,3,\,4} = \pm\,\alpha_m\, y$, the general solution will be presented in the form

$$Y_m(y) = Y_m^{\text{omog}} + Y_m^{\text{part.}}, \qquad (9)$$

where

$$Y_m(y) = A_m \cosh \alpha_m y + B_m \sinh \alpha_m y + \\ + C_m \alpha_m y \cosh \alpha_m y + D_m \alpha_m y \sinh \alpha_m y + Y_m^{\text{part.}} \quad (10)$$

Therefore the deflection becomes:

$$w(x,y) = \sum_{m=1}^{\infty} \left(A_m \cosh \alpha_m y + B_m \sinh \alpha_m y + \right. \quad (11)$$
$$\left. + C_m \alpha_m y \cosh \alpha_m y + D_m \alpha_m y \sinh \alpha_m y + Y_m^{\text{part.}} \right) \sin \alpha_m x$$

where the integration constants A_m, B_m, C_m, D_m are obtained using boundary conditions written for the sides parallel to x axis, these boundary conditions can be of any type.

For the plate loaded uniformly over the entire surface, using relation (5), and (8) follows:

$$Y_m^{\text{part.}} = \frac{p_m}{\alpha_m^4 D} = \frac{4p}{Dm\pi\alpha_m^4} = \frac{4pa^4}{D\pi^5 m^5}, \quad (12)$$

m = 1, 3, 5, … .

Further it will be presented the calculation of a square plate (fig. 2) simply supported on the sides $x = 0$ and $x = a$, clamped on the side $y = 0$ and free on the side $y = b$. The dimension of the plate is 6x6 m and it thickness δ = 15 cm. The modulus of elasticity of the material $E = 2{,}31*10^7$ kN/m^2 and Poisson ratio $\nu = 0{,}2$. The plate is loaded with a uniformly distributed load $p = 10$ kN/m^2.

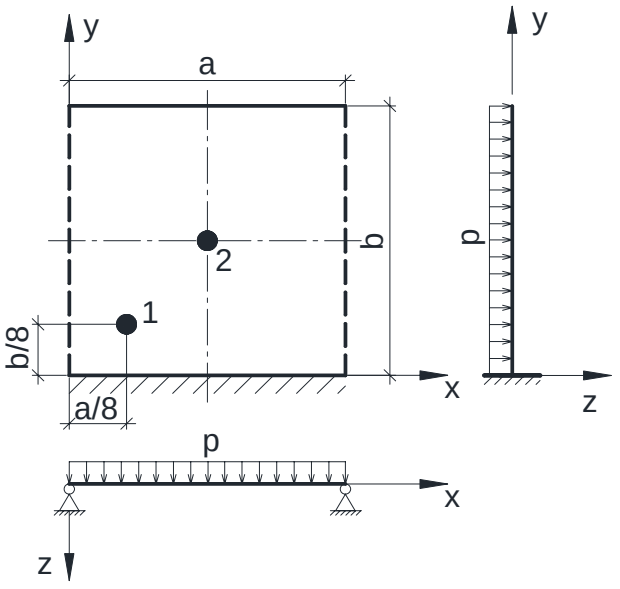

Figure 2. Plate with different boundary conditions.

The boundary conditions are:

- for the clamped side ($y = 0$) $\begin{cases} w = 0 \\ \dfrac{\partial w}{\partial y} = 0 \end{cases}$; (13)

- for the simply supported sides ($x = 0$, $x = a$)

$$\begin{cases} w = 0 \\ M_x = 0 \end{cases} \Rightarrow \begin{cases} w = 0 \\ \dfrac{\partial^2 w}{\partial x^2} + \nu \dfrac{\partial^2 w}{\partial y^2} = 0 \end{cases}; \quad (14)$$

- for the free side ($y = b$)

$$\begin{cases} M_y = 0 \\ Q_y^* = 0 \end{cases} \Rightarrow \begin{cases} \dfrac{\partial^2 w}{\partial y^2} + \nu \dfrac{\partial^2 w}{\partial x^2} = 0 \\ \dfrac{\partial^3 w}{\partial y^3} + (2-\nu) \dfrac{\partial^3 w}{\partial x^2 \partial y} = 0 \end{cases}. \quad (15)$$

From the boundary conditions we obtain the integration constants A_m, B_m, C_m, D_m.

$$A_m = -Y_m^{\text{part.}} = -\frac{4pa^4}{D\pi^5 m^5};$$

$$B_m = \frac{(3+\nu)(1-\nu)C^2 + 2\nu C - (1-\nu^2) - \nu(1-\nu)\kappa S}{(3+\nu)(1-\nu)C^2 + (1+\nu)^2 + (1-\nu)^2 \kappa^2} \cdot Y_m^{\text{part.}}$$

$$C_m = \frac{(3+\nu)(1-\nu)CS + \nu(1+\nu)S - \nu(1-\nu)\kappa C - (1-\nu)^2 \kappa}{(3+\nu)(1-\nu)C^2 + (1+\nu)^2 + (1-\nu)^2 \kappa^2} \cdot Y_m^{\text{part.}}$$

$$D_m = -\frac{(3+\nu)(1-\nu)CS + \nu(1+\nu)S - \nu(1-\nu)\kappa C - (1-\nu)^2 \kappa}{(3+\nu)(1-\nu)C^2 + (1+\nu)^2 + (1-\nu)^2 \kappa^2} \cdot Y_m^{\text{part.}}$$

where $C = \cosh \alpha_m b$, $S = \sinh \alpha_m b$, $\kappa = \alpha_m b$.

Internal efforts expressed through the deflection are obtained with the relations:

$$\left.\begin{aligned} M_x &= D \sum_{m=1}^{\infty} \left(\alpha_m^2 Y_m - \nu Y_m'' \right) \sin \alpha_m x; \\ M_y &= D \sum_{m=1}^{\infty} \left(-Y_m'' - \nu \alpha_m^2 Y_m \right) \sin \alpha_m x; \\ M_{xy} &= -D(1-\nu) \sum_{m=1}^{\infty} \alpha_m Y_m' \cos \alpha_m x; \\ Q_x &= D \sum_{n=1}^{\infty} \left(\alpha_m^3 Y_m - \alpha_m Y_m'' \right) \cos \alpha_m x; \\ Q_y &= D \sum_{n=1}^{\infty} \left(\alpha_m^2 Y_m' - Y_m'' \right) \sin \alpha_m x; \end{aligned}\right\} \quad (16)$$

The table below presents the results for the investigated plate (fig.2) in the points 1, 2, obtained using Fourier series and the results obtained using finite element method for different mesh and result deviation using FEM from analytical solution.

Mention that the FEM programs (SCAD, ANSYS, Robot, etc.) contain triangular, quadrilateral, etc. elements connected only in nodal

points and each node has three degrees of freedom: θ_{xi}, θ_{yi}, w_{xi} .

Table 1. Results obtained using Fourier series and using FEM.

The strain calculated in the given point	Fourier series	Results and deviations obtained using FEM for nxn mesh			
		4x4		8x8	
		Value [kNm/m]	Deviation [%]	Value [kNm/m]	Deviation [%]
M_{x1}	0,35	0,73	109	0,63	80,5
M_{y1}	-6,52	-7,08	8,6	-5,63	-13,7
M_{xy1}	-8,52	-9,38	10,0	-9,0	5,6
M_{x2}	21,0	21,2	0,8	20,0	-4,7
M_{y2}	9,14	10,8	17,9	9,3	1,7
M_{xy2}	0	0	0	0	0

Table 1. (continuation)

The strain calculated in the given point	Results and deviations obtained using FEM for nxn mesh			
	16x16		32x32	
	Value [kNm/m]	Deviation [%]	Value [kNm/m]	Deviation [%]
M_{x1}	0,45	28,9	0,41	17,5
M_{y1}	-6,1	-6,5	-6,18	5,24
M_{xy1}	-8,77	2,9	-8,71	2,2
M_{x2}	19,7	-6,0	19,7	-6,3
M_{y2}	8,94	-2,2	8,87	-3,0
M_{xy2}	0	0	0	0

The results essentially differ using finite element method when approaching corners of the plates where moments tend to infinity. Similar results are obtained for plates of different sizes and loads.

There is no warning that existing elements in different computer programs (SCAD, Lira, ANSYS etc.) doesn't allow to describe conditions more complicated than clamped support. For free sides, in general, boundary conditions can't be described using elements with three degrees of freedom in the node.

CONCLUSIONS

1. For stress calculations, the existing computing programs (SCAD, Lira, ANSYS etc.) are not able to give accurate results to satisfy all cases of boundary conditions except the clamped side.

2. Plate corner points are singular points for which the finite element method should use special elements that would take into account the behavior of the solution in this points.

3. To perform calculations with finite element method with high accuracy there were developed special finite elements with an increased number of degrees of freedom in nodes, but implementing them in computer programs is difficult, so they are missing.

4. An alternative to FEM is boundary element method (BEM) which is free from the mentioned gaps, because the implementation of special elements in the method is more simple. The contour elements that will be implemented will allow us to satisfy different boundary conditions. These elements can be used including the asymptotic behavior of solutions in singular points.

The author expresses sincere thanks to his supervisor Dr. hab. prof. Gheorghe Moraru who contributed with his observations to improve this paper.

Bibliography

1. ***Konchakowskij Z.*** *Plity'. Staticheskie raschety', Moskva, Strojizdat, 1984.*

2. ***Moraru Gh.****, Introducere în metoda elementelor finite şi de frontieră*, Chişinău, U.T.M., 2002.

3. ***Perel'muter A., Slivker V.*** *Raschetny'e modeli sooruzhenij i vozmozhnost' ih analiza, Kiev, Stal', 2002.*

4. ***Timoshenko S., şi Woinowsky-Krieger S.*** *Theory of plates and shells, New York, McGraw-Hill,1959.*

Recommended for publication: 07.03.2013.

THE CHOICE AND OPTIMIZATION OF A COMPOSITE MATERIAL USED TO RENOVATE THE BEARING-TYPE JOINTS

L. Malai
State Agrarian University of Moldova

1. INTRODUCTION

The main purpose of the research carried out in this paper is the choice and optimization of a composite material used to renovate the bearing – type joints with the solutions of high performance. In order to reach this purpose the main objectives have bun set these objectives are: the study of the influence of some factors of the material through identification and qualitative and quantitative quantification of the share of the nature and the composite material adherence on metal substrates, the PCM being compared with the adherence of the matrix material. The composite material chosen for the test has as matrix the polyamide PA12 reinforced with molybdenum disulphide, different mass percentage of glass microspheres and basalt microfibres.

2. MATERIAL AND METHOD

The object of the research was chosen to be metalopolymeric tribological action couplings renovated with PCM, the constitution of the material intake used in the compensation of waste wear parts. The matrix was the polyamide PA12 (OCT 6-05-425). The CM adherence was compared with the adherence of the basic material. The reinforcement of the composite material was carried out with the following agents: molybdenum disulphide DM-1 (TU 48-19-133-90), used to improve the reaction of the composite material to load and wear fatigue; empty glass microspheres (glass microballoons) MC-BP gr.5 (TU 6-48-91-92), with the following chemical composition: SiO_2:76-78 %; Na_2O: 10-12 %; CaO: 6 %; ZnO: 1-1,5 %; B_2O_3: 4 %, density 0,37-0,42 g/cm^3, resistance to compression -150 kg/cm^2 (grinding -10%); humidity-not more than 0,3%; basalt microfibres used to increase the resistance to traction, rigidity, contraction during formation; lubrication improvement.

The composite was prepared by mixing the components in a ball mill ZE-101 during 30 minutes at the speed of the drum of 80...120 m^{-1}. the sorting of the basalt microfibres took place in a grinding device Ц-10 with the following sorting through a reciprocating sieve.

The coverage was applied by pressing at heat substrate by substrate of carbon steel of ordinary quality in hidraulic press DV 2428. the dimensions and the form of the samples were established according to the studied characteristics. Technological parameters were maintained in semi – automatic system.

The researches were carried out according to the matrix – the program with 3 factors Box-Benkin shown in chart 1 and the obtained data were processed applyind the following program STATGRAPHICS: Special ► Experimental design ► Create design ► Response surface.

The adherence was estimated through the method of pins with an open device described in [4]. The wear was determine data the friction machine SMT according to the scheme of the segment tree in the conditions of limited lubrication (1 oil drop SAE 10W-40 la 400 m. of path) under the load P_c = 1,5 MPa and the sliding speed v_r = 0,63 ms^{-1}.

3. RESULTS DISCUSSIONS

Competent choice of the materials used to renovate the bearing-type joints is a very important technological stage. These materials must have a range of features that should assure work capacity at least at the level of new pieces. In this aspect PCM presents a number of advantages in comparison with traditional materials used in cars repairing industry.

The main advantage of PCM in comparison with traditional materials is the possibility to obtain some unique characteristics owing to rational and controlled combination between the basic polymer and many other materials for reinforcement. Though reinforcing agents have specific individual characteristics, they may significantly change their characteristics in combination the way you want, both their own characteristics and the characteristics of the basic material.

The possibility of the modulation of PCM characteristics and thus obtaining a new various

range of physical and mechanic characteristics, that are important to assure the use in a lot of procedures of used pieces renovation in general and the use of PCM on, polyamide basis is motivated, its efficiency of PCM on polyamide basis is [1,2,5,6].

It is known that in order to assure a desired reliability level of the joints renovated by PCM, the compensating wear layer must have a good adherence with the layer in which it is applied to resist the loads that appear during exploitation and to have good resistance to wear.

At the same time, reinforcing agents often influence the resistance to adherence inadequatly, even unexpectedly. That is why, when creating a new PCM it is important to study its adherence in comparison with the basic material simultaneously with the dominant exploitation characteristics.

Next, we are going to present the results of the researches concerning the resistance of PCM adherence and its resistance to wear in the condition of friction with lubrication (these situation occur very often with agricultural machines and processing industry machines).

The adherence has been estimated for PCM applied on carbon steel layers in delivery status the function of the constituents concentration. For this research the polyamide PA12 (OCT 6-05-425), has been used as matrix it is a kind of polyamide with improved resistance to ultra-violet radiation action and to weather conditions it has increased resistance to wear and shocks showing phisico-mechanical characteristics with a large temperature scale, having the smallest density of all known today polyamides. At the same time, it is resistance to the majority of chemicals solvents (aliphatic and aromatic hidrocarbons, ketones, esters, ethers, oils, etc.).

The quantification of the influence of the constituents, concentration on coverings adherence was made through the relative adherence determined as the relation beteveen PCM estimated adherence and the matrix material adherence that is of the polyamide PA12. There has been studied CM adherence at the substrates of carbon steel in delivery state the function of constituents, concentration. After statistical processing of the

Table 1. The program of the experiments

Nr. crt.	Encoded values			Natural values, %		
	x1	x2	x3	X1 (MoS2)	X2 (Hallow glass microspheres MC-BII)	X3 (Basalt fibres)
1.	1	0	-1	5	20	2
2.	0	1	-1	3	30	2
3.	0	0	0	3	20	4
4.	-1	0	-1	1	20	2
5.	1	1	0	5	30	4
6.	0	-1	1	3	10	6
7.	0	0	0	3	20	4
8.	-1	-1	0	1	10	4
9.	1	0	1	5	20	6
10.	0	-1	-1	3	10	2
11.	1	-1	0	5	10	4
12.	-1	1	0	1	30	4
13.	-1	0	1	1	20	6
14.	0	0	0	3	20	4
15.	0	1	1	3	30	6

experimental data there have been obtained the following equation of regression, that in coded coordinates, adiquatly describes the evolution of the relative adherence the function of constituents, concentration:

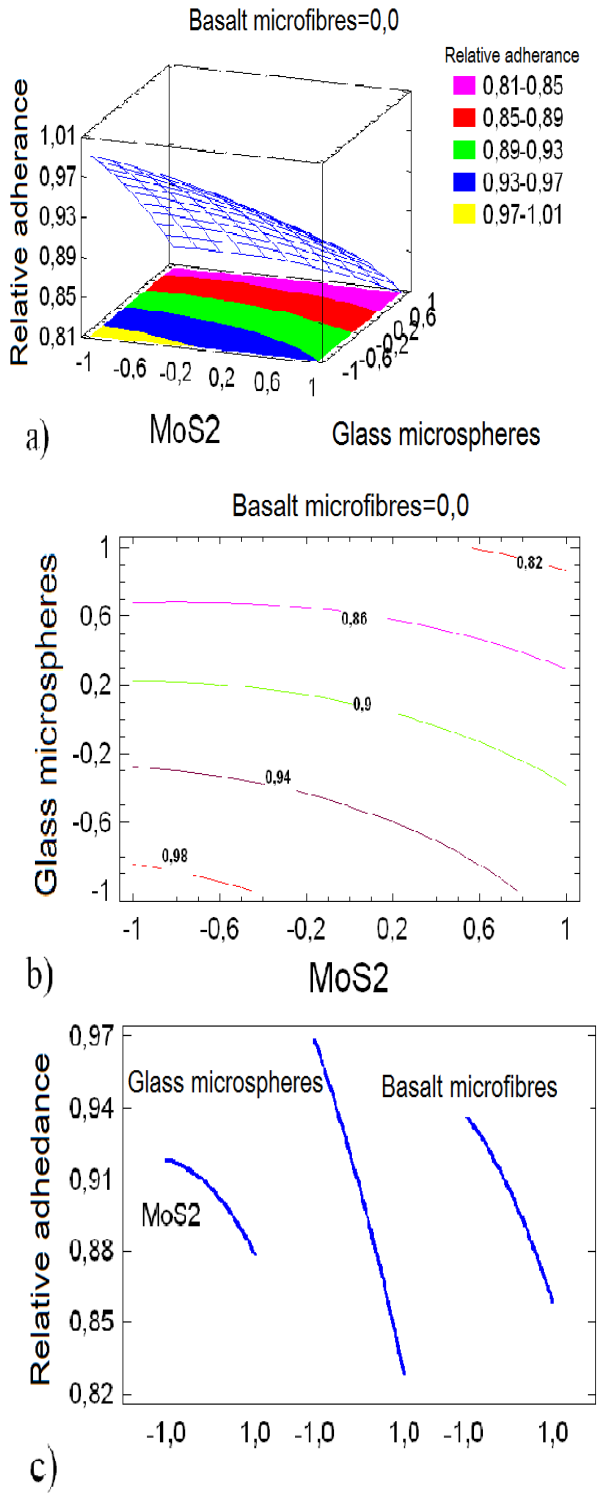

Figure 1. The estimation of PCM relative adherence the function of constituents concentration for level 0 (the concentration of basalt microfibres 4%): *a) the response surface, b) the responce levels and c) dominants effects*.

$$A_r=0,907-0,02x_1-0,07x_2-0,04x_3-0,008x_1^2+0,01x_1x_2+0,01x_1x_3-0,083_2^2-0,03x_2x_3-0,008x_3^2, \quad (1)$$

where A_r is the adhesion in MPa; x_1, x_2 and x_3 represent the percentage of the components in coded coordinates and MoS_2, - glass microsferes and basalt microfibres**.**

In figures 1 and 2 are presented the graphics of the studied PCM relative adherence the function of constituents concentration for various levels of response factors.

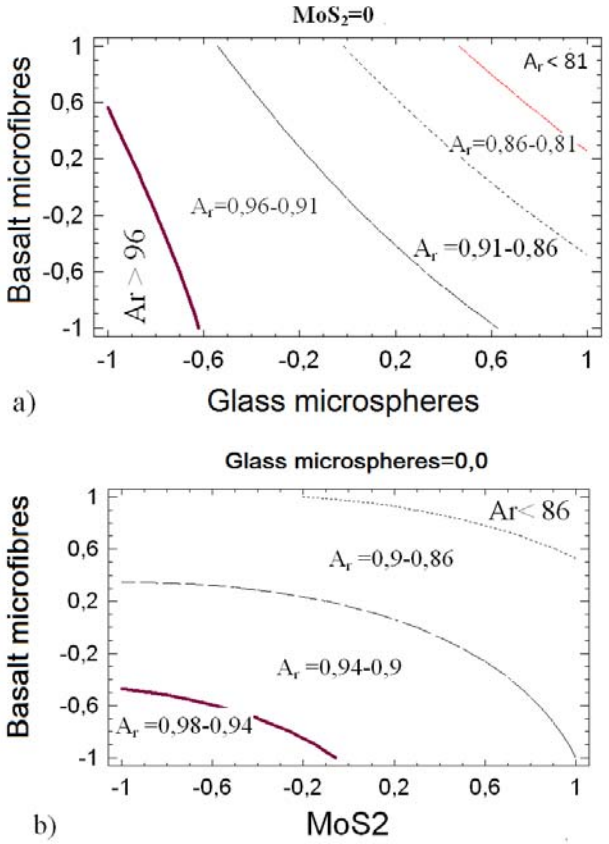

Figure 2. The estimation of PCM relative ad herence the function of constituents concentration for various levels of response factors: *a) MoS_2=0; b) eglass microspheres=0.*

According to the analysis of equation 1 and the graphics from figures 1 and 2 we, may state that all the reinforcing agents influence negatively PCM adherence at the substrates of carbon steel (b_1, b_2 *and* b_3 differ from 0 having negative values), the dominant influence belongs to glass microspheres ($|b_2| = 0,07>|b_1|$ *and* $|b_3|$), *than follow basalt microfibres* ($|b_3| > |b_1|$). This fact is explained by the higher percentage of glass microspheres in comparison with the percentage of molybdenum disulphide and basalt microfibres. At the same time we may state that the influence of MoS_2 contents on the adhesion isn't significant ($b_1 < 0$ and $b_{22} = 0$), having under certain condition the growth of the

contents of glass microspheres and basalt microfibres (b_{12}.and $b_{13} > 0$).

4. CONCLUSIONS

1. The analysis of the data from specialty literature shows the possibility to use the polyamide PA12 as wear compensator at the renovation of component machine pieces of agricultural machines and of processing industry machines. The polyamide PA12 improves exploitation properties by reinforcing them with molybdenum disulphide, glass microspheres and basalt microfibres.

2. According to the experimental studies of the composite material relative adherence based on polyamide we may state that studied reinforcing agents influence negatively the adherence of the filler at the substrates of carbon steel.

3. It's necessary to continue the researches in order to find some improvement methods for PCM polyamidic adherence at metalic substrates as wellas to study adherence stability during exploitation in various environments.

Bibliography

1. Marian Gr. *Contribuţii teoretico-experimentale la studiul fiabilităţii pieselor şi îmbinărilor utilajului agricol recondiţionate cu compozite pe bază de polimeri: Teza de doctor habilitat în tehnică: 05.20.03. – Chişinău, 2005. – 252 p.*

2. Sîrghii V. *Contribuţii la asigurarea tehnologică a fiabilităţii pieselor utilajului agricol recondiţionate cu aplicarea compoziţiilor din mase plastice: Teza de dr. în tehnică: 05.20.03. – Chişinău, 2007, 252 p.*

3. Marian Gr., Gorobe V., Ţapu V. *Perspektivy ispol´yovaniâ poristyh polimernyh kompozicij pri vosstanovlenii soprâženii s zazorom. În: Doklady Meždunarodnoj naucno-praktičeskoj konferencii, Minsk, 2009, p. 62-63.*

4. Marian Gr., Gorobe V., Ţapu V., Sîrghii V . ş.a*. Sporirea gradului de aderenţă a compozitelor poliamidoepoxidice prin aplicarea straturilor intermediare de conversiune. In: Ştiinţa Agricolă. Univ. Agrară de Stat din Moldova. 2006, nr. 1, p. 75 - 79.*

5. Koleasko I. *Issledovanie i razrabotka tehnologii vosstanovleniâ s.-h. tehniki poliamidnymi pokrytiâmi: Teza de cand. în şt. tehnice: 05.20.03. – Chişinău, 1980. – 152 p.*

6. *Dudcak V.* *Razrabotka tehnologii vosstanovleniâ detalej sel´skohozâistvennoi tehniki kompozicionnymi polimernymi pokrytiâmi: Teza de cand. în şt. tehnice: 05.20.03. – Chişinău, 1985. – 143 p.*

Recommended for publication: 22.01.2013

MICRO HYDRO POWER STATION WITH HYDRODYNAMIC ROTOR

PhD, assoc. prof. V. Bostan
Universitatea Tehnică a Moldovei

INTRODUCTION

The research of the systems for conversion of renewable sources of energy (RSE) and their elaboration is of great importance for Republic of Moldova being in complete agreement with European Union policies and commitments of the Republic of Moldova toward the increase of the RSE quote in the energy production up to 20% in 2020. Systems for conversion of the kinetic energy of the free water flow into electric or mechanical energy are using turbines in the absence of dams, thus eliminating the negative environmental impacts such as noise pollution, excessive sedimentation, low water quality, effects on aquatic fauna. The kinetic energy of free water flow is a recommended energy source available continuously and it can be efficiently harnessed by floatable micro-hydro power stations in order to meet the energy needs of consumers, particularly in remote rural areas. As working elements in such small-scale hydro-electric power stations are used Garman type rotors with oblique axis blades, Darrieus rotors, multi-blade rotors, Gorlov type turbines. The anchored power stations require a foundation to which the working elements, multiplicator and electric generator placed on a resistance frame are anchored. In contrast with anchored power stations, the floating micro-hydro power stations can be placed in the areas with higher flow rate and at further distances from the river banks. Moreover, they can be grouped and positioned appropriately to form a hydro power farm in order to convert more efficiently the flowing river kinetic energy. Nowadays, various types of floating micro-hydro power stations are being used with either horizontal or vertical axis.

Based on carried out research [1], there is proposed a constructive concept of two flow turbines with 3 and 5 blades with NACA hydrodynamic profile. These turbines have been used to design and manufacture four configurations of floatable micro hydro power stations for the conversion of river kinetic energy [2].

In order to increase the conversion efficiency it is necessary to optimize the hydrodynamic profile of the blades taking into account the turbine dimensions, angle of attack and exploitation conditions. Since conversion efficiency highly depends on the hydrodynamic profile of the blades, it is important to minimize the deformations of the blades due to hydrostatic pressure and applied forces. Therefore, it is important to design and analyze a resistance structure for the blades that will preserve the prescribed design shape parameters, along both the blade length and height.

2. TURBINE WITH HYDRODYNAMIC BLADES

Hydrodynamic rotor consists of main shaft 2 (fig.1), horizontal rods 1 and blades 4 with NACA 0016 hydrodynamic profile assembled in semi shaft 3 with the possibility to rotate around them. Under the action of hydrodynamic forces, the blades 4 rotate with angular velocity ω depending

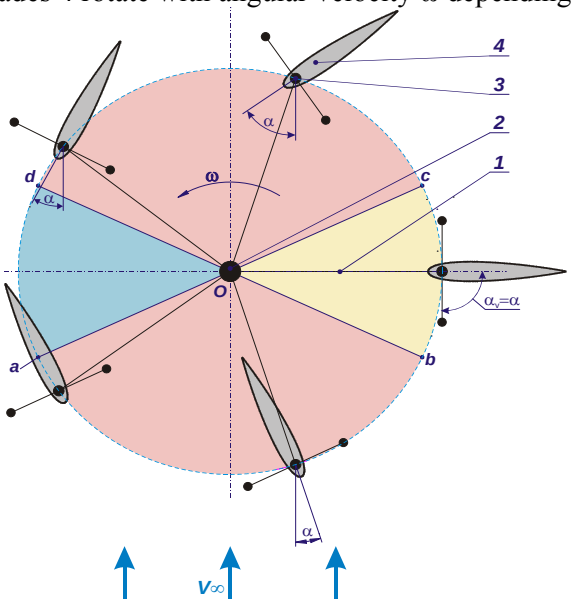

Figure 1. Conceptual scheme of vertical axis turbine with hydrodynamic blades.

on the water flow velocity $\vec{V}_\infty$, blades angle of attack α and rotor diameter D (diameter of location of blade semi shaft axes).

To identify the character of influence of hydrodynamic effects on a blade with NACA symmetric profile in its rotational motion around

centre *O*, four specific areas of blade-fluid interaction are defined: upstream area *Oab*, downstream area *Ocd*, transition from upstream to downstream area *Obc* and transition from downstream to upstream area *Oda*.

Maximum efficiency of flow kinetic energy conversion into useful mechanical energy can be realized if a blade with hydrodynamic profile contributes to the development of a total torque T_Σ under the action of hydrodynamic force during one complete rotation. To achieve this condition it is necessary that blades 3 be oriented under an optimum (from the point of view of conversion efficiency) angle of attack α with respect to the flow direction for each area crossed by every blade during its complete rotation.

3. DETERMINATION OF HYDRODYNAMIC COEFFICIENTS

Consider a blade with symmetric hydrodynamic profile placed in a water stream with uniform velocity $\vec{V}_\infty$ (fig. 2). In the fixing point O' of the symmetrical blade with rod OO' two coordinate systems are considered: $O'xy$ system with axis $O'y$ oriented in the direction of the velocity vector $\vec{V}_\infty$ and $O'x'y'$ system with axis $O'y'$ oriented along the rod OO'. Points A and B correspond to the trailing and the leading edges, respectively. The angle of attack α is the angle between the profile's chord AB and the direction of the velocity vector $\vec{V}_\infty$, and the positioning angle φ is the angle formed by the velocity vector direction and OO'.

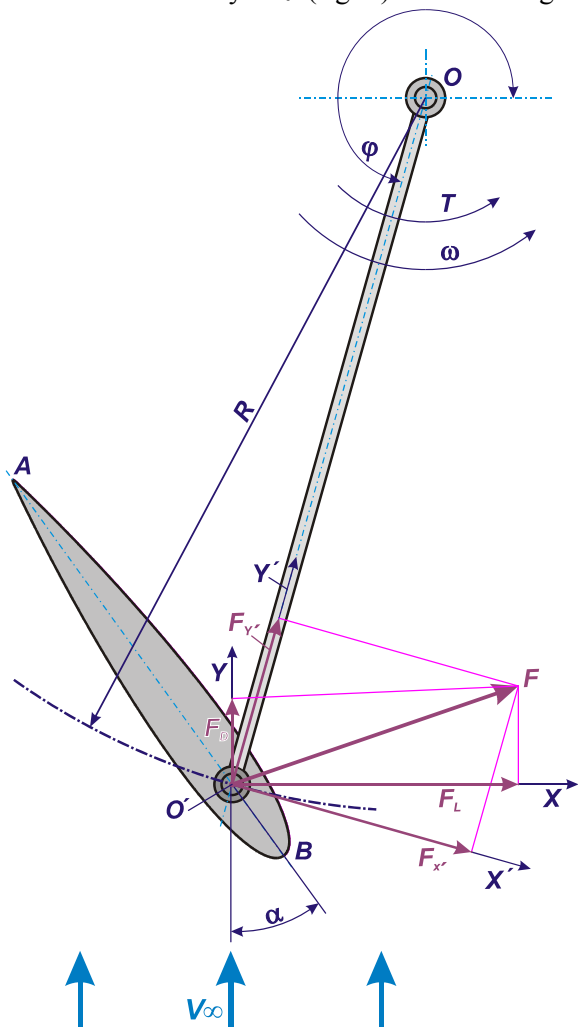

Figure 2. Hydrodynamic profile blade

The hydrodynamic force $\vec{F}$ has its lift and drag components in directions O'x and O'y, respectively, given by:

$$F_L = \frac{1}{2} C_L \rho V_\infty^2 S_p, \quad F_D = \frac{1}{2} C_D \rho V_\infty^2 S_p, \qquad (1)$$

where ρ is the fluid density, V_∞ is the flow velocity, $Sp=cH$ (c is the length of chord AB, and H is the blade height) represents the lateral surface area of the blade, and C_L and C_D are dimensionless lift and drag hydrodynamic coefficients. The hydrodynamic coefficients C_L and C_D are functions of the angle of attack α, Reynolds number Re and hydrodynamic shape of the blade. The symmetric shape of the hydrodynamic profile is chosen from the library of NACA 4 digits aerodynamic profiles and the profile chord length is considered unitary.

The components of hydrodynamic force in coordinate system $O'x'y'$ are:

$$\begin{aligned} F_{x'} &= -F_L \sin\varphi + F_D \cos\varphi, \\ F_{y'} &= F_L \cos\varphi + F_D \sin\varphi. \end{aligned} \qquad (2)$$

The torque developed by blade i at the rotor shaft O is

$$T_i = F_{x'} \cdot |OO'|, \qquad (3)$$

and the total torque developed by all blades is

$$T_\Sigma = \sum_{i=1}^{N_b} T_i, \qquad (4)$$

where N_b is the number of rotor blades.

In order to compute the lift hydrodynamic coefficient a panel method is being used. Thus, the fluid is considered incompressible and inviscid, and its flow plane and potential [3, 4]. The flow potential Φ in point $P'(x,y)$ is obtained by superposition of a uniform velocity flow, a distribution of sources with strength $q(s)$ and a distribution of vortexes with strength $\gamma(s)$ on profile C:

$$\Phi(P') = V_\infty x\cos\alpha + V_\infty y\sin\alpha + \oint_C \frac{q(s)}{2\pi}\ln(r)ds - \oint_C \frac{\gamma(s)}{2\pi}\theta ds, \quad (5)$$

where s denotes the arc length measured along profile C, and (r,θ) are the polar coordinates of P' relative to the point on C corresponding to arc length s.

The computation of the flow potential Φ uses a collocation method in which profile C is discretized with N boundary elements E_j with endpoints P_j and P_{j+1}. It is assumed that the vortex strength $\gamma(s)$ is constant, and the source strength $q(s)$ is piecewise constant on each boundary element E_j with value q_j, $j=1,\ldots,N$. Breaking the integrals in (5) along each element gives:

$$\Phi = V_\infty x\cos\alpha + V_\infty y\sin\alpha + \sum_{j=1}^{N}\int_{E_j}\left(\frac{q_j}{2\pi}\ln(r) - \frac{\gamma}{2\pi}\theta\right)ds, \quad (6)$$

where unknowns γ and q_j are determined from imposing boundary and Kutta conditions on collocation points $M_j\left(\bar{x}_j,\bar{y}_j\right)$ chosen to be the midpoints of E_j. Let u_j and v_j be velocity components in M_j. Boundary and Kutta conditions are:

$$\begin{aligned} &-u_j\sin\theta_j + v_j\cos\theta_j = 0,\ \mathrm{j}=1,\ldots,N \\ &u_1\cos\theta_1 + v_1\sin\theta_1 = -u_N\cos\theta_N + v_N\sin\theta_N, \end{aligned} \quad (7)$$

where θ_j denotes the angle formed by element E_j and x-axis. The velocity components in point M_i are determined by the contributions of velocities induced by sources and vortexes on each boundary element E_j:

$$\begin{aligned} u_i &= V_\infty\cos\alpha + \sum_{j=1}^{N}u_{ij}^{s}q_j + \sum_{j=1}^{N}u_{ij}^{v}\gamma, \\ v_i &= V_\infty\sin\alpha + \sum_{j=1}^{N}v_{ij}^{s}q_j + \sum_{j=1}^{N}v_{ij}^{v}\gamma, \end{aligned} \quad (8)$$

where $u_{ij}^{s}, v_{ij}^{s}, u_{ij}^{v}, v_{ij}^{v}$ are the influence coefficients.

Let β_{ij}, $i\neq j$, be the angle between P_jM_i and M_iP_{j+1}, and set $\beta_{ii}=\pi$. Let $r_{ij} = \left|M_iP_j\right|$ and define $D_{ij} = r_{i,j+1}/r_{ij}$. Boundary and Kutta conditions (7) together with equations (8) lead to a linear system with unknowns γ and q_j:

$$\left[A_{ij}\right]_{i,j=1}^{N+1}\begin{bmatrix} q_1 \\ q_2 \\ \vdots \\ q_N \\ \gamma \end{bmatrix} = \begin{bmatrix} b_1 \\ b_2 \\ \vdots \\ b_N \\ b_{N+1} \end{bmatrix} \quad (9)$$

with coefficients A_{ij} and b_i given by formulas with $i,j=1,\ldots,N$:

$$\begin{aligned} A_{ij} &= \frac{1}{2\pi}\left(\sin\Delta_{ij}\ln D_{ij} + \beta_{ij}\cos\Delta_{ij}\right), \\ A_{i,N+1} &= \frac{1}{2\pi}\sum_{j=1}^{N}\left(\cos\Delta_{ij}\ln D_{ij} - \beta_{ij}\sin\Delta_{ij}\right), \\ A_{N+1,j} &= \frac{1}{2\pi}\left(\beta_{1,j}\sin\Delta_{1j} + \beta_{N,j}\sin\Delta_{Nj} - \cos\Delta_{1j}\ln D_{1j} - \cos\Delta_{Nj}\ln D_{N,j}\right) \\ A_{N+1,N+1} &= \frac{1}{2\pi}\sum_{j=1}^{N}\left(\sin\Delta_{1j}\ln D_{1j} + \sin\Delta_{Nj}\ln D_{N,j} + \beta_{1j}\cos\Delta_{1j} + \beta_{Nj}\cos\Delta_{Nj}\right) \\ b_i &= V_\infty\sin\left(\theta_i-\alpha\right),\ i=1,\ldots,N, \\ b_{N+1} &= -V_\infty\cos(\theta_1-\alpha) - V_\infty\sin(\theta_N-\alpha), \end{aligned}$$

where $\Delta_{ij} = \theta_i - \theta_j$. For more details see [1, 2].

Linear system (9) provides the values of γ and q_j, using which the tangential components of velocity are computed:

$$u_{\tau i} = u_i\cos\theta_i + v_i\sin\theta_i.$$

The local pressure coefficient on the discretized profile is computed from

$$C_{p,i} = 1 - \left(\frac{u_{\tau i}}{V_\infty}\right)^2. \quad (10)$$

The hydrodynamic forces acting on the boundary element Ej are given by:

$$\begin{aligned} f_{xj} &= C_{p,j}\left(y_{j+1}-y_j\right), \\ f_{yj} &= C_{p,j}\left(x_{j+1}-x_j\right). \end{aligned} \quad (11)$$

The total force is the sum of contributions of each boundary element:

$$F_x = \sum_{j=1}^{N}f_{xj},\ F_y = \sum_{j=1}^{N}f_{yj}. \quad (12)$$

Lift coefficient is then given by:

$$C_L = -F_x\sin\alpha + F_y\cos\alpha. \quad (13)$$

Next phase after the computation of the velocity distribution in potential flow around the profile consists in the computation of boundary layer parameters divided into two sub-steps: laminar boundary layer and turbulent boundary layer [5-7]. The boundary layer starts at the stagnation point and follows the profile along the upper or lower surface in direction of trailing edge (fig. 3).

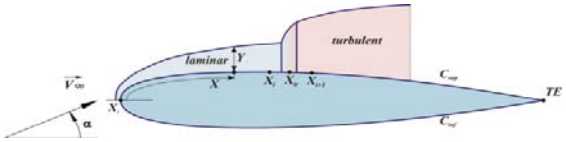

Figure 3. Transition from laminar to turbulent boundary layer.

The computation of laminar boundary layer parameters is based on the Von Karman integral-differential momentum equation:

$$\frac{d\theta}{dx}+\frac{\theta}{V}\left(2+\frac{\delta^*}{\theta}\right)\frac{dV}{dx}=\frac{1}{2}C_f, \qquad (14)$$

where V represents the velocity of the boundary layer exterior part in the considered point, δ^* is the displacement thickness, θ is the momentum thickness and C_f denotes the local friction coefficient on the profile surface. Introducing shape parameter $H=\delta^*/\theta$, allows to rewrite equation (14) as follows:

$$\frac{d\theta}{dx}+(2+H)\frac{\theta}{V}\frac{dV}{dx}=\frac{1}{2}C_f. \qquad (15)$$

Introducing the kinetic energy thickness θ^* Von Karman equation (14) leads to

$$\frac{d\theta^*}{dx}+3\frac{\theta^*}{V}\frac{dV}{dx}=2C_d, \qquad (16)$$

where C_d denotes the dissipation coefficient. Introduce in (16) the second shape parameter $H^*=\theta^*/\theta$ to get:

$$\theta\frac{dH^*}{dx}+H^*(H-1)\frac{\theta}{V}\frac{dV}{dx}=2C_d-\frac{1}{2}H^*C_f. \qquad (17)$$

In order to determine all boundary layer parameters, equations (15) and (17) are coupled with Falkner-Skan semi-empirical correlations between H^* and H, [6]:

$$H^*=\begin{cases}0.076\dfrac{(H-4)^2}{H}+1.515, & \text{if } H<4,\\ 0.04\dfrac{(H-4)^2}{H}+1.515, & \text{otherwise.}\end{cases} \qquad (18)$$

Also, let $\mathrm{Re}_\theta=\mathrm{Re}\cdot\theta\cdot V$ and assume that

$$\frac{1}{2}\mathrm{Re}_\theta C_f=F_1(H),\ 2\mathrm{Re}_\theta\frac{C_d}{H^*}=F_2(H),$$

where

$$F_1=\begin{cases}0.01977\dfrac{(H-7.4)^2}{H-1}-0.067, & \text{if } H<7.4,\\ 0.022\dfrac{(H-7.4)^2}{(H-6)^2}-0.067, & \text{otherwise,}\end{cases} \qquad (19)$$

$$F_2=\begin{cases}0.00205(4-H)^{11/2}+0.207, & \text{if } H<4,\\ \dfrac{-0.003(H-4)^2}{1+0.02(H-4)^2}+0.207, & \text{otherwise.}\end{cases} \qquad (20)$$

Multiply equation (15) by Re_θ and let $\omega=(\mathrm{Re}_\theta)^2$. Re-arrange terms to obtain:

$$\frac{1}{2}V\frac{d\omega}{dx}+(2+H)\omega\frac{dV}{dx}=F_1(H). \qquad (21)$$

Multiply equation (17) by Re_θ/H^* and re-arrange terms to get:

$$\omega V\frac{d(\ln H^*)}{dH}\frac{dH}{dx}+(1-H)\omega\frac{dV}{dx}=F_2-F_1. \qquad (22)$$

Then, equations (21) and (22) are rewritten as follows

$$\begin{aligned}&\frac{1}{2}V(x)\frac{d\omega}{dx}+(2+H)\omega A(x)=F_1(H),\\ &\omega V(x)F_3(H)\frac{dH}{dx}+(1-H)\omega A(x)=F_4(H),\end{aligned} \qquad (23)$$

where

$$A(x)=\frac{dV}{dx},$$
$$F_3(H)=\frac{d(\ln H^*)}{dH},$$
$$F_4(H)=F_2(H)-F_1(H).$$

The system of nonlinear ODE (23) coupled with initial conditions

$$\omega(0)=\frac{F_1(2.24)}{4.24A(0)},$$
$$H(0)=2.24,$$

is solved by backward Euler method, in which functions F1 and F4 are linearized in vicinity of Hj. Method is iterated till either the transition from the laminar layer to the turbulent layer is predicted or trailing edge TE is reached.

The transition from laminar to turbulent boundary layer is located by Michel criterion, [8]. Let $\mathrm{Re}_x=\mathrm{Re}Vx$ and

$$\mathrm{Re}_{\theta\max}=1.174\left(1+\frac{22.4}{\mathrm{Re}_x}\right)\mathrm{Re}_x^{0.46}. \quad (24)$$

Then, transition takes place if $\mathrm{Re}_\theta>\mathrm{Re}_{\theta\max}$ with transition point being the root of linear interpolation of $\mathrm{Re}_\theta(x)-\mathrm{Re}_{\theta\max}(x)$.

The computations of the turbulent boundary layer parameters are done by applying the Head's model based on the Von Karman integral equations for turbulent boundary layer, [6]. Let Q denote the flow volume in the boundary layer at an arbitrary point x, $\delta^*=\delta-Q/V$ be the displacement thickness and $E=d\left(V\theta H_1\right)/dx$ be the entrainment velocity. According to the Head's model the dimensionless velocity E/V depends only on H_1, that in its turn, depends only on H. Cebeci and Bradshow [6] have considered the empirical relations

$$E/V=0.0306(H_1-3)^{-0.6169}, \quad (25)$$

$$H_1=\begin{cases}0.8234(H-1.1)^{-1.287}+3.3, H\le 1.6,\\ 1.5501(H-0.6778)^{-3.064}+3.3, H>1.6\end{cases} \quad (26)$$

Last equation to determine the unknowns θ, H, H_1 and C_f is the Ludwieg-Tillman wall friction law:

$$C_f=\frac{0.246}{10^{0.678H}\,\mathrm{Re}_\theta^{0.268}}. \quad (27)$$

Combining Von Karman integral equation and relations (25)–(27) provides a system of ODE:

$$\frac{dY}{dx}=g(Y,x), \quad (28)$$

where $Y=\begin{bmatrix}\theta & H_1\end{bmatrix}^T$ and

$$g(Y,x)=\begin{bmatrix}-\frac{\theta\left(H_1+2\right)}{V}\frac{dV}{dx}+\frac{1}{2}C_f\\ -\frac{H_1}{V}\frac{dV}{dx}-\frac{H_1}{\theta}\frac{d\theta}{dx}+\frac{0.0306}{\theta\left(H_1-3\right)^{0.6169}}\end{bmatrix}.$$

The initial values are the final values supplied by the laminar boundary layer step. The numerical integration of system (28) is done by Runge-Kutta method of order 2, namely:

$$Y^*=Y_j+h_jg(Y_j,x_j),$$
$$Y_{j+1}=Y_j+h_j\left(\frac{1}{2}g(Y_j,x_j)+\frac{1}{2}g(Y^*,x_j)\right),$$

that is iterated either till the trailing edge is reached or till the separation of the turbulent layer occurs. The drag coefficient C_D is computed from Squire-Young formula [9]:

$$C_D=2\left(\theta V^\lambda|_{x_{TE},C_{upper}}+\theta V^\lambda|_{x_{TE},C_{lower}}\right), \quad (29)$$

where $\lambda=\left(H|_{x_{TE}}+5\right)/2$.

4. TORQUE AND FORCES ACTING ON THE MULTI-BLADE HYDRODYNAMIC ROTOR

Consider a rotor with diameter 4 m and 5 hydrodynamic blades with NACA 0016 symmetrical profile with chord length 0,8 m and height 1,4 m. The numerical methods, described in previous section, are used to compute the hydrodynamic coefficients $C_{L,ref}$ and $C_{D,ref}$ for the symmetrical profiles selected from the NACA library of aerodynamic profiles with a reference chord length $c_{ref}=1\,m$. The coefficients corresponding to the profile with the chord length 0,8 m are calculated from the relations:

$$C_L=1,3C_{L,ref},\ C_D=1,3C_{D,ref}.$$

The magnitude of the hydrodynamic force $\vec{F}$ acting on the blade, its tangential and normal components $F_{x'}$ and $F_{y'}$ versus the positioning angle are presented in fig. 4 (a). Fig. 4 (b) shows the torque $T_{r,i}$ developed by a single blade versus the positioning angle.

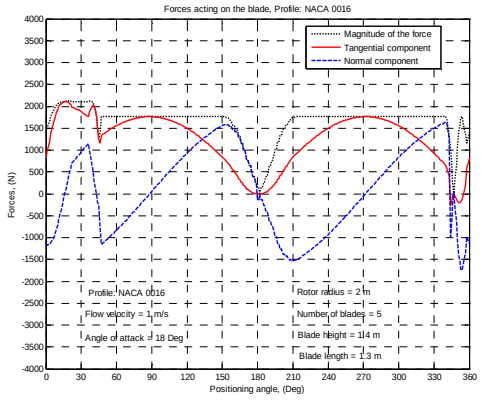

(a)

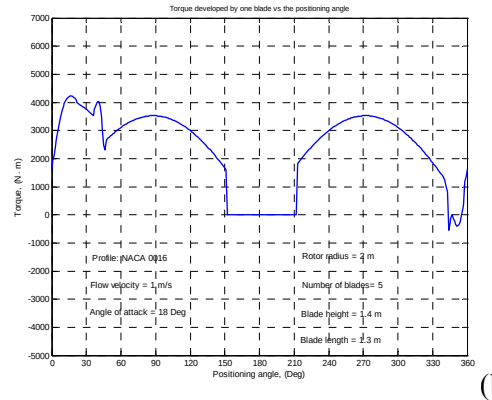

(b)

Figure 4. Hydrodynamic force components (a) and torque (b) versus the positioning angle.

Fig. 5 (a) shows the total torque at the rotor shaft $T_{r\Sigma}$ developed by all blades versus the

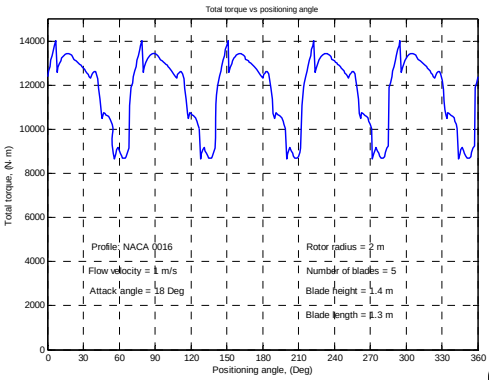

(a)

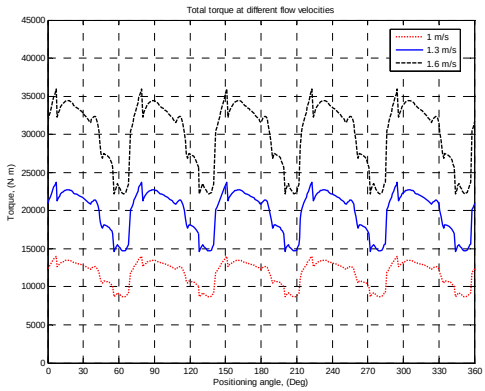

(b)

Figure 5. Total torque developed by 5 blades (a) and total torque for various flow velocities (b).

positioning angle, while Fig. 5 (b) shows the total torque $T_{r\Sigma}$ for three water flow velocities V_∞ .To determine the optimal working angle of attack it is necessary to compute the value of the torque for several values of the angle of attack: $\alpha = 15^o,\ 17^o,\ 18^o,\ 20^o,$ (fig. 6).

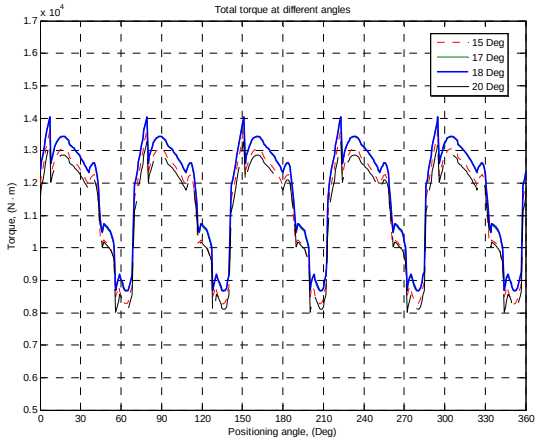

Figure 6. Torque developed by 5 blades versus the positioning angle.

5. HYDRODYNAMIC BLADE WITH SCREENS FOR DIRECTING THE FLUID FLOW IN THE BOUNDARY LAYER

Consider a laminated composite material shell composed of the following layers as shown in fig. 7: first layer bidirectional lining of type E fiberglass and polyetheric resin matrix; second layer has two sub-layers consisted of chopped fiberglass linings with an armoured polypropylene lining between them; third layer is again a chopped fiberglass lining in a polyetheric matrix; and the fourth is a gelcout covering layer.

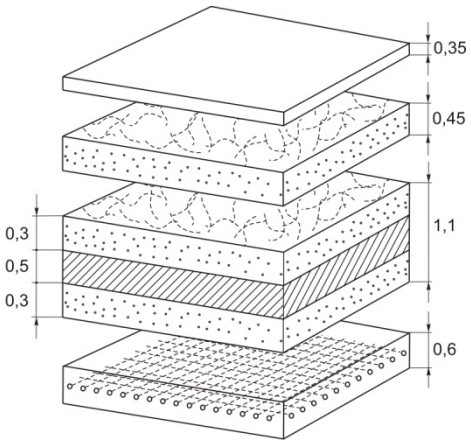

Figure 7. The structure of the composite material blade cover.

The computation of the material constants was performed using the manufacturer recommendations. The Young modulus for the

composite layer is $E = E_m V_m + E_f V_f$, where E_m and E_f are Young modulus for matrix and fiberglass, respectively, and V_m and V_f are the volume fractions of the matrix and fiberglass, [10]. Poisson coefficient is computed similarly. Thus, the following values have been obtained: Young modulus $E = 13,2GPa$ and Poisson coefficient $\nu_{12} = 0,3$.

Two FEM models have been considered: a section of the hollow blade discretized with finite elements Solsh190 and a section of the blade injected with polyurethane foam (density $0,6kg/cm^3$, $E = 0,95GPa$, $\nu = 0,24$) discretized with Solsh190 elements (lateral cover) and Solid45 elements (interior), [11, 12]. In both cases the lateral cover is made of laminated composite materials with thickness 2,6mm. The blade is subjected to hydrodynamic forces corresponding to the flow velocity of 2m/s and hydrostatic pressure. The maximum value of the forces acting on the blade is 11 kN. In the hollow hydrodynamic blade with composite material cover with thickness 2,6mm the maximal displacement is 4,3mm and the maximal stress value is approximately 38MPa. The stresses and displacement distributions are similar with those of hollow blade with aluminum cover. In fig. 8 there are presented displacements and the main stresses in the injected with polyurethane foam blade with the same thickness of lateral cover: displacements u_x (a), u_y (b) and u_z (c), and main stresses σ_1 (d), σ_2 (e) and σ_3 (f). While carrying out research on Computational Fluid Dynamics (CFD) of blade-fluid interaction it was stated the existence of fluid turbulent flow in the boundary layer, the intensity of which depends on its flow speed. To reduce the influence of this phenomenon on the conversion efficiency it is proposed to equip the blades with screens *1* for directing fluid flow in the boundary layer. Screens are spaced from one another at distance $h_b = \frac{1}{6}(V+1)$ and their peripheral profile is the equidistance with prominence

$$e = \tau_e c,$$

where c is the length of the blades chord, V is the flow velocity and parameter

$$0,02c \le \tau_e \le 0,06c .$$

Constructively the blade (fig. 9) consists of modules *2* with height h_b separated by screens *1*. Each module consists of sub-modules *3* with common composite coating. Modules *2* and

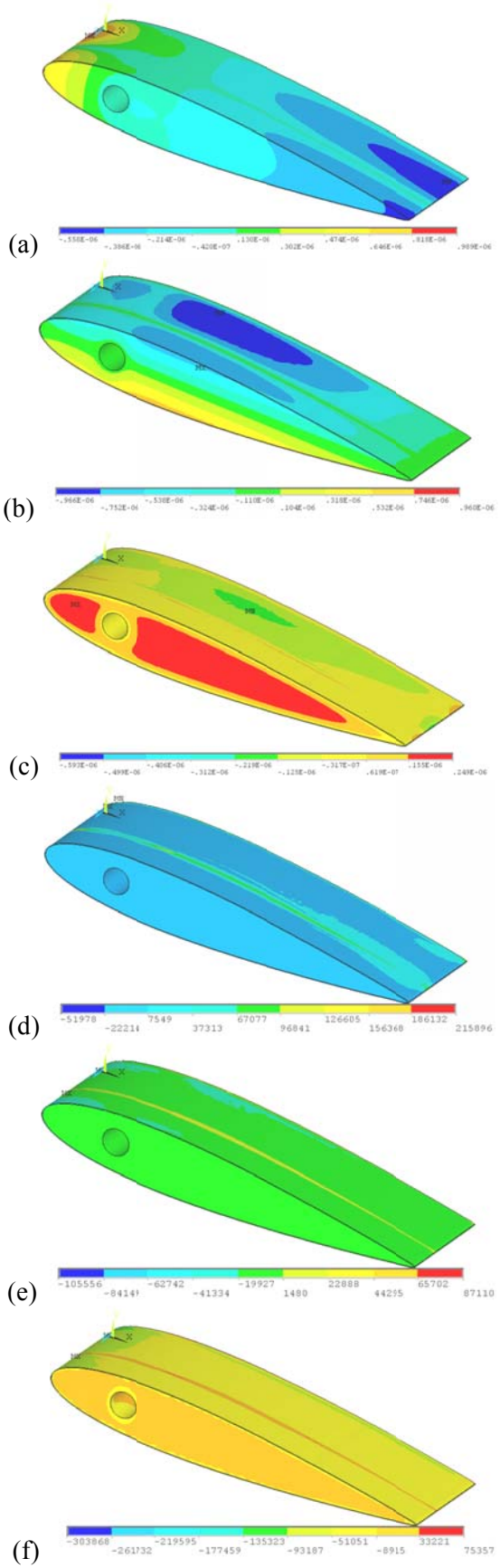

Figure 8. Displacements and main stresses in the blade injected with polyurethane foam and composite material cover with thickness 2,6 mm: u_x (a), u_y (b), u_z (c), σ_1 (d), σ_2 (e) and σ_3 (f).

screens *1* are assembled on a common shaft *4* mounted in levers *5* of rotor and fixed to rod *6*. The number of modules is determined depending on the total height *H* of the blade.

To manufacture the composite material side cover of modules *2* with hydrodynamic profile, the reversed (mirror) profile moulds (fig. 10) were executed using numerical control milling machine with 5 degree mobility. Fig. 11 shows the manufacturing of a blade (a, b) and the general view of a finished blade with modified hydrodynamic profile, manufactured on the basis of composite materials technologies.

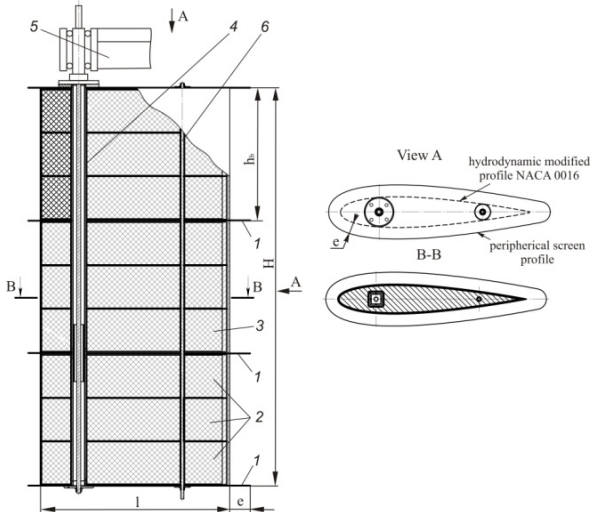

Figure 9. Blade construction.

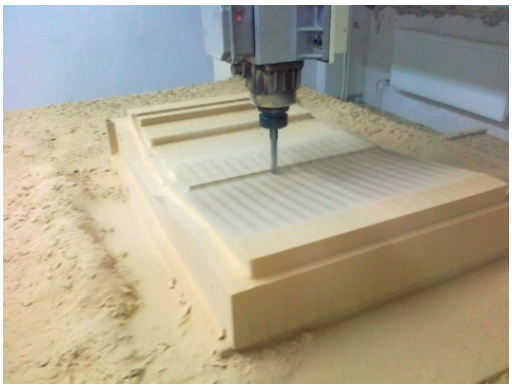

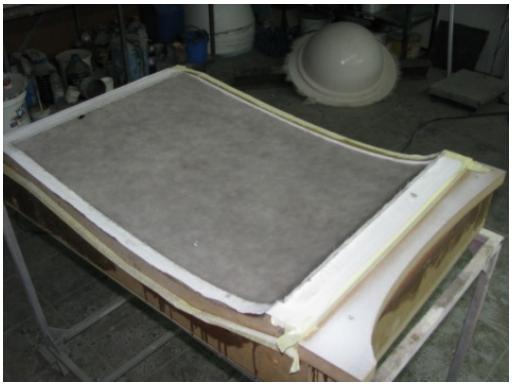

Figure 10. Manufacturing of reverse moulds.

(a)

(b)

(c)

Figure 11. Hydrodynamic blade manufacturing (a, b) and finished blade (c).

6. DIFFERENTIATED ORIENTATION MECHANISM OF BLADES

To increase energy conversion the blades *3* must be oriented towards the fluid flow direction at a variable angle of attack α, depending on the passed area (upstream, downstream and transition areas). For this purpose on the semi shaft *4* of each blade *3* (fig. 12) a rod *5* is attached placed perpendicular to the blade cord respectively and equipped with two rotating sleeves *6* located with the possibility of changing distance *l* from the blade semi shaft.

Guides *7*, *8* and *9* are mounted at rotor periphery, and rotating sleeves *6* roll in contact on their guide surface. The profile of guides and their position with respect to the location of rotor centre defines the angle of attack α and the evolution of its change for each blade during a full rotation. Thus, any blade in each point of its circular motion path is positioned at the same angle of attack α. At any point of the motion trajectory of the blades *3*, angle α can be modified depending on the flow velocity V_∞ by varying the location parameter *l* of the rotating bodies *6* to the semi shaft axes *4* of blades *3*.

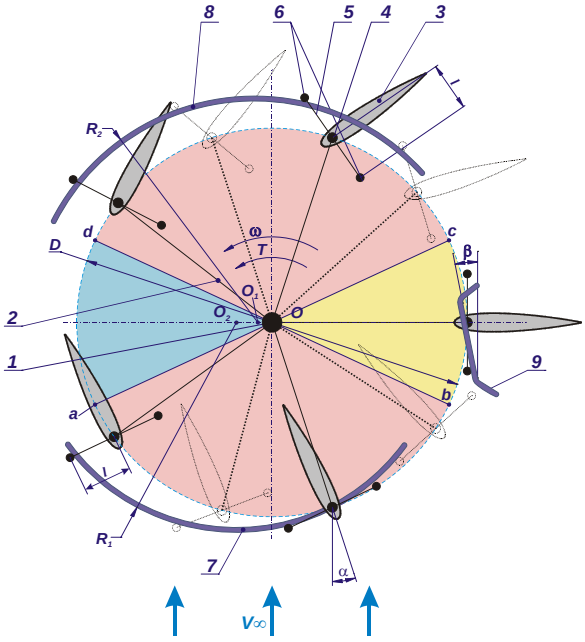

Figure 12. Differentiated orientation mechanism of blades.

Based on carried out research the optimal hydrodynamic profile and angle of attack were identified; their differentiated orientation mechanism was designed with account of requirements and constructive-kinematical solutions specified below.

Profile of guides *7*, *8* and *9* and their location shall provide individual positioning of each blade under optimal differentiated angle of attack α depending on the area of the blade-fluid interaction considering the flow rate of water flow. This condition is achieved by: location in the upstream area *Oab* of the rotor of circular guide *7* with radius R_1 and with the origin in the centre O_1 moved at distance OO_1; location in the downstream area *Ocd* of another circular guide *8* with radius R_2 and with the origin in the centre O_2 moved at distance OO_2, and in the upstream-downstream transition area by location of the rectilinear guide *9* positioned under angle β with respect to the flow direction. In this case the interaction of the rotating sleeves *6* of rods *5* with the guide profile, the blades are positioned in order to ensure that hydrodynamic forces developed by blades in all three areas *Oab*, *Ocd* and *Oda* contribute to torque development of the rotor shaft *1*, that in its turn will lead to increased energy conversion efficiency.

Also, in order to ensure the stability of blades *3* positions during their interaction with the fluid, semi shafts *4* are placed on the axis of symmetry of the hydrodynamic profile at distance $|BW|$ (fig. 13) from the blade edge determined from relation:

$$|BW| = 0,25c - k, \text{ with } \Delta \le k \le k_{\max}$$

Where c is the length of the blade chord, k is the distance ensuring condition of stability of blade positioning in fluid

$$R_k > 0, \tag{30}$$

$\Delta \in [25,40]mm$ denotes the parameter that depends of chord length c change in the interval (800–1300) mm, and k_{max} is the maximum distance determined from the condition ensuring admissible friction forces in the kinematic coupling rotating sleeve- guide.

In case of blade rotation $0 < \varphi < 2\pi$ at a variable angle of attack α, the orientation mechanism of blades should ensure stability of their positioning (fig. 13), which can be achieved if the reaction force in the kinematical coupling rotating sleeve – guide satisfies condition (30). On the other side, from the condition of minimizing unnecessary friction forces in kinematic couplings rotating sleeve – guide it follows that

$$R_{k,\max} = \tau R_k, \tag{31}$$

where $R_{k.\max}$ is the maximum reaction in the kinematic couplings rotating sleeve – guide and

parameter $\tau \in [1,2,\ 1,5]mm$. Reaction R_k in higher order kinematical coupling sleeve – guide can be expressed by relation:

$$R_k = \frac{F_L h}{l}, \tag{32}$$

where F_L is the hydrodynamic force developed at blade-fluid interaction, h is the distance between the blade semi shaft axes and the action line of the hydrodynamic force, and l denotes the distance between the blade semi shaft axes and sleeve (rotating body).

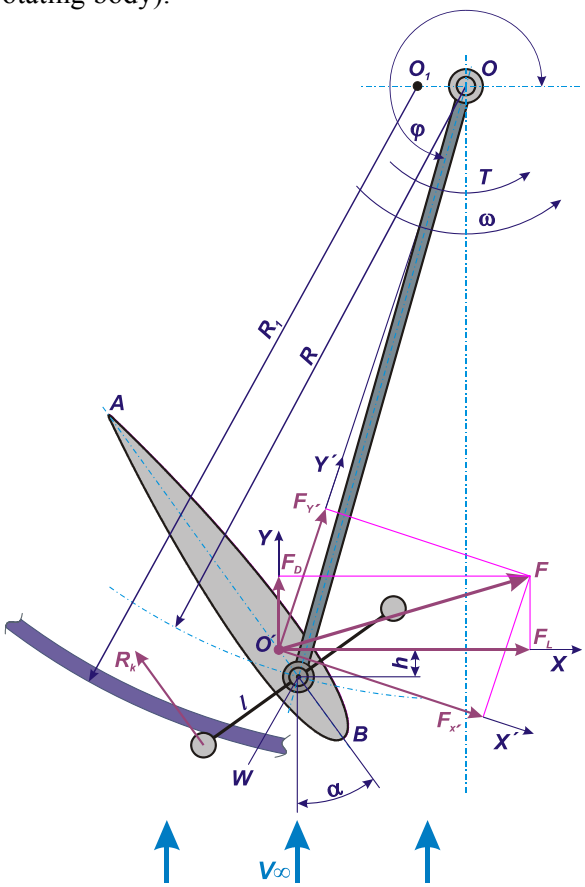

Figure 13. Stability of blade positioning in orientation mechanism.

From relation (32) results that in order to ensure the stability of blade positioning in its rotational motion in the fluid while respecting condition (30), it is necessary to identify the point W of location of blade semi shaft as well as the influence of the pitch moment, the turbulence regime, boundary layer parameters etc.

Installation of rotating bodies *6* in rods *5* with possibility of changing their distance l from the blades *3* semi shaft axis *4* ensures repositioning of blades depending on the flow rate of water flow, and thus provides conversion efficiency increase.

Profile shape of guides *7*, *8* and *9* and their location calculated with regard of rotor diameter D, and with consideration of the influence of the flow velocity of water flow on the correct positioning of blades, ensures in the result blades *3* orientation at variable angles of attack α depending on the area of blade-fluid interaction, namely:

- in upstream area *Oab*: $12^o \le \alpha \le 25^o$;
- in downstream area *Ocd*: $25^o \le \alpha \le 90^o$;
- in the upstream to downstream transition area *Obc*: $12^o \le \alpha \le 90^o$.

Differentiated positioning of the blades under variable angle of attack provides increased energy conversion by efficient exploiting of hydrodynamic forces developed by blades and reducing hydraulic resistance forces acting on the blades in their rotation around the hydraulic rotor main shaft.

7. CONCLUSIONS

The hydraulic turbine with 5 hydrodynamic profile blades assures conversion of 49.5% of the energetic potential of water stream with velocity 1.3 m/s. The optimal orientation of the blades with respect to water stream direction (enabled by differentiated orientation mechanism) assures participation of all blades (even those moving upstream) in generating the torque at the rotor shaft.

The modular blades with composite materials cover injected with polyurethane foam and resistance structure with 4 transversal screens assure minimal local deformations and prevents an early boundary layer separation that will not influence significantly the water flow and efficiency of energy conversion. Experimental testing of the micro hydropower station MHCF D4x1,5E in real field conditions confirmed that the hydropower station with hydrodynamic 5−blade rotor assures the conversion of the energy at the rotor shaft to the generator clams with efficiency of 77.5%.

Bibliography

1. Bostan V. *Computational Analysis of Hydrodynamic Effects in Hydraulic Flow Turbines (Part 1), Annals of University of Craiova, Electrical Engineering series, No.35, 2011, pp.83-92.*

2. Bostan I., Gheorghe A., Dulgheru V., Sobor I., Bostan V., Sochirean A. *Resilent Energy Systems. Renewables: Wind, Solar, Hydro, Topics in Safety, Risk, Reliability and Quality, Vol. 19, Springer, 2012.*

3. Moran J. *An Introduction to Theoretical and Computational Aerodynamics, John Wiley and sons, 1984.*
4. Katz J., Plotkin A. *Low Speed Aerodynamics, From Wing Theory to Panel Methods, Mac-Graw Hill, 1991.*
5. Batcelor G.K. *An Introduction to Fluid Dynamics, Cambridge University Press, 1970.*
6. Cebeci T., Bradshaw P*. Momentum Transfer in Boundary layers, Hemisphere Publishing Corportation, 1977.*
7. Reynolds W.C., Cebeci T. *Calculation of Turbulent Flows, Topics in Applied Physics Series, Springer-Verlag, Vol.12, 1978.*
8. Michel R. *Etude de la Transition sur les Profiles d'Ales, Onera Report, 1/1578A, 1951.*
9. Squire H.B., Young A.D. *The Calculation of the Profile Drag of Aerofoils, R.&M.1838, ARC Technical Report , London, 1938.*
10. Jones R. M. *Mechanics of Composite Materials, 2nd Edition, Taylor & Francis, 1999.*
11. *ANSYS 10.0, User's Guide.*
12. *ANSYS 10.0, Advanced Analysis Techniques Guide.*

Recommended for publication> 21.02.2013.

STUDY OF MACROPORES AND CRACKS IN STRUCTURAL LIGHTWEIGHT CONCRETE

[1]A. Goldman,[2]G. Fishman, [3]V. Toporet, [3]A. Rashcovoi
[1]Academic College in Ariel, and Technion – IIT in Haifa, Israel
[2]Academic College in Ariel, Israel
Technical University of Moldova in Chişinău

1. INTRODUCTION

One may characterize the GFC as Lightweight High Performance Concrete, as it combines superior properties of High Performance Concrete (HPC) such as very high density with substantially reduced bulk unit weight [2]. Unlike other known lightweight concretes, GFC does not contain any lightweight aggregate. It incorporates HPC as matrix, containing normal aggregate of course, that is, "HPC matrix". Light unit weight of GFC is achieved by introduction of polymer macrofiller grains.

The HPC itself is known since early eighties. The worldwide "HPC boom" in concrete science and technology took place as a result of two major developments. One of them was Condensed Silica Fume, or microsilica, first introduced into concrete technology as early as fifty six years ago. The other development (High Range Water Reducing Admixtures HRWRA, or super plasticizers) took place some twenty years later. Today, the HPC covers a wide range of cement-based products, offering very-to-ultra high strength, very high density, and substantially improved durability in aggressive environments. Its compressive strength is 80-160 MPa, and it can be as high as 800 MPa [3, 4]. The HPC is often considered as more fragile than conventional 20-60 MPa concrete. Consequently, the field of HPC applications is not as wide as one might predict two decades ago. The mechanisms of the HPC fracture remain unclear in some of their aspects [5, 6].

Being relatively fragile, the HPC is known for possessing the "true composite" behavior [3, 4, 7, 8], which resembles that of some natural rocks [7]. Fiber reinforcement can make it less fragile and can significantly improve its fracture toughness. This method is efficient, and thus it is widely accepted. However, the use of fibers actually did not yet widen the range of HPC applications, and in several aspects it is not intended to.

From this point of view, the application of HPC as the matrix to produce its lightweight version, that is GFC, is expected to improve the fracture toughness, much like it is achieved by introducing fibers. Steel fibers can take tensile stresses while cracks propagate in concrete under external loads. Lightweight polymer macrofillers that produce voids in GFC are also intended to partially arrest the crack propagation [9, 17]. The fracture toughness can therefore be improved, and so one can see the incorporation of voids into the HPC matrix as another possibility of improving the fracture behavior of the HPC. Several studies have shown the possibility of controlling stress concentrations, and crack propagation by changing the size and the content of voids [10, 11, 12, 13].

Computerized Tomography (CT) in medicine is known for years. Yet, one may qualify its application in concrete research as relatively new, whereas the CT has been used for studying mainly crack patterns [15] and void distributions [16, 19]. In this study, the CT serves for studying the distribution of polymer macrofiller grains and their impact on crack propagation in the mass of the HPC matrix. Some observations on crack patterns by this technique, and by Scanning Electron Microscopy (SEM), are represented as well.

2. SCOPE OF INVESTIGATION

Beside fibers, introduction of some water-soluble polymers can also produce an impact on the elasticity of cementations matrix, thus improving the fracture behavior. The price shall be certain, although limited, reduction of strength [6, 8]. Use of lightweight polymer grains as macrofillers, which can actually serve as voids of given sizes in hardened HPC is another possibility. Their presence shall affect the mechanisms of crack development, possibly reducing stress concentrations and speed of crack propagation [9, 12]. The polymer is chemically inert in cementations systems, while its grain size varies between approximately 2 and 6 mm. The unit weight of such grains shall be low enough to be negligible when compared to that of cementations components.

The influence of thus created voids on the macrostructure and crack distribution in GFC is

being investigated. We have suggested that proper introduction of voids by means of macrofiller grains is beneficial for controlling strength and fracture behavior. This is aimed at developing various lightweight structural elements of buildings.

3. RESULTS AND DISCUSSION

The trial GFC mix, aimed at checking its feasibility, was first prepared in 2001. It was based on a typical HPC mix design containing microsilica and commercially available super plasticizer. This mix served as the matrix for the GFC, as well as for the reference.

Another series of testing was conducted in 2003 as an introductory part of the Ph.D. research. It has included (a) an HPC mix with Portland cement of EN type 52.5, microsilica (10% by weight of cement), and a commercial super plasticizer; and (b) three GFC mixes, containing polymer macrofiller grains (13%, 23%, and 41% of total mix volume). Properties of fresh mixes were defined according to Israeli Standard (IS) 26, part 2. Compressive strength was measured following IS 26, part 4. Mechanical testing was conducted using the "Sercomp 7" system manufactured by Controls Group Ltd. in Italy. The results are shown below it Table1.

Significant reduction of compressive strength and modulus of elasticity, which fits the increase of the macrofiller content, is observed. The bulk unit weight is also reduced, although to a smaller degree. Yet, mechanical properties of GFC remain satisfactory at all levels of the macrofiller content [18, 19].

The experiment was aimed also at evaluating the influence of the macrofiller content on major properties of fresh and hardened HPC, while no changes are introduced into its own mix design. The results indicate that one can achieve a significant reduction of bulk unit weight, however on the account of mechanical properties. On one hand, the bulk unit weight can be as low as roughly 2000 kg/m^3, and even 1600 kg/m^3, while keeping satisfactory level of compressive strength [18, 19]. On the other hand, the reduction of compressive strength, and probably of other mechanical properties, can be very significant. One shall take into account the dependence of these results on the initial strength of the HPC matrix.

Table 1. Results of mechanical testing.

Properties	Reference HPC 2001	GFC 2001	Reference HPC 2003	GFC 1 2003	GFC 2 2003	GFC 3 2003
Compressive strength, MPa, at:						
1 day	-	-	34.7	29.0	20.4	-
7 days	59.8	34.0	71.3	45.8	33.1	17.0
28 days	78.0	47.2	84.7	54.7	38.8	21.8
Modulus of elasticity, MPa	46,000	35,000	-	-	-	-
Bulk unit weight, kg/m^3	2426	2018	2445	2223	2074	1614
Standard slump, mm	-	-	110	90	170	170
Filler content, volume %	-	≈25	-	13	23	41
Percentage of bulk unit weight reduction	-	16.8	-	9.1	15.2	34.0
Percentage of 28 days compressive strength reduction	-	39.5	-	35.4	54.2	74.2

These tests have clearly confirmed the feasibility of achieving structural lightweight concrete without lightweight aggregate, while controlling its mechanical properties and weight by means of a lightweight polymer macrofiller.

The whole idea of GFC is viable only if proper distribution of macrofiller grains in the concrete volume is achieved (fig. 1). According to the observations, several factors shall have an effect on movement and positioning of macrofiller grains in the mass of fresh concrete.

It is believed, that these factors can be divided between two groups, representing separately the influence of aggregate and paste. The most

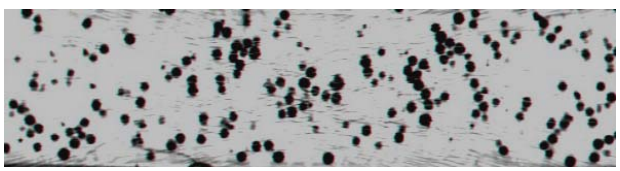

Figure 1. Typical distribution of macrofiller grains in the 70x280 mm cross section (x-ray CT image).

influential group of factors is introduced by the aggregates, namely by their grain size, grading, and volume content.

One should therefore expect a correlation to exist between the maximal size $\mathbf{D_a}$, fineness modulus **FM**, and volume $\mathbf{V_a}$ of aggregate, and correspondent parameters of the macrofiller, such as average size $\mathbf{D_f}$, and volume $\mathbf{V_f}$. Assuming that unit volume of concrete consists of paste and aggregate, and taking into account the volume of paste $\mathbf{V_p}$, one may express the content of macrofiller as follows:

$$V_f = (1- V_a-V_p)\cdot D_f/D_a, \qquad (1)$$

where the constituent $\mathbf{D_f/D_a}$ is macrofiller - to-aggregate size ratio. Somewhat alike aggregate-to–paste volume ratio, this one is believed to influence the workability of fresh concrete. The major impact it produces is however on distribution of macrofiller introduced into concrete**.** Regarding the distribution, the fineness modulus **FM** shall be taken into account as well. The above ratio can thus be given as $\mathbf{FM_f/FM_a}$. The influence of aggregate parameters on the macrofiller distribution is shown in fig. 2 and in fig. 3.

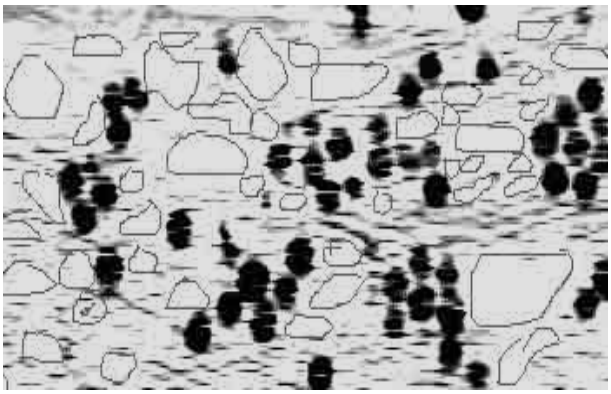

Figure 2. Positioning of macrofiller particles and coarse aggregate grains (reconstruction of X-rays CT image).

The distribution in fig.3 was obtained in an HPC mix whereas the aggregate-to-paste ratio is relatively high. This is typical for the "traditional" HPC. One can see that coarse aggregate grains can form zones where groups of macrofiller particles are entrapped. From this point of view, the aggregate size and volume content, as given by expression (1) seem to play the major role. It has been suggested, that the optimal aggregate size is roughly similar to that of macrofiller, as well as their grading, that is, $\mathbf{FM_f/FM_a \approx 1}$ [14]. As to the aggregate content, it shall vary, thus allowing variability of the macrofiller content, which in its turn leads to controlling the unit weight and other related properties of Lightweight High Performance Concrete (GFC).

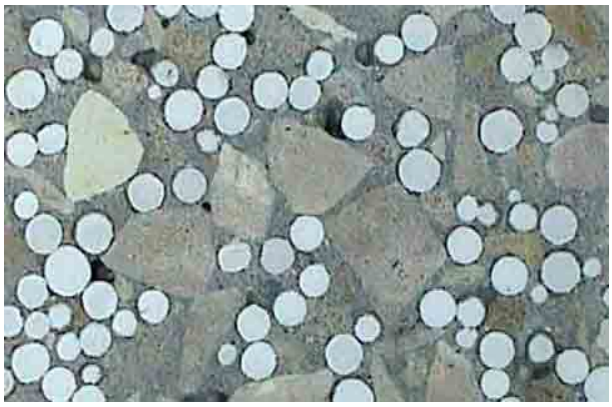

Figure 3. Typical distribution of macrofiller particles between coarse aggregate grains.

Under these conditions, and providing the paste content $\mathbf{V_p}$ in a fresh mix is constant, one can describe the mechanism of controlling the properties of GFC as follows:

$$V_f = k(1-V_a), \qquad (2)$$

The lower is the aggregate content, the larger amount of the macrofiller can be introduced. The coefficient **k** is a constant depending on paste content $\mathbf{V_p}$, if $\mathbf{FM_f/FM_a \approx 1}$ as given above.

Another group of factors is induced by paste. As long as the aggregate content is relatively high, it can provide proper distribution of macrofiller as shown in fig. 2 and fig. 3 above. The role of paste becomes significant in two cases: (a) when lowering the aggregate content in order to increase the amount of macrofiller, and (b) when the aggregate size is smaller than that of macrofiller ($\mathbf{FM_f/FM_a<1}$). Paste of composition typically found in High Performance Concrete contains very efficient super plasticizers (HRWRA). Under certain conditions, such paste can by itself provide proper distribution of macrofiller particles by well known dispersion mechanisms, induced by HRWRA [14].

The system of voids created by the lightweight macrofiller is believed to have two major effects on mechanical properties of concrete. It may increase the potential of absorbing fracture energy, thus improving fracture behavior of the HPC matrix [6, 14]. Consequently, it shall be able of arresting the crack propagation [9, 12]. The latter effect has been observed by multiple X-rays CT scanning (fig. 4), and it has been verified by SEM investigation (fig. 5).

Figure 4. Fragments of X-rays CT scans showing cracks ending at macrofiller spheres.

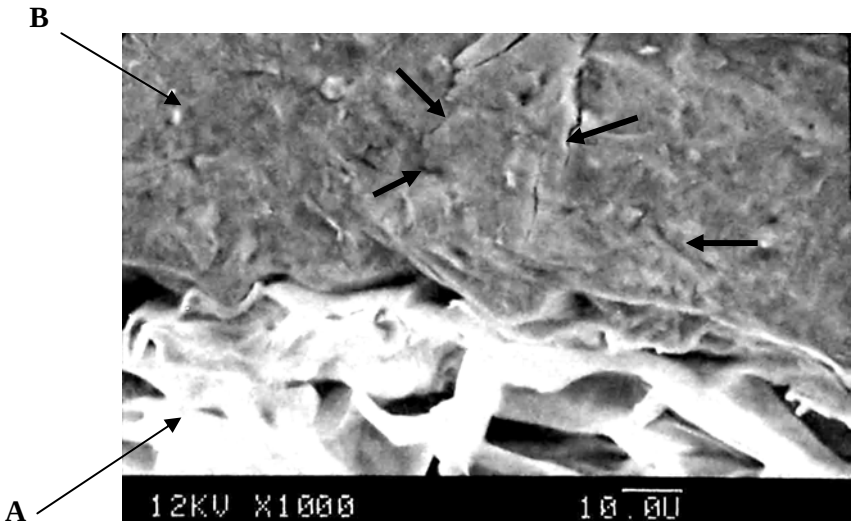

Figure 5. SEM image of boundary zone between polymer macrofiller particles (A) and HPC matrix (B): arrows show crack patterns in the HPC matrix.

4. CONCLUSIONS

1. Proper distribution of lightweight polymer macrofiller in the mass of concrete can be achieved mainly by adjusting aggregate volume content, if its average size is similar to that of macrofiller particles.

2. Paste can be of significance for proper distribution of macrofiller when aggregate size and/or volume content are lowered. Paste may influence macrofiller distribution through dispersion mechanisms induced by super plasticizers.

3. Crack propagation in HPC containing polymer macrofiller can be controlled. Spherical macrofiller particles can serve for arresting crack development, which has been confirmed by combined X-rays CT and SEM study.

ACKNOWLEDGMENTS

Authors are thankful to the Technical University of Moldova for making possible and coordinating this study. We are grateful to the Academic College in Ariel, where the experimental work has been carried out, for providing laboratory facilities.

Bibliography

1. Pruteanu N., Fishman G., Goldman A. *Composition for Preparation of Lightweight High Strength Concrete, Patent MD 2772 C2 2005.05.31, Chişinău, Moldova, 2005.*

2. Goldman A. *Properties of Concretes and Pastes with Microsilica, M.Sc. Thesis, Technion IIT , Haifa , 1987.*

3. Goldman A., Bentur A. *Bond Effects in High Strength Silica Fume Concretes, ACI Materials Journal, 1989, vol. 86, pp. 440-447.*

4. Shah S. P. *Materials Aspects of High Performance Concrete, First Int. Conf. on High Strength Concrete (UEF), Kona, Hawaii, 1997, pp. 504-511.*

5. Ali M. A. , White R.N. *On expending ACT 318 to High Strength Concrete, First Int. Conf. on High Strength Concrete (UEF), Kona, Hawaii, 1997, pp.554-567 .*

6. Goldman A. *Mechanisms of Strengthening in Cementitious Systems Containing Microsilica, D.Sc. seminar, National Building Research Institute, Technion IIT, Haifa, 1988.*

7. Aitcin P.-C. *High-Performance Concrete, E and FN SPON, London & New York, pp. 442-445.*

8. Goldman A. *High Performance Concrete: From Late Seventies to Nowadays, 2005 (in progress).*

9. Fishman G. *Private Communication, Netanya, Israel, July 200 .*

10. Broek, D, et. al., *Applicability of fracture toughness data to surface flaws and to corner cracks at holes, Nat. Aerospace Inst. Amsterdam, Report TR 71033 (1971).*

11. Bowie, O. L. *Analysis of an infinite plate containing radial cracks originating at the boundary of an internal circular hole, Journal of Math, and Physic., 25 (1956) pp. 60-71.*

12. Fishman G. *Stress Concentration Examples. Part 1., Meridian Ingineresc, Journal of Moldavian Engineering Association and TUM in Chişinău, No. 3, 2004, pp. 46-48.*

13. Fishman G. *Stress Concentration Examples. Part 2, Elliptical Hole, Meridian Ingineresc, Journal of Moldavian Engineering Association and TUM in Chişinău, No. 3, 2005, pp. 79-82.*

14. Goldman A. *Private Communication, Haifa, Israel, March, 2003.*

15. Saleh H. H. and Livingston R. *The Use of X-Ray Computed Tomography (CT) Techniques to Study the Internal Structures of Concrete, NDT.net, 2nd MENDT Proceedings, vol. 9, No. 06, pp. 01-06.*

16. Garboczi E. J. *Three-Dimensional Mathematical Analysis of Particle Shape Using X-Ray Tomography and Spherical Harmonics: Application to Aggregates Used in Concrete, Cement and Concrete Research, vol. 32, No. 10, October 2002, pp. 1621-1638.*

17. Fishman G. *On Controlling Pore System in Lightweight Concrete, Seminar, Technical University of Moldova, October 10, 2004.*

18. Fishman G. *Technology for High Resistance Easy Concrete Bearing Elements, Ph. D. dissertation, Technical University of Moldova, May, 2006.*

19. Fishman G. and Goldman A. *Technology of Lightweight Concrete with Controllable Pore Formation, Meridian Ingineresc, Journal of Moldavian Engineering Association and TUM in Chişinău, No. 4, 2005, pp. 82-85.*

Recomandat spre publicare: 11.01.2013

EFFECTIVE TECHNOLOGIES OF PRODUCTION OF BUILDING MATERIALS AND ARTICLES

[1]Ya. Zubrilina, T. Lupashku[2], E. Shamis[1]
[1]Technical University of Moldova
[2]Institute of Chemistry of the Academy of Sciences of Moldova

1. COMMON VIEWS

The present preposition includes not only one but several new technologies: building articles on basis of gypsum-cement- puzzolane binder (GCPB); semifinished products from extra-fine basalt fiber (EFBF), first of all basalt wool; quasi-composite building articles from GCPB and EFBF.

It is known that compositions of gypsum bindings and Portland cement are instable. Within the limits of 1-3 months after building mortar making strength decreases and the result of it is destruction.

This result from three-sulphate forming of calcium hidro-sulfo-alumenate on base of calcium sulfate and highly basic calcium aluminates, which contain Portland cement. Hence ettringite forms in composition, which is called “cement bacillus”.

A.V. Volzhenskij offered a composition on base of gypsum, Portland cement and active mineral (puzzolane) admixture comprising silica in active state.

Pozzolanic admixture permits to decrease strength of the calcium hydroxide and under existing conditions highly basic calcium aluminates cannot exist. So in opinion of researchers forming:

- mono- sulfate form $3CaO \cdot Al_2O_3 \cdot CaSO_4 \cdot 12H_2O$;
- hodro-granates $3CaO \cdot Al_2O_3 \cdot nSiO_2$ (6-2n) H_2O;
- hydro- aluminum-silicon $3CaO \cdot Al_2O_3 \cdot CaSiO_3 \cdot 12H_2O$;
- gypsum $CaSO_4 \cdot 2H_2O$ and theirs solid solutions.

Many years' experience in application of GCPB in building trade had confirmed deductions of researches. In recent years was produced improved form of quick-hardening binding on gypsum – composite gypsum binding (CGB), which also can be used in offered technologies.

Nomenclature of articles: elements of indoor and outdoor walls, dividers – slot-comice blocks and plates, elements of reinforced concrete monolithic overlaps – insert-blocks and plates for floor beds. All these elements are made from cellular GCPB having compression durability of 5,0 – 6,0 MPa, the density 800 – 1000 kg/m^3 with basalt-fiber inserts with density of 45 kg/m^3. From the above-enumerated elements it is possible to fully complete the whole constructive surface body of the building – incombustible, enough durable to resist the seismic, wind and other major exposures. The buildings from the above-enumerated elements are supposed to be erected in combination with metal and reinforced concrete monolithic constructions. The wall from the proposed elements by thickness of 300 mm assures the same heat shielding, as the wall from break with thickness up to 2450 mm.

By the result of the researches it was possible to receive from GCPB inclusively under production conditions, close-meshed rapid-setting for articles for heightened durability but without preliminary preparation of foam or input in forming mixture of gas-forming compounds.

Innovative technical solutions of the equipment and taking, that completely provide manufacturing of materials and articles with a preset predicted and higher performance were developed and tested in industrial practice. With density 1000kg/m^3 the actual compression strength made 17,2 MPa, bending strength – 4,7 MPa. Knauf offered by the company possesses the characteristic 4,5 MPa & 2,2 MPa.

Primary equipment includes kneading-and-mixing machine of continuous operation that effectuates cavitational-flush mixing of GCPB or another mineral biding material and water. Activation of mixture (build up of durability characteristics) is taking place during process of its preparation. This is reached due to the special regimes of production process allow in defined order to obtain materials of the programmed density and durability. Kneading-and-mixing machines moves above the forms of the articles, in which it discharges the newly prepared mixture. Gypsum articles are taken out from form in 15-20 minutes after the forms were supplied with mixture, due to natural rapid hardening without any thermal processing or other artificial exposure. Further the articles are

vectored to the chamber where excessive moisture evacuation is effectuated.

Major facts, defining significance of new building technologies complex, are as follows:

- ubiquitous abundance of the initial row material; natural origin of host materials with a high scale time-approved durability; optimum characteristics of the articles – fire resistance, heat-shielding, acoustical absorption, water-, biological-, cold-, weather resistance etc.; promptitude of development of production and construction of objects, inclusively in areas exposed to extreme effects (natural disasters, military operations, man-caused catastrophes, terrorist acts);
- versatility of articles for construction for buildings and structures of different purpose and of any constructive schemes; possibility of usage in buildings of the diverse architecture; simplicity and briefness of the new technologies of production of building articles; compact, parterre placement of the equipment of technological lines; high performance of usage building items in buildings and structures constructed in any climatic zones of the planet.

2. POTENTIAL USAGE OF TECHNOLOGIES

Offered building technologies and products are characterized as ecologically clear, energetically efficient, stable in extreme situations, economically efficient. They can be recommended for usage in construction of buildings of any constructive schemes and floor quantity practically in all climatic zones.

The complex of offered technologies is approved in trial manufacture in 90-‘s in Russia (Moscow) within the framework of the Federal program “*Energosberejenie Rossii*”, the Moscow city program of the Ministry of science and technologies in Russia.

As region of initial industrial realization of new building technologies the Republic Moldova is supposed. Here there is a necessary base, free capacities, relatively inexpensive and insufficiently loaded working and technological personnel, highly skilled scientists and the engineers participating in elaboration of offered technologies. The marketing researches have shown that in Moldova there is a steady demand for the offered building products, determined by their technical and economic advantages in comparison with analogues.

In Moldova offers have got the approval of the state authorities in the form of the Assignment of the president of Moldova # 05/5–100A from August, 8, 2001, Decision of the Government # 421 from April, 5, 2002, branch building programs.

The elaborated investment project including the marketing-plan and the business-plan, has confirmed expediency of the organization of such a manufacture in Moldova. The potential opportunity of realization of the presented technologies and their production in neighboring countries is also determined in this project.

Technologies can be of interest in regions with a cold climate (for example, the north Russia, the Scandinavian countries, Canada, Alaska). They represent special interest for regions with excess seismic activity.

In our opinion, offers can be recommended for the building market of USA, in particular, for construction of buildings of a little floor quantity. Here special value is got with opportunities of creation of enough strong structures, capable to resist to influence of fire, radiation, seismic loading, but to provide a minimum of costs in construction. Moreover, the important factor in support of offers is energy efficiency not only in production, but also during the operation of building.

3. ADDITIONAL INFORMATION

Elaboration of a complex of offered technologies was carried out 40 years in Moldova, Russia and Ukraine.

At the first stage of researches (60-70-s’) the technology of thin-walled volumetric blocks on GCPB was created, and for the first time in the world building practice in 1961 in Kishinau trial manufacture of volumetric blocks of sanitary-engineering units and engineering communications was organized. Then the technology was widely realized in USSR, now in Moscow two factories of a building industry make these products, providing needs of city construction.

At the second stage (70-s- the beginning of 90-s’) the general technology of modular construction with usage of rapid-setting materials on GCPB and aerostatic flying devices (dirigible balloons) was elaborated for transportation and installation of large volumetric blocks. Models of such volumetric blocks were made and tested in 1972 in Kiev with our participation, and the model of the specialized dirigible balloon was constructed and tested in 1991 in Ulyanovsk.

At the third stage (90-s and in present time) the elaborations were conducted in

Moldova and Russia and in 1997-99 in Moscow trial manufacture of effective building production offered technologies was organized.

Exhibits of the offered technologies were submitted and have got an approval on a number of the international exhibition:

- on the third International exhibition-congress "High Technologies. Innovations. Investments". In Sank-Petersburg in 1998.
- on the International Exhibition "Dorogy-98" in Moscow in 1998
- on the exhibition "*Rosstrojexpo*" in Moscow in 1999
- on CEI Summit Economic Forum in Budapest (Hungary) in 2000
- on the International Exhibition "Moldconstruct'2001" and "*Moldconstruct*'2006".

At the present time elaborators carry out the preparation of a batch production of building products on the offered high technology technologies in Kishinaw. Simultaneously technologies continue to be improved.

4. ECONOMIC PARAMETERS

Costs of creation and start – up of the unified process module UTM-1 with the annual capacity 20,0 thousand m^3 of building articles and 8,0 thousand m^3 of basal wool make up 1230,75 thousand $USD.

According to the business-plan data the annual receipts from sales of production at prices of Moldavian building market make up 2944,0 thousand $USD.

Total cost of this production represents 2240,0 thousand $USD.

Annual profit will make up 704,0 thousand $USD.

Bibliography

1. Voljenskij A.V., Stambulko V.I. *Ferronskaja A.V. Gipso-czementno-puccolanovy'e i betonny'e izdeliya. – Moskva: Gosstrojizdat,1971.*

2. Eger S.M., Ishkov Yu.G., Shamis E.E. *Dirizhabli dlya severny'h rajonov//Promyshlennyj transport. – M.:1988, #2.*

3. Kostikov V.I., Smirnov L.N., Shamis E.E. *Programma "Bazalt": tehnologii i izdeliya dlya stroitel'stva. – M.: 1999, - #2 (5-6).*

4. Kostikov.V.I., Shamis E.E. *i dr. Gipsobazal'tovye stroitel'nye izdeliya i tehnologii/ Stroitel'nye materialy, oborudovaniya, tehnologii XXI veka. – M.: 1999. - #3-4.*

5. *Shamis E.E. Ob''yomno-blochnoe domostroenie s primeneniem by'strotverdeyushhih materialov. – Kishinyov:Kartya Moldoveneaska',1971.*

6. *Shamis E.E., Smirnov L.N. I dr. Tehnologii gipsobazal'tovy'h stroitel'ny'h izdeliy'//Bazal'tovoloknisty'e materialy': Sbornik statej. – M.:Informkonversiya, 2001.*

7. *Shamis E.E., Moorichev V.B. Using Lighter Than Air Vehicles (Dirigibles) in Housing Construction. Proceeding of the Interagency Workshop on LTA Vehicles. FTL Report R75-2, Massachusetts Institute of Technology, Cambridge, Massachusetts, 1975.*

Recommended for publication: 17.01.2013

RELIGIOUS FREEDOM TODAY - EMPEROR CONSTANTINE'S EDICT OF MILAN: 1700 YEARS LATER

This year therefore marks the 17th centenary of the official recognition of Christianity, which was accorded the same rights as all other religions throughout the Roman Empire, thus instituting the concept of religious tolerance. It is exactly 1700 years since the Emperor Constantine gave official

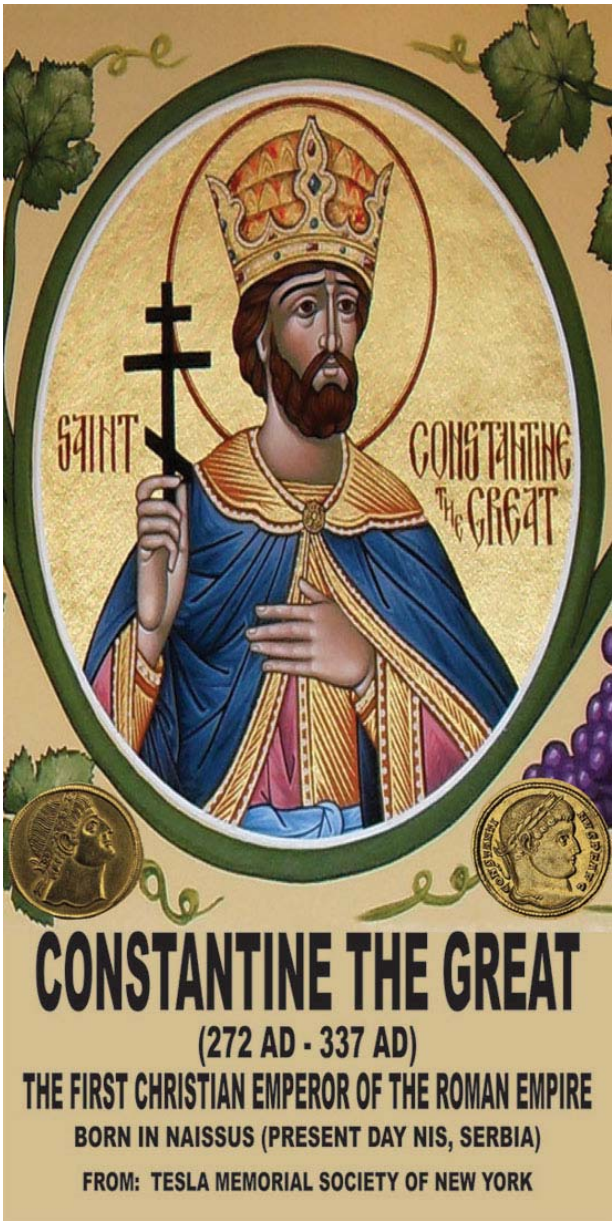

recognition to Christianity. 1700 years have passed since 313 when, through the Milan Edict of Toleration, Emperor Constantine granted freedom of conscience and freedom of worship to all cults, thus putting an end to centuries of persecution against Christians in the Roman Empire. Since then, Christians have enjoyed religious freedom, which has allowed the development of current European society.

"*In … 313 … Licinius (the eastern Roman emperor) and Constantine (the western emperor) had met in Milan. The occasion was the marriage of Licinius to Constantine's half-sister, Constantia. But the two emperors used the occasion to discuss matters of state and agreed on a policy concerning the practice of religion. During the summer of 313 Licinius sent letters to provincial governors…in the East,in Asia Minor and Syria, granting Christians the rights they had already acquired in the West and restoring their property. This letter has often been called the "Edict of Milan" but the term is a misnomer. It was not an edict but a letter posted by Licinius from several cities in the East, such as Nicomedia, the residence of the emperor. Like other official correspondence, however, it was written in the name of both emperors and its content reflects the hand of Constantine*". Licinius's letter, involved all religions, not just Christianity; it went beyond mere toleration and embodied a more robust idea of religious freedom, based on the conviction that true faith and true worship cannot be compelled; and it treated the Church as a corporate body with legal rights, including property-owning rights. Thus the not-really-an-Edict of Nicomedia and Elsewhere cemented into the foundations of the West ideas first sketched by the Christian philosopher Lactantius: that coercion and true religious faith don't mix because "God wishes to be adored by people who are free". The rather humane provisions of the mis-named "Edict of Milan" were not infrequently ignored in subsequent western history; but that doesn't alter the fact that the "Edict" had a profound and, in many respects, beneficial influence on the future of the West. The Edict of Milan marked not only the legalization of Christianity but the birth of the concept of religious tolerance in the western world, granting freedom of expression to all faiths and religions, that has endured to the present day. The ensuing 1700 years have seen Christianity implanted in every nation on earth, though not without sporadic persecutions, bloody and bloodless, that continue to the present day. In his Edict which we celebrate today, Saint Constantine was "*more modern*" and more noble than many of the rulers who came after him, or who govern today, when millions of Christians suffer throughout the world.

Here are some of the major points that the Edict stressed:

1) Freedom in worship is "*of profit to all*

mankind". Man's relationship with God is his "*first and chiefest care*", and in order for everyone to flourish in this pursuit, the State shouldn't interfere.

2) Freedom of religion is beneficial to the State. The authors stated that the purpose of the Edict was for "*establishing public tranquility*". Religious oppression facilitates violence and strife among citizens of the same society.

3) Civil equality belongs to all people regardless of one's religion. In many areas of the empire, Christians were not allowed to own land and many churches were dispossessed of their properties. This Edict restored land to Christians and condemned any such civil discrimination based on religion.

4) The Emperors believed that this Edict would win divine favor, resulting in success and happiness in their realm.

What led to such a historic decision? In the turbulent year 312 AD, while preparing for a decisive battle, Constantine received a vision: *In hoc signo vinces* – By this sign you shall conquer. Profoundly struck by the message, Constantine took the Christian symbol of the first two letters of the Greek word for Christ (X and P, the one superimposed on the other, known as the Chi-Rho symbol) and ordered his soldiers to mark their standards with this sign before going into battle. He and his troops marched to victory against the army of rival emperor, Maxentius, at Rome's Milvian Bridge – where even today tourists can stroll across the River Tiber.

Subsequently, Constantine gave orders for the construction of a basilica over the burial ground of St Peter himself. After many changes over the centuries, today a magnificent and imposing St Peter's Basilica and Square inspire reverential awe and welcome pilgrims from across the globe. To further commemorate the emperor's victory, the Arch of Constantine was erected near the Coliseum where his predecessors had amused themselves with the blood of Christian martyrs - a sharp contrast, indeed. Patient observers can follow the battles and conquests of the emperor on the numerous panels comprising the arch. Constantine, though considered the first Christian emperor, and while appreciative of divine intervention and victory in battle, did not always live or rule by Christian virtue. History tells us that he executed his son by his first wife, and somehow his second wife disappeared one day and soon was found dead. Constantine did become baptized shortly before he died in 337 AD.

All Christians can jointly celebrate this anniversary of Christianity. The Ecumenical Patriarchate of Constantinople, in conjunction with the Council of the Bishops' Conferences of Europe (CCEE), is commemorating the 1700th anniversary of the Edict of Milan by hosting a conference devoted to religious freedom. The following are the main ideas from the Patriarchal and synodal encyclical on the 1700th anniversary since the edict of Milan (the Patriarch Bartholomew, May 19, 2013, Constantinopole).

„By the Mercy of God Archbishop of Constantinople-New Rome and Ecumenical Patriarch!

To the Plentitude of the Church: Grace and Peace from God.

"Blessed is our God, who so deemed" and orders all things for all people, who has led us to "this day of the Resurrection" when "all has been filled with light, heaven and earth alike."

This year marks the 1700th anniversary since the issue of the Edict of Milan about religious freedom. Therefore, we are communicating to the Church in all places and times in order to address a message of hope, love, peace and optimism from the most holy Apostolic and Patriarchal Ecumenical Throne in as much as the Church is the continual presence of God. "Whoever has seen the Son has seen the Father" (John 4:9), and whoever has seen the institution of the Church has seen the divine-human Lord and the Holy Spirit, who are with us.
The Church is precisely such an institution in freedom. "Such is Christianity: it grants freedom to those in slavery." (St. John Chrysostom, Homily IX on 1 Corinthians 193).

As a result of the Edict of Milan, the persecutions against Church and religion, previously licit, ceased; and for the first time in human form, freedom of religious conscience was instituted in the world. However, the freedom that Christ granted us (see Gal. 5:1) is not mere "form" and "letter". It is genuine freedom, which we are always seeking in order that all things may become "new." Otherwise, how can we possibly expect a new heaven and a new earth?

Until the time of Constantine the Great, the history of the world, namely the period of "Old Israel" before Christ, and after the divinely incarnate presence of the "New Israel," the free expression of conscious faith is replete with problems and persecutions to the point of martyrdom by blood for the sake of truth.

***

History recounts the persecution of individuals who shared a different perspective and faith about God from that proclaimed by the worldly authorities or the society, which they inhabited.

The captive children, who refused to worship the irrational and arrogant human ruler claiming the features of God, cried out aloud in the pit: "let all God's works praise the Lord." In so doing, they prefigured the freedom brought by the Lord, "who became as one under the law so that he might win those under the law." (see 1 Cor. 9:20)

***

In ancient Athens, the Philosopher Socrates was condemned to death on the charge that he accepted the gods worshipped by the city. Similarly, there are many individual persecutions recorded by the classical Greek authors about those who supported different beliefs, such as the example of the persecution of Anaxagoras of Clazomene, who claimed that the sun is a fiery rock, or Diagoras of Milos, who criticized the ancient idolatrous mysteries and discouraged citizens in these. There is not doubt that physical or ideological persecutions through the centuries, which sometimes led and continued to lead to death by martyrdom, nevertheless did not abolish religious tolerance among people, as this was formally proclaimed in the Edict of Milan.

***

The Roman emperors had an absolutist mentality, rendering themselves leaders even of religion. Indeed, they reached the point of demanding recognition for their divine status, which required equivalent honor.

The rejection of Christians of such imperial demands provoked anger in as much as it questioned imperial authority. The result anthropocentric worldview was the well-known merciless persecutions, which filled many shrines with martyrs who "washed their robes and made them white in the blood of the lamb." (Rev. 7:14)

Ultimately, the persecutions against religion affirmed the words of St. John Chrysostom: "One who fights against God can never destroy good to the end; instead, such a person may perhaps not feel that he is doing something terrible at the outset of his daring act. However, if he persists in his madness he can never lay a warring hand on God, because he will never avoid the hand of the invincible God." (To those Opposed to the Monastic Life 1, PG 47.319)

***

Emperors Constantine the Great in the East and Licinius in the West accepted the fact that, after three centuries of harsh persecution against the Christians, religious hatred and constant oppression resulted in no benefit for the empire. Therefore, they decided to allow Christians the freedom to practice their faith and worship of God. The content of the ever-relevant Edict of Milan in the 313 AD, which reflects the will of Constantine the Great, "who understood the craft of bitter warfare," constituted the basis of the freedom of religious conscience that was recognized many centuries later.

***

The Edict of Milan contains advanced positions on religious freedom, expressed in thirteen sections. It institutes principles which are foreign for that period of the fourth century but which still remain principles and signposts, even if some claim that these principles can also be fully applied in a world that lies in evil and in justice, where darkness prevails instead of righteousness and light.

The Edict confesses and declares: respect for the thought and will of every person to care for the divine affairs as he wills; regard and respect for the divine and freedom of choice in religious matters to Christians and all people without discrimination; the return without delay to the community of Christians, the Church and the Synod of places of worship and other assets which were seized and taken from them; and all these things in order that "the divine care, which protects us and which we have already experienced in many situations, may remain securely with us forever."

***

This Edict and the consequent reformations of Constantine the Great introduced to the world the concept of human rights. For the first time the above-mentioned values were established: respect of religious tolerance, freedom of expression of religious conscience – values of human life – and all such values, which comprise the basis of the relevant legislation that is valid today and the various contents of occasional declarations by international organizations and state bodies.

Constantine the Great, who received his vocation from above, embraced all people, citizens and faithful, believers and unbelievers, thereby becoming a servant of the peaceful welfare and the salvation of all humanity. From his time onward, the Church of Christ transfigures institutions and regenerates the world, precisely as the burning bush on Mt. Sinai that was not consumed, the Womb that contained the uncontainable, namely Life in order that we may have life. (see John 10:10)

*****

If we carefully observe the history of the world since that time, especially today, after 1700 years from the declaration of the Edict of Milan by Constantine the Great, we sadly ascertain that the various regulations about religious freedom have unfortunately been violated on numerous occasions in the past, not only against Christians, but sometimes even by Christians themselves against their fellow Christians and against the adherence of other religions.

Regretfully, when Christians became the majority within society, there were some instances of overzealous tendencies. One of the more contemptible instances of such spiteful conduct among Christians was the great schism and division of the One Church, which ignored in later generations that "Christ is not divided" (1 Cor. 1:13) and that we humans are "earth and ashes." (Sir. 10:9) We overlooked and continue to overlook the aguish of the division of the seamless garment of the Lord, the Church, both locally and in every parish as One, Catholic, and Apostolic. Thus, as another "furnace of evil" (Prov. 16:30), we no longer enjoy love, peace, and tolerance; nor do we ask ourselves and one another the crucial question: "shall not the judge of all the earth do what is just" (Gen. 18:25) for us as well?

*****

Last century, the Orthodox Church in particular was persecuted relentlessly by the atheist regime and other states, which depended on this regime ideologically, especially in the countries of Eastern Europe. In some countries, Christians are still, to this day, treated with great disfavor, despite the fact that many international treaties have now been universally recognize the right to religious freedom.

The relevant reports on religious oppressions by the appropriate international organizations are replete with specific examples of religious oppression against Christian religious minorities in particular as well as individual Christians.

To this very day, unfortunately, we must emphasize that religious tolerance and freedom of worship are an achievement of civilization. There are vast regions of the world that are inhabited by people, who do not tolerate a different religious faith from theirs. Religious persecutions continue to exist, even if they do not assume the same form as persecutions of the early Christians. Various unfavorable discriminations against adherents of several religious faiths still persist and are sometimes intensely oppressive. In many cases, religious fanaticism and fundamentalism prevail, so that the Edict of Milan is still relevant in our times and addresses those people, who, despite the passing of 1700 years since its declaration, have yet to apply it completely.

*****

As we observe the journey of humanity from this sacred Center of Orthodoxy, we can freely admit that, despite the rapid progress of science and human discoveries, unfortunately the world has as a whole has not yet reached the noble concept and perception of religious freedom and that we still need a collaborative effort to achieve this goal.

Nonetheless, contemporary religious persecutions against Christians once again reveal the power of faith and the grace of sanctity.

*****

Fathers, Brothers, and Children in the Risen Lord,

The anniversary that we celebrate is a crucial sign. It signifies that, when man loses his unity with the Church, whose constitution lies in the Trinitarian unity, he also loses his freedom. For one loses oneself when one loses all others. Everything in the Church is illumined by the Trinitarian unity, particularly the Eucharistic sacrament, which comprises the very heart of the Church as a gift from the Father through the Son in the Holy Spirit. If man preserves the Trinitarian unity, man is preserved as person and communion. If we preserve and experience this unity, the divine – human unity, then we preserve the unconfused and undivided unity of the two natures in Christ, which are extended to us as a blessing in the unity of truth and life, institution and grace, law and freedom. Those things that appear antithetical in fact interpenetrate without change and without alteration in accordance with the model of the Theotokos, who brought the opposites into the same. At the same time, this interpenetration reveals the constant presence at all times and in all places of Christ, divine and human, who continues to journey in the field of history with another form. He journeys with every person who struggles searches and despairs not in order to grant "magical solutions" as some sensory narcotic but in order to open his eyes, grant new senses and lift him toward heaven, while bringing down to earth the Holy Spirit which enters our earthly knead as a Trinitarian leaven.

No human institution, even if labeled ecclesiastical, can contain, tolerate, and satisfy the man, who breathe God within and desires what lies beyond, namely ongoing perfection in Christ. Nor is it possible for such a man to be satisfied with any promise or worldly perspective when he thirsts for the inconceivable and humanly inaccessible. All human existence cries "No!" to every secular

institution, which supposedly claims that it leads to the mystery of life and salvation.

Every mechanical and seemingly "good" spiritual institution is "only" ready is frail, dissolved and non-existent. Therefore, the Lord, who knows all things and guides human hearts, came to shatter these "prisons" so he was persecuted and continues to be persecuted. However, in the end He was victorious in His Resurrection. He destroyed deceit. He overthrew the bankers' tables and the merchants' benches, namely those who had converted God's temple into "a house of commerce." (John 2:17) He liberated humanity from the "curse" of the law. (Gal. 3:13) Through His descent into hades, "chains were broken, gates were shattered, tombs were open, and the dead were brought to life." (Aposticha, Great Vespers, Holy Friday)

Thus, all those who were "dead" from love, freedom, human rights, faith, hope, expectation, light, righteousness, truth, life, passed over into light: "and none was left dead and buried." (Catechetical Homily of St. John Chrysostom)

And thus was constituted the holy Church, which through the ages, the martyrs, the ascetics and the righteous, despite persecutions and human temptations, is no "prison," but freedom and, like death, powerful love. As the herald of this truth through the centuries, the Church is the continuation and consequence of the womb of another Mother, "wider than the heavens," which gives birth to freedom. Thanks to the Church, all of us are children of the free woman (Gal. 4:31), children of freedom, which is acquired through obedience to the divine truth and love. If human institutions are afraid of human freedom, either dispelling, or disregarding, or even abolishing it, the institution of the Church, generates free persons in the Holy Spirit. And the Spirit constitutes the entire institution of the Church in as much as it "breathes where it wills but you do not know where it comes from or where it goes. So it is with everyone who is born of the Spirit." (John 3:8) The indefinable nature of freedom is the rock of our faith.

***

The Wisdom of God, the Lady Theotokos our Pammakaristos and Conciliation, St. Demetrios Kanavis, St. George the Trophy-bearer of the Phanar, and all the saints of our Church are not keepers of the law but legislators according to St. Symeon the New Theologian. The institution of the Church is charismatic, and the charismata of the saints function as institutional signposts for the faithful of the Church.

One can truly and experientially say that charismatics do not exist but in fact become and are continually born for charisma is not granted as a static quality, but as a blessing, which is granted perpetually. Charismatics are those who are truly free because they are aware of the ultimate weakness of humanity and goodness of God. Such is the teaching that has trickled down to us from the Edict of Saint Constantine.

Those who see everyone else good and pure, regarding themselves as being "beneath all creation," possess the grace of compunction and humility. They recognize the gifts of inner rest and illumination, they regard nothing as their own achievement, nor do they exploit any opportunity to expand their "authority" by "undermining" others, namely by limiting the freedom of others. The saints marvel at God's ineffable love and spontaneously return this love directly to the Giver of al gifts. This is precisely what renders the saints worthy of continually receiving gifts that are new, greater, spotless, spiritual, a blessing for all creation, general achievements. In turn, they continue to reserve to have no high regard for themselves. Their highest regard is God.

As soon as they become aware that the world honors them, the saints are surprised, worry, and withdraw. They retire behind the curtain of feigned foolishness or ignorance, which in fact is true freedom. They are comfortable because they live, follow, and contribute to the flow of divine blood and grace within the body of the Church community.

***

Brothers and Sisters in the Lord,

Human rights and the freedom of religious conscience are gifts which were "once given to the saints" (Jude 1:3), but which are constantly acquired along the journey of life. They are acquired through the experience of communion in Christ within the harmonious cosmic liturgy. We have been talking for 1700 years about the freedom of human conscience. However, the Orthodox Church always – and particularly in the recent years of global changes within the last tragic century – foresees and discerns in its entirety the "prevalence in the world of peace, righteousness, freedom, fraternity and love among all peoples, and the elimination of all racial and other distinctions," as would be decided by the coming Holy and Great Synod.

These sacred gifts are experienced through grace in the Divine Liturgy, where the creation of the world is revealed. It is humanly impossible to comprehend the magnitude of our freedom because we do not

respect human beings as the image of God. And if we do not love our neighbor, we do not truly love God.

In this world, people naively imagine that "all things are fluid and nothing is permanent and it is not possible to cross the same river twice" (Heraclitus), namely that all things come and go and are forgotten, while human stones and graves cover them.

The Lord granted us the mystery of memory in freedom, when he proclaimed that "nothing is covered up that will not be uncovered" (Luke 12:2) and that all things culminate in the truth of freedom in Him and in the sense of doxological gratitude "for all that we know and do not know."

Therefore, beyond external differences and distances, beyond worldly changes and exchanges, beyond the "rational" West and East, from the creation of the world we have seen God's love, which dispels the falsehood of deceit like an irruption in silence, granting us the truth of life as a blessing of freedom and unity, as a journey of surprises leading to the endless journey toward Pascha, which is Jesus Christ Himself. "It was no messenger or angel but His presence that saved" (Is. 63:9) us in freedom and for freedom. He is with us after His ascension, "neither separated nor distant from us." (Kontakion of the Feast of the Ascension) He stands beside us even when it appears that He abandoned us. Finally, He grants us the assurance that He is always present manifesting His glory in love and kenosis, depicted in icons as the king of glory in His resurrection, delivering Adam and Eve from hell, even while hanging peacefully on the wood of the Cross in ultimate humiliation.

***

"Great are you, O Lord, and wondrous are your works, and no word suffices to Hymn your wonders." In any case, "every hymn is inadequate, hastening to describe the multitude of Christ's great compassion."

Our Modesty, together with our brothers in the Holy Spirit and concelebrants in the Lord, stand before the "empty tomb" with the myrrh-bearing women and behold that "the stone has been moved." We witness in ecstasy and awe the Risen Lord, who trampled down death by death, liberating us from the bonds of flesh and consuming hades, while granting us life.

Thus, on the occasion of our commemoration of the granting to Christians of the right to freedom of faith and worship, from this sacred Center of Orthodoxy, which has served in captivity the true freedom of humanity in Christ and of the ecclesiastical body, we express our intense concern, anxiety and protest for the ongoing persecutions throughout the world. In particular, today we fervently pray for the Christian populations of the geographical regions of the Middle East, who experience frequent murders, kidnappings, persecutions and threats, which have culminated in the kidnapping of two brother Hierarchs, whose whereabouts are still unknown, namely the distinguished and most reverend Metropolitan Paul of Aleppo, well-known for his spirituality and significant ecclesiastical, social and educational ministry, as well as the Syrian Jacobite Metropolitan Yohanna Ibrahim of Aleppo.

We wholeheartedly share in the pain, sorrow and challenges faced by Christians in the Middle East and Egypt, and especially in the ancient and senior Patriarchate of Antioch. Beyond any political stance, we categorically condemn once again the use of all forms of violence, appealing to the rulers of this world to respect the fundamental human rights of life, honor, dignity and property, recognizing and praising the peaceful lifestyle of Christians as well as their constant effort to remain far from turmoil and trouble.

We express our concern as the Church of Constantinople that, 1700 years after the issue of the Edict of Milan, people continue to be persecuted for their faith, religion and conscientious choices.

The Ecumenical Patriarchate will never cease, through all the spiritual means and truth at its disposal, to support the efforts for peaceful dialogue among the various religions, the peaceful solution to every difference, and a prevailing atmosphere of toleration, reconciliation and cooperation among all people irrespective of religion and grace.

In condemning every form of violence as contrary to religion, we proclaim from the Ecumenical Patriarchate that truly great is "the mystery of our religion; God was revealed in flesh, vindicated in spirit, seen by angels, proclaimed among gentiles, believed in the world, taken up in glory" (1 Tim. 3:16), governs the world and the affairs of the world in accordance with His incomprehensible will and judgment, and will come again in glory as the righteous judge of the entire world.

To Him be glory, might, power, honor, worship, and the kingdom to the endless ages of ages. Amen"

Column written by professor Valeriu Dulgheru, Ph.D. Dr. Sc. from Technical University of Moldova

THE PHYSICS OF CREATIVITY AND THE CREATIVITY OF EVOLUTION

„The creation of the universe is usually envisaged as an abrupt event that took place in the remote past. It is a picture reinforced both by religion and by scientific evidence for the 'big bang'. What this simple idea conceals, however, is that the universe has never ceased to be creative"

Paul Davies

As the contemporary physicist, Paul Davies (1988), notes above, creativity is ongoing within the history of the physical universe. Creation did not end at the beginning, however conceived; it was only getting started. Especially in the West, we do not see the physical cosmos as a creative (or selfcreative) reality. We follow a Newtonian model of the universe in which matter is dead and inert, simply pushed and pulled about by physical forces (Lombardo, 2006a); and/or we accept the Judeo-Christian explanation that God created all the forms of nature at the beginning of time.

Yet, contrary to both Newton and *Genesis*, within contemporary cosmology and evolutionary theory, the universe is generally viewed as possessing an ongoing history of creative and emergent realities. Further, creativity within nature appears (to a degree) to be cumulative, building upon what existed before but equally transcendent in manifesting novel realities that go beyond what existed before. In essence, natural evolution is a creative process, ongoing, cumulative, and yet transcendent.

If indeed this view of natural creativity is correct, then creativity need not involve an intelligent or purposeful agent generating it (contradicting the divine source theory of creation). Moreover, the foundational dynamics and underpinnings to creativity in humans (intelligent and purposeful agents) exist within nature itself; creativity is not something unique in humans. What, indeed, do we know (or at least surmise) regarding the creative process in the evolution of nature. By the time of Darwin, nature was no longer seen as a stable reality created by God as it presently is. Rather nature, both biological and geological, was understood to be dynamical with a long history of change. Even the heavens no longer seemed stable or eternal as most ancients believed (Green, 1959). For Darwin, living species evolve and hence emerge through a gradual process of natural selection of variable offspring. Biological evolution of the new is driven, at least in part, through adaptation to environmental conditions which change over time as well. Further, there is both becoming and passing away, for species disappear (go extinct) as well as emerge. Further still, living forms are interconnected, provoking each other into change, through competition over resources and niches; there is a clearly a selfprovoking quality to creation within nature. Based on such natural processes, out of simple beginnings emerge a great variety and complexity of biological forms. This envisioned evolutionary process involves both cumulative growth and progressive differentiation.

More recently, Stephen Gould and Niles Eldredge add to this vision of creative biological evolution the idea that the emergence of new species is often relatively sudden (in geological terms) rather than slow and steady as Darwin envisioned it. There is "*punctuated equilibria*". Species may stay relatively unchanged for extended periods and then holistically and quickly transform; the process is not slow and piecemeal. Regardless of what instigates these sudden shifts a frequently cited cause is dramatic environmental change creative evolution is Gestalt-like and relatively quick.

The contemporary biologist Lynn Margulis further proposes that biological evolution at times has involved symbiosis, where distinct species integrate forming more complex species. She contends that this is how eukaryotic cells (cells with nuclei) emerged, through a coming together of prokaryotic cells (cells without nuclei). Nature, in fact, is filled with symbiotic relations and interdependencies. Hence, the creative evolution of the new is not simply driven by competition; there is also integration among simpler forms, whether the forms physically merge or simply develop reciprocal living arrangements. What emerges out of such symbiotic integrations is something new and creative. Self-organization in natural evolution is a theme that frequently shows up in contemporary open systems or complexity theory. Progressively, especially over the last century, principles of self-organization and evolution have been applied not only to biology but to nature as a whole. What Darwin was describing in his theory of biological evolution was just one piece of a general cosmological process.

For Ilya Prigogine, diverse types of natural systems evolve through self-organization. Natural systems undergoing increasing turbulence can jump upward to higher levels of organization and complexity; hence, the expression "order out of chaos" is used to capture a fundamental dimension of evolutionary change within nature. Connecting with ancient themes, chaos is viewed as a prelude (even necessary condition) for creation.

Pulling together Darwin and Prigogine, Stuart Kauffman argues that the evolution of life involves both competition and natural selection, and self-organization–an integrative, complicating process.

Moreover, for Kauffman the emergence of more complex natural forms is to a great degree unpredictable; the universe is filled with novel, emergent realities that cannot be predicted from simpler constituents that preceded them. In arguing for such a view, now framed at a cosmic level, Kauffman aligns himself with the great twentieth century philosopher Alfred North Whitehead who stated that "*The ultimate metaphysical ground is the creative advance into novelty*".

Anticipating Kauffman, the philosopher, J. T. Fraser (1978), also weaves together the themes of order and chaos in his explanation of the ongoing evolution of nature, as well as similarly arguing that new levels of complexity cannot be predicted or understood relative to lower levels of complexity. A further common theme found in such theories is that creation occurs at the interface of order and chaos, of structure and flow.

Building on such ideas, Kevin Kelly argues that self-organization is a result of the interaction of many parts within a system, rather than the coordination of parts from some top-down command center. There is no need for a singular creator orchestrating or generating the emergence of the new. Hence, there is an unpredictability and "*out of control*" quality to this pluralistic process of interactive self-organization.

As we move into the new Millennium, the theory that the cosmos as a totality has evolved through a succession of creative jumps in complexity has become fundamental to the scientific picture of nature. Distilling the essence of this vision, Harold Morowitz presents a list of twenty-eight creative steps in the emergence of everything within the universe each step conceptualized as more complex than preceding steps. This comprehensive panorama of the ongoing act of creation includes the successive emergence of stars, galaxies, chemical elements, solar systems, planets, geospheres, cells, animals, mammals, hominids, tools, agriculture, cities, and philosophy. Creation is not guided or orchestrated from above in this process; creation is not planned out; creativity is intrinsic, pervasive, and essential to the dynamics of the universe itself. What's more, it is an adventure, filled with novelty and unpredictability, rather than a foregone conclusion.

To recapitulate: cumulative growth; ongoing change and creativity; differentiation and syntheses; relatively sudden holistic transformations; chaos, unpredictability, novelty, and adventure; and self-organization all show up as fundamental themes in the modern scientific vision of creative evolution in nature. But there is more. The art movement of Futurism, which emerged early in the twentieth century, began its manifesto with the following words: "*We want to sing the love of danger, the habit of energy and rashness...We declare that the splendor of the world has been enriched by a new beauty: the beauty of speed*". And indeed, the pace of change in contemporary times seems to be speeding up, perhaps to the point of a mad frenzy.

Many argue that evolution has been accelerating across the great panorama of cosmic time and that what we see in our contemporary world (how quick things move, how fast things change) is simply a manifestation of this general natural phenomenon of accelerative evolution. As Murray Gell-Mann notes, evolution in the cosmos has moved through roughly six fundamental levels of increasing complexity and organization: the physical quantum; physical macro-gravitational; chemical; biological; cultural; and technological. For Gell-Mann (1994), each stage brings with it a faster, more complex process for further evolution. That is, evolution is evolving, and each stage finds a way to speed up the process of more change, more increasing complexity and order. To drive this basic point home, when scientists and historians are asked to identify key advances in the history of life on the earth, they generally agree on which constitute the most important jumps forward and, if plotted on a graph, the key identified jumps are coming closer and closer together in time.

As Toffler (1971) and Gleick (1999), among others, point out, we live in an era of accelerative change for Gleick, it is "*the acceleration of just about everything"*. Though Kurzweil (1999, 2005) primarily applies the "*Law of Accelerating Returns*" to the exponential growth of information technology, the same basic principle can be applied to all forms of change in human society. Innovations (ideas and inventions) feed back into the entire social-technological system, stimulating further changes and developments. Growth is a positive feedback loop; creation feeds on creation, hence, the accelerative growth of natural evolution. As David Christian points out, the most salient and dramatic fact within recent human history that seems responsible for the rapid evolution of society and technology is the accelerative growth of human innovation. Humans, coupled with their technologies, are highly creative beings–an advanced expression of the creative evolutionary process in nature and it is our evolved creative capacity that is generating the accelerative speed of change within our world.

References:

Th. Lombardo. Creativity, Wisdom, and Our Evolutionary Future.// Journal of Futures Studies, September 2011, 16(1): 19 - 46

Column written by professor Valeriu Dulgheru, Ph.D. Dr. Sc. from Technical University of Moldova

PERSONALITIES FROM THE MERIDIANS OF THE ENGINEERING UNIVERSE

CRISTEA MATEESCU

Cristea Mateescu was born on the 11th of August 1894 at Caracal. His father was a clerk, and his mother a housewife. He attended the primary school in his native town, then „Carol I" secondary school in Craiova and High school in Buzau. He passed the entrance examination at the National School of Bridges and Roads of Bucharest in top position. He got his engineer degree in 1919 and he continued his studies in Switzerland between 1920 –1921 and in France between 1921 – 1922.

During these internships which were financially supported by the Romanian Academy, he studied especially the display of water falls and of the lakes for hydroelectric plants. In France he met professor Denis Fydoux who helped him visit several hydroelectric plants, opening his professional career.

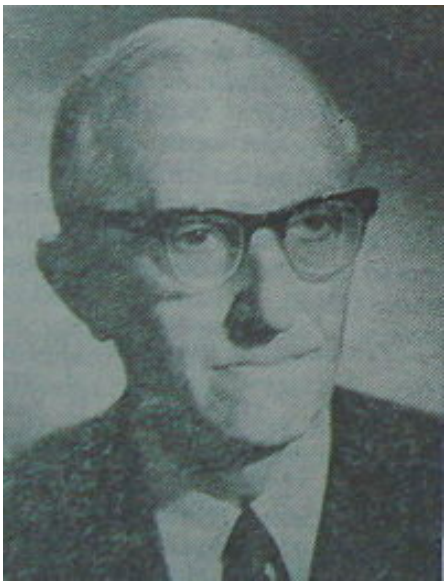

Rhetorical questions

My imagination can go further and I can ask myself if engineer Cristea Mateescu, born at 15 km from the Olt River, having a passion for hydroelectric arrangements, had ever thought, that the Olt River would be radically transformed along 350 km in order to build 31 hydroelectric plants with an installed power of 1.112,8 MW and an electric production of 3.040,6 GWh/year.

Had he ever imagined that, at Râmnicu Vâlcea, it would be build in 1974 a hydroelectric plant whose dam would have 34 metres height and it would be supplied from a lake with a surface of 319 ha and 319 million m^3 of water? This make me think of the hydroelectric plant from Ioneşti, inaugurated in 1978 and whose dam is 14 m height and which is supplied from a lake with the surface of 466 ha and 25 million m^3 of water. I am also thinking of the hydroelectric plant from Turnu, built in 1981 and whose dam is 44 m height, and its lake has a surface of 154 ha and 13 million m^3. What can we say about the hydroelectric plant from Drăgăneşti, built in 1988 whose lake with a surface of 1000 ha goes beyond the bridge that crosses the Olt river, covering the beach where the child Cristea Mateescu used to sunbathe with his friends?

Finally, we shouldn't forget about the hydroelectric plant from Izlaz whose construction will begin soon.

Certain answers

I don't know if the engineer Cristea Mateescu imagined all these achievements, but I know for a fact that his first scientific paper was about the electric plant from Sadu-Gorj. He remarked himself within scientific community in 1927 with the paper "The Rationale Arrangement of the superior part of the river Ialomița". He organized and led, for the first time in Romania, a department for the hydro-energetic study of the rivers Prahova, Ialomița, Târlung, Buzău-Bâsca, Siret. It is known for sure that he designed the hydroelectric plant from Sadu V- Sibiu, with a dam built with rockfill and reinforced concrete, the first one of this type in Romania. The river Sadu was used for obtaining electricity along the history. Let us present some information about it. In 1896 the first hydro-electric plant was built along this river, Sadu I. In 1907 in uphill it was built the second one, Sadu II, and in 1955 the hydroelectric plant Sadu V, supplied from Negoveanu lake with a dam of 62 m height.

It is known for sure that the engineer Cristea Mateescu participated in the designing

of the dam from Valiug, built between 1946 and1949, that he participated in the designing of the hydro-electric plant from Bicaz, built between 1951 and 1960. It is also known for sure that he was the head of the designing team of the hydro-energetic complex from Corbeni, built between 1958 and 1966. Fortunately, Cristea Mateescu lived enough to see or to read about the hydro-energetic arrangement of the river Olt which started in 1974.

Engineer at Electric Plant

In 1922, after graduation, he was employed at "*Electrica*" Company where he worked until 1926. Within this context I want to mention that the Electric Plant from the Peles Castle started to function in August 1884. In 1899 it is inaugurated the Hydroelectric plant from Sinaia, the biggest in Romania at that time. In 1898 the Romanian Society for Electric and Industrial Companies was set up. It managed the energetic activity of Prahova area.

On the 11th of May 1901, this society changed its name in "*Electric*a" Society Ltd. We can conclude that Cristea Mateescu started his professional career in one of the most important hydro-electric companies from Romania.

Professor

His results as a student, his specializations in Switzerland and France, his results as an engineer recommended him for a teaching career. In 1936 he became assistant at the rational mechanics and material resistance course.

In 1938 he defended his Ph.D. thesis with the subject "*La résolution des systèmes hyperstatiques par deux méthodes récentes-critique et extension des méthodes Filipescu et Cross*".

He became associate professor in 1939, and then professor in 1946. He taught several disciplines, among which the regime and water arrangement at the Construction Institute of Bucharest. This was the name of the present Technical Institute of Construction of Bucharest It must be mentioned that he was the head of the Hydraulic Construction Department between 1950 and 1964.

Other accomplishments

Cristea Mateescu became an engineer at the National School of Bridges and Roads, so in his CV there are included also projects for famous civil constructions, for example "*Asigurarea Română*" ARO-Patria block from Bucharest.

Complex personality

He was editor-in-chief at "Hydro-techniques" journal. He was a collaborator at the national electrification plan. He was the president of the Romanian National Committee for Big dams during 1957-1963. He evoked in his works the contributions of two great Romanian engineers: Alexandru Davidescu and Ion Ionescu. He was chosen associate member of the Romanian Academy in 1955 and full member in 1974.

He died on the 14th of June 1979 in Bucharest.

Column written by professor eng .Gheorghe Manolea, University of Craiova, Doctor Honoris Causa of Technical University of Moldova from Chişinău

CALENDAR – ANNIVERSARIES

2 April 1793 -220 years since **Thomas Addison** birth, (April 1793 – 29 June 1860), a renowned English physician and scientist, professor, doctor.

6 April 1483 - 530 years since **Rafael Sanzio** birth (6 apr.1483 – 6 apr.1520) **(**better known as **Raphael),** an Italian painter and architect of the High Renaissance, one of the greatest artists of all times (6 April 1483 – 6 April 1520).

8 April 1973 - 40 years since **Pablo Picasso** death, was a Spanish painter, sculptor, printmaker, ceramicist.

10 April 1813- 200 years since **Joseph-Louis Lagrange** death**,** (25 January 1736 – 10 April 1813) was a French mathematician, astronomer and physicist, of Italian origin.

12 April 1808- 205 years since **Costache Negruzzi** birth, was a Romanian poet, novelist, translator and politician. (12 April 1808 – 24 August 1868).

29 April 1893 -120 years since **Harold Urey** birth, was an American physical chemist whose pioneering work on isotopes earned him the Nobel Prize in Chemistry in 1934. He played a significant role in the development of the atom bomb .

23 May 1883- 130 years since **Dimitrie Leonida** birth, Romanian engineer, energy specialist, scientist, professor (23 May 1883 – 14 March 1965).

24 May 1923 -90 years since **Radu P. Voinea** birth, engineer, professor of theoretical mechanics. President of the Romanian Academy (24 May 1923–11 May 2010).

31 May 1883 -130 years since **Onisifor Ghibu** birth**,** was a Romanian teacher of pedagogy, member of the Romanian Academy, politician, journalist, one of the great personalities of Romanian culture, called the ”Bessarabia Apostle "

6 June 1933 - 80 years since **Heinrich Rohrer** birth, was a Swiss physicist who shared half of the 1986 Nobel Prize in Physics .

19 June 1623 - 390 years since **Blaise Pascal** birth, French mathematician, physicist, inventor, writer and philosopher. In 1642, he started some pioneering work on calculating machines Between 1658 and 1659 he wrote on the cycloids.

22 June 1963 -50 years since **Maria Tănase** death, was a renowned singer of folk music; considered one of the most talented voices of Romanian folklore.

24 June 1883 - 130 years since **Victor Franz Hess** birth, was an Austrian-American physicist, and Nobel laureate in physics. He discovered cosmic rays (24 June 1883–17 December 1964)

24 June 1918 – 95 anniversary since the inauguration of the first airmail flight in Canada, between Montreal and Toronto.

24 June 1848 – 165 anniversary of the Fântânele Battle, Transylvania, during the Revolution of 1848, between the Romanian revolutionary army and Hungarian forces.

Column supported by Zinaida Stratan

Industrial Design
Student projects

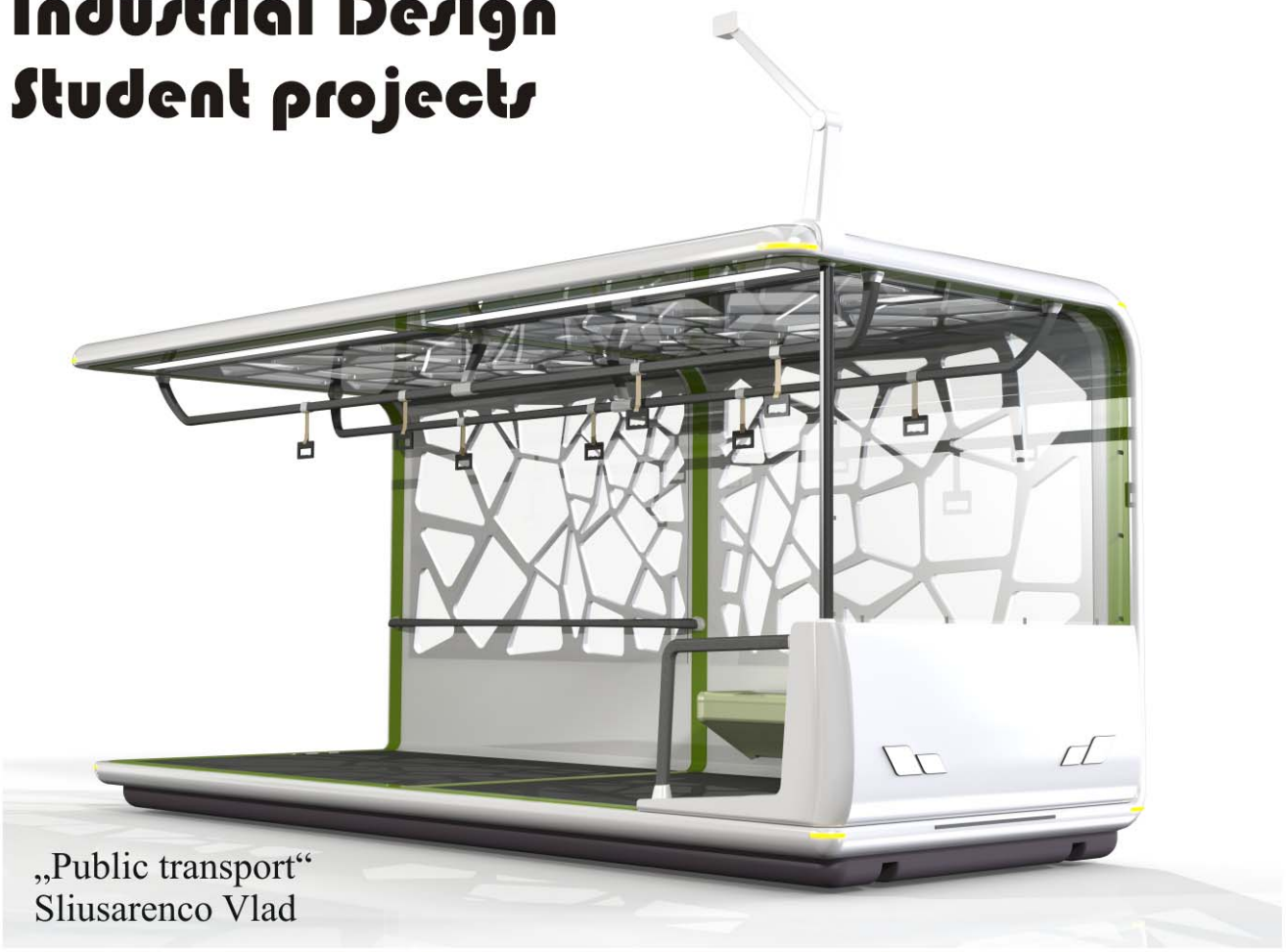

„Public transport“
Sliusarenco Vlad

„Packing for sunflower oil“
Gogu Anatoli

Technical University of Moldova
Bd. Stefan cel Mare 168, Chisinau, Republica Moldova
Tel.: (373 22) 44-50-07, e-mail: podborschi.valeriu@gmail.com